ETH

Eidgenössische Technische Hochschule Zürich
Swiss Federal Institute of Technology Zurich

PEDG 2014
Tutorial

# Mains Interfaces for Future 400 $V_{DC}$ Distribution Systems and Electric Vehicle Battery Charging

**Johann W. Kolar, Roman Bosshard**

Power Electronic Systems Laboratory,
ETH Zurich, Switzerland
www.pes.ee.ethz.ch

# Outline

# Introduction

# 400$V_{DC}$ Distribution Systems

- ► Future Datacenters
- ► Future Hybrid AC & DC Microgrids

# ▶ AC vs. Facility-Level DC Systems for Datacenters

- **Reduces Losses & Footprint**
- **Improves Reliability & Power Quality**

— **Conventional US 480V$_{AC}$ Distribution**

Source: intel 2007

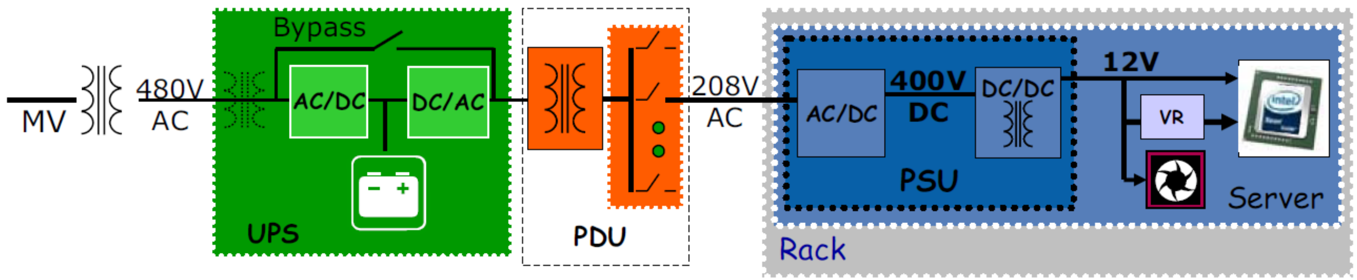


— **Facility-Level 400 V$_{DC}$ Distribution**

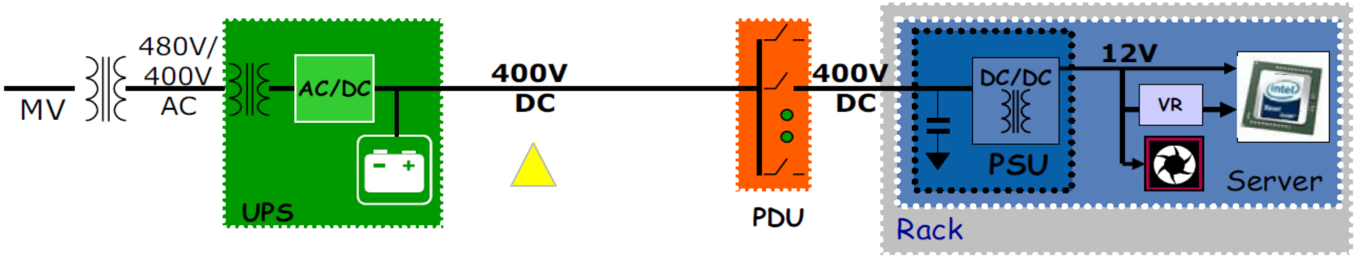


- **Proposal for Public +380V$_{DC}$/-380V$_{DC}$ Systems by Philips, EMerge ALLIANCE, etc.**

# ▶ Smart Grid Concept

Source: Borojevic 2010

- **Hierarchically Interconnected Hybrid Mix of AC and DC Sub-Grids**

  - Distr. Syst. of Contr. Conv. Interfaces
  - Source / Load / Power Distrib. Conv.
  - Picogrid-Nanogid-Microgrid-Grid Structure
  - Subgrid Seen as Single Electr. Load/Source
  - ECCs provide Dyn. Decoupling
  - Subgrid Dispatchable by Grid Utility Operator
  - “Virtual Power Plants”
  - Integr. of Ren. Energy Sources

- **ECC = Energy Control Center**

  - Energy Routers
  - Continuous Bidir. Power Flow Control
  - Enable Hierarchical Distr. Grid Control
  - Load / Source / Data Aggregation
  - Up- and Downstream Communication
  - Intentional / Unintentional Islanding for Up- or Downstream Protection
  - etc.

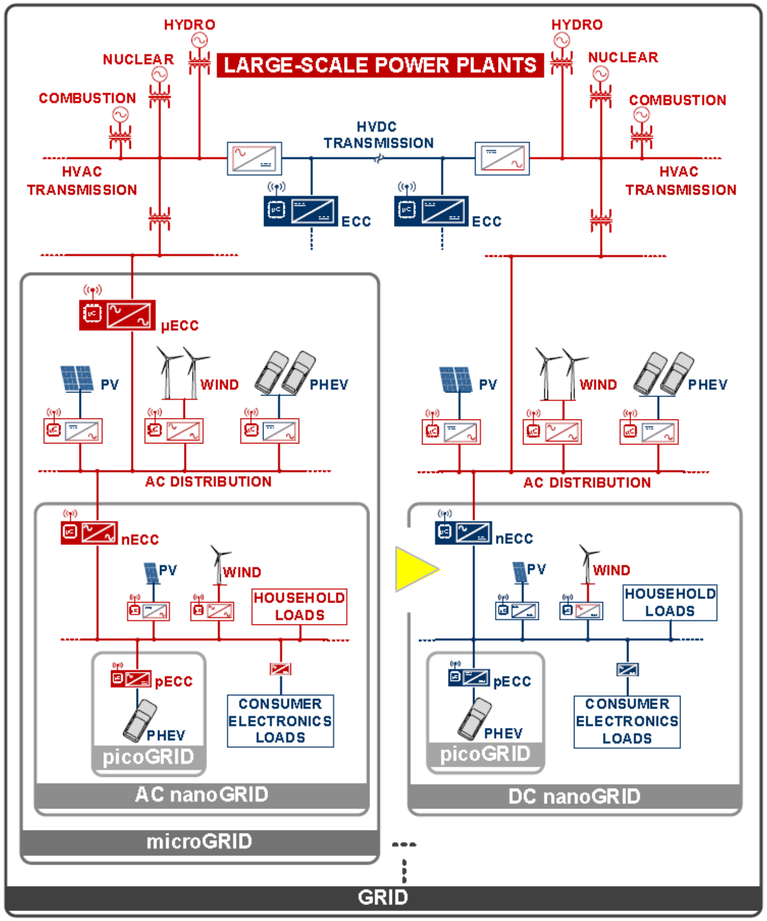

# ▶ Smart Home / Microgrid

→ **Energy Trading (Scheduling of Power Supply / Consumpt., Operating Reserves, Power Quality Services, Energy Storage / Balancing etc.; Smart Meters**

→ **Smart Picogrid (Smart Homes, Smart Buildings etc.)**

Source: P. Tenti ECPE Workshop 03/2013

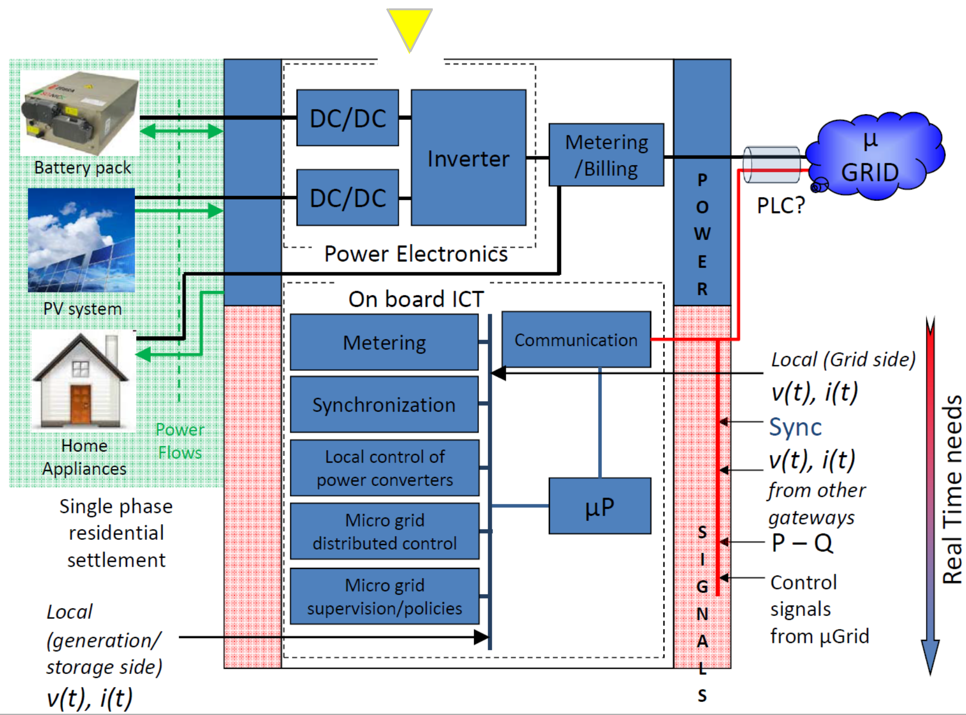


**Energy Gateway – Functional diagram**

■ **Distributed Control of Power Electronic Interfaces in Smart Picogrids**

# EV Charging

- Charging Levels
- AC/DC Power Conversion Partitioning
- Operating Range of 3-Φ PFC Rectifier Systems

# Electrical Ratings of EV Chargers

▶ SAE J1772 Definition (USA)

- AC Level 1: 120 V, 16 A → 1.92 kW
- AC Level 2: 204-240 V, 80 A → 19.2 kW
- AC Level 3: n/a → ≥ 20 kW

- DC Level 1: 200-450 V, 80 A → 36 kW
- DC Level 2: 200-450 V, 200 A → 90 kW
- DC Level 3: 200-600 V, 400 A → 240 kW

▶ IEC 62196 Definition (Europe, Int.)

- Mode 1: 1x230 V / 3x400 V, 16 A → 7.68 kW
- Mode 2: 1x230 V / 3x400 V, 32 A → 15.36 kW
- Mode 3: 3x400 V, 32-250 A → ≥ 20 kW

- Mode 4: ≤ 1000 V, 400 A (DC) → 240 kW

▲ SAE J1772 Combo Connector for AC or DC (Level 1-2)

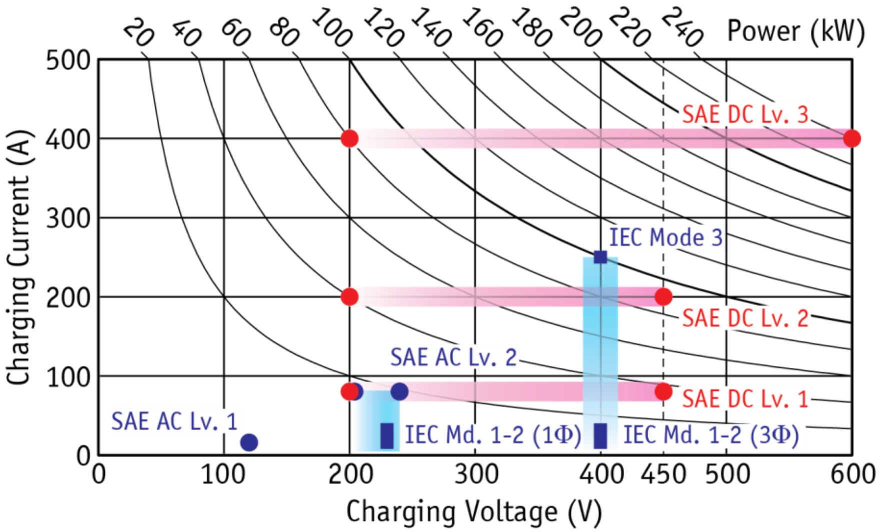

# EV Battery Charging – Requirements

- **Plug-in Hybrid EV (Toyota Prius)**
  - 23 km El. Range @ 4.4 kWh Capacity
  - Battery Voltage: 200 V
  - Charging Time: 2.5 h (L2, 3.8 kW)

- **Passenger EV (Nissan Leaf)**
  - 200 km Range @ 24 kWh Capacity
  - Battery Voltage: 360 V
  - Charging Time: 6-8 h (L2, 3.3 kW)
    0.5 h (L3, 50 kW)

- **Electric Passenger Bus (TOSA 2013)**
  - 19 m / 133 Passengers
  - 40 kWh Battery Capacity
  - Charging: 15 sec @ 400 kW
    3-4 min @ 200 kW

# EV Charging – Basic Power Electronics Topologies (1)

## ■ Basic Requirements

- Wide Input/Output Voltage Range – Voltage Adaption
- Mains Side Sinusoidal Current Shaping
- Isolation of Mains and Battery (?)
- Output Battery Current Control
- Maintainability (No Inverter/Motor Integration)

## ■ Basic Topologies

- Non-Isolated
- Isolated Single-Stage (Matrix-Type)
- Isolated Two-Stage

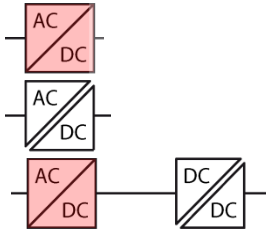


- Battery could Integrate a DC/DC Conv. & Communication Interface (Monitoring, Distributed Control) – *SMART Battery*

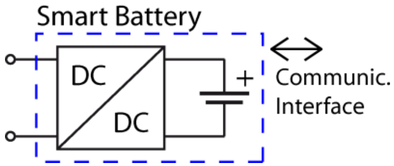

# Remark: 3-Φ Rectifier Common-Mode Output Voltage

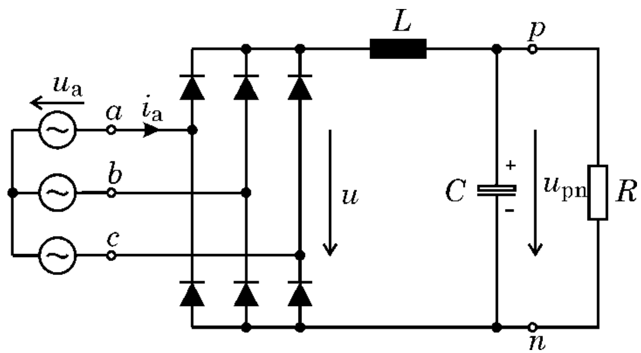


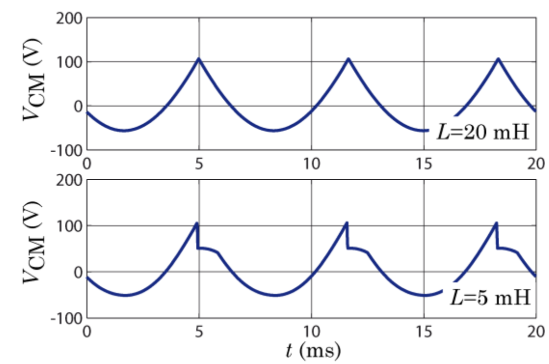


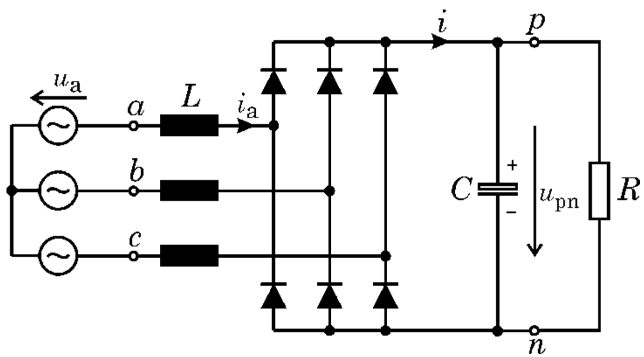


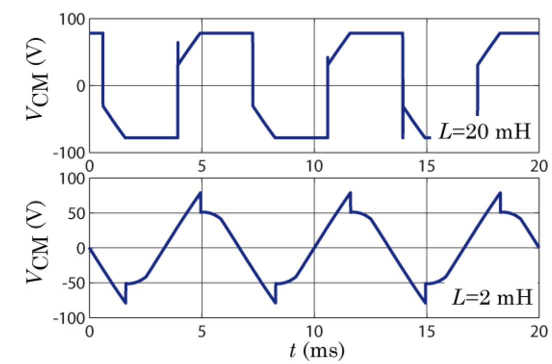


- Output shows Low-Frequency Common Mode Voltage;
- Load/Battery Cannot be Connected to Ground (Isolation Required)

# EV Charging – AC/DC Power Conversion Partitioning

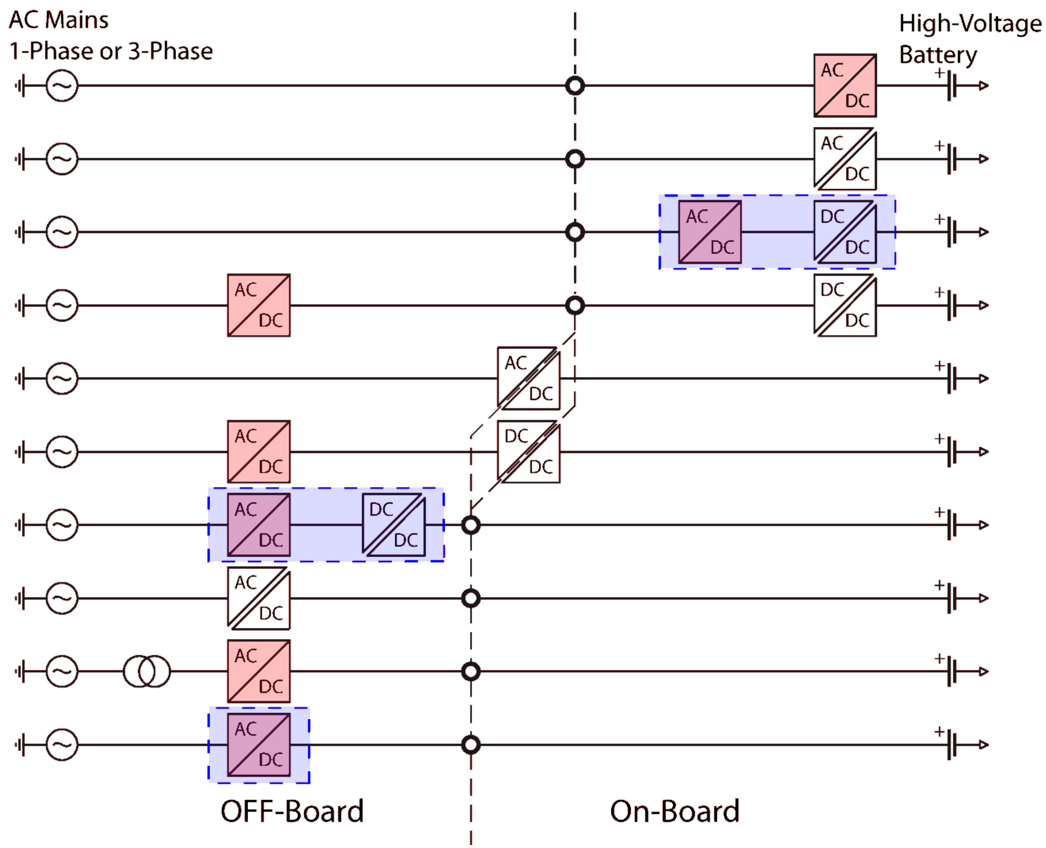


- - - - Standard Solutions

# Operating Range of 3-Φ PFC Rectifier Systems

- Boost Type
- Buck Type

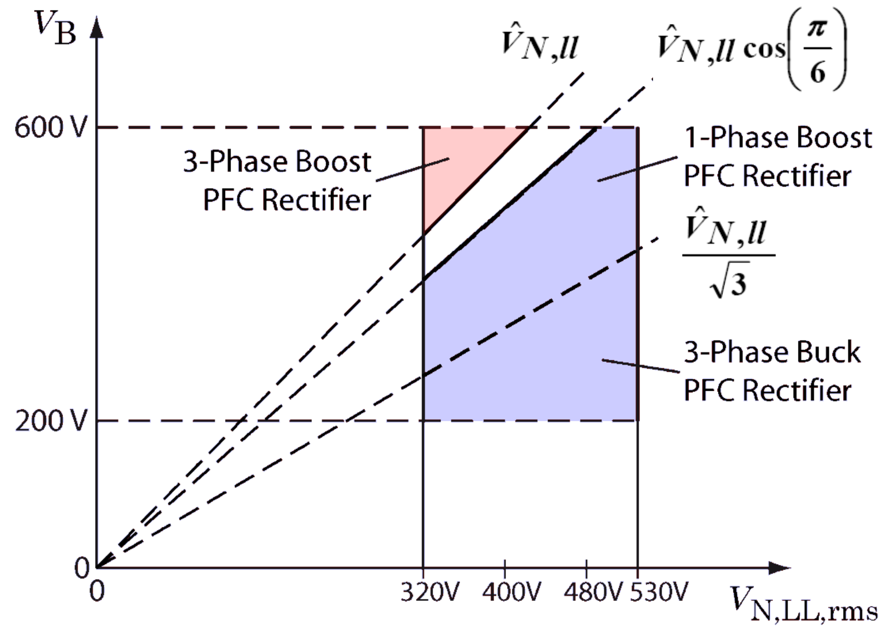


$V_B$ ........... Battery Voltage
$V_{N,ll,rms}$ ... RMS Value of Mains Line-to-Line Voltage

# Potential Ancillary Grid Services of EV Chargers / EVs

- Peak Power / Failure Mode Grid Support - Utilizes Storage of Charging Station / EVs
- Reactive Power Compensation / Supply - No Storage Required / No Battery Wearout
- Active Filtering of Grid Side Harmonics - No Storage Required / No Battery Wearout

- Bi-Directional Grid Interface Required
- Grid-Code / Standardization Required
- Economic Models Need to be Developed

**J. W. Kolar, T. Friedli,**
*The Essence of Three-Phase PFC Rectifier Systems - Part I*, IEEE Transactions on Power Electronics, Vol. 28, No. 1, pp. 176-198, January 2013.

**T. Friedli, M. Hartmann, J. W. Kolar,**
*The Essence of Three-Phase PFC Rectifier Systems - Part II*, IEEE Transactions on Power Electronics, Vol. 29, No. 2, February 2014.

# Boost-Type 3-Φ PFC Rectifier Systems

– **Unidirectional**
– **Bidirectional**

# ▶ Classification of Unidirectional Rectifier Systems

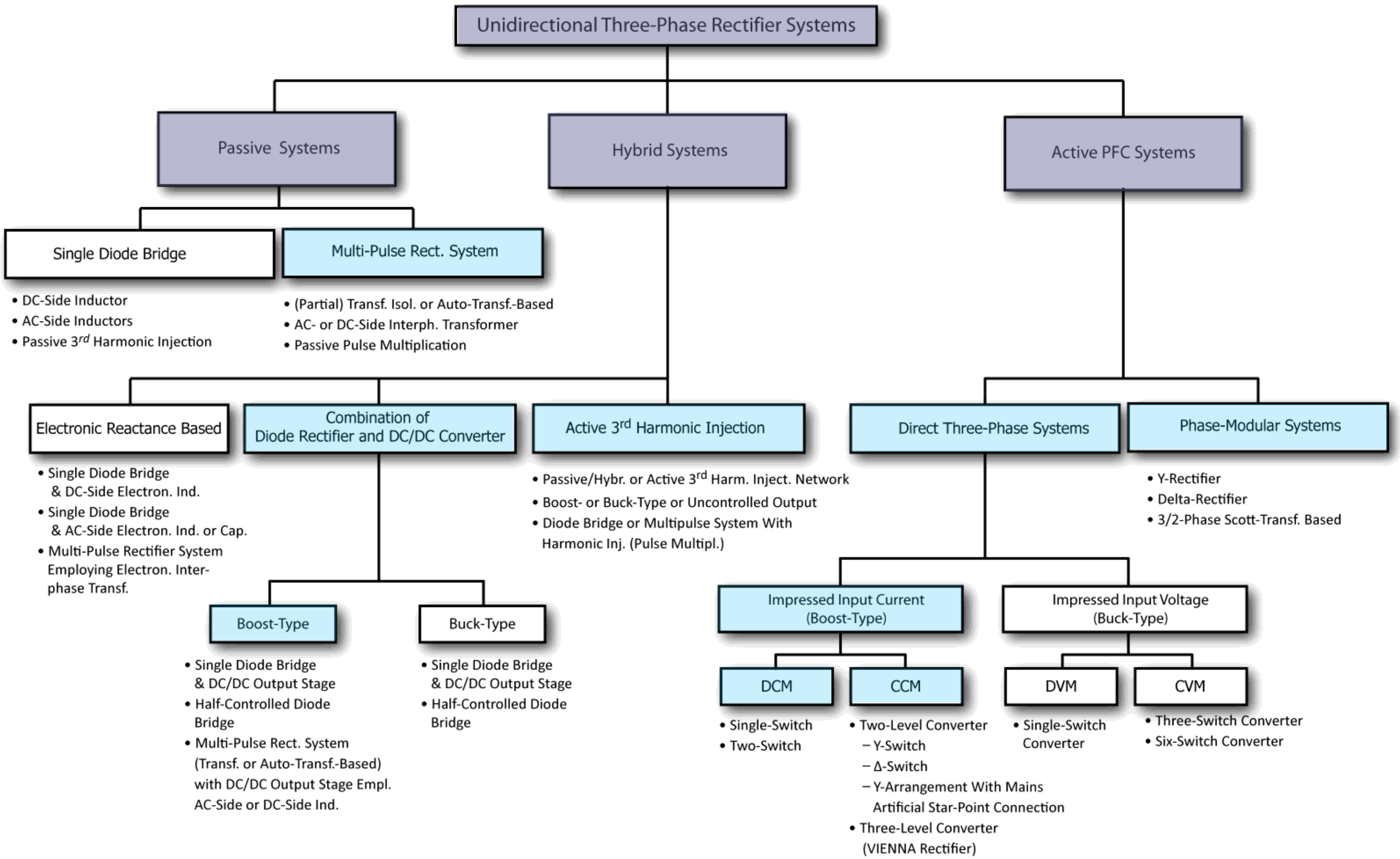

# ▶ Classification of Unidirectional Rectifier Systems

- **Passive Rectifier Systems**
  - Line Commutated Diode Bridge/Thyristor Bridge - Full/Half Controlled
  - Low Frequency Output Capacitor for DC Voltage Smoothing
  - Only Low Frequency Passive Components Employed for Current Shaping, No Active Current Control
  - No Active Output Voltage Control
- **Hybrid Rectifier Systems**
  - Low Frequency and Switching Frequency Passive Components and/or
  - Mains Commutation (Diode/Thyristor Bridge - Full/Half Controlled) and/or Forced Commutation
  - Partly Only Current Shaping/Control and/or Only Output Voltage Control
  - Partly Featuring Purely Sinusoidal Mains Current
- **Active Rectifier Systems**
  - Controlled Output Voltage
  - Controlled (Sinusoidal) Input Current
  - Only Forced Commutations / Switching Frequ. Passive Components

■ **Phase-Modular Systems**
- Phase Rectifier Modules of Identical Structure
- Phase Modules connected in Star or in Delta
- Formation of Three Independent Controlled DC Output Voltages

■ **Direct Three-Phase Syst.**
- Only One Common Output Voltage for All Phases
- Symmetrical Structure of the Phase Legs
- Phase (and/or Bridge-)Legs Connected either in Star or Delta

# Phase-Modular Systems

*Y-Rectifier*
*Δ-Rectifier*

# ▶ Classification of Unidirectional Rectifier Systems

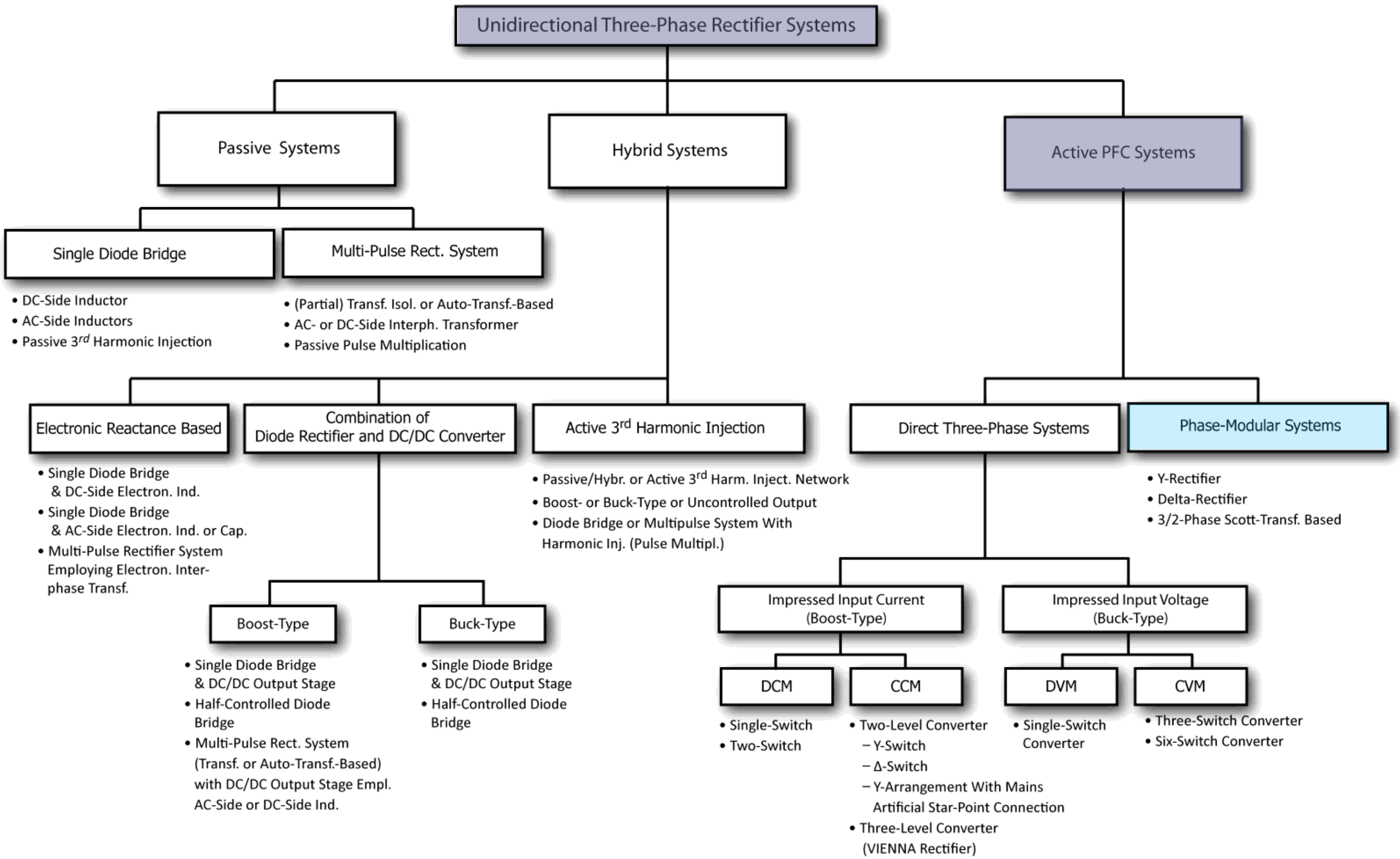

# 1-Φ PFC Rectifier Topologies

► **Three Basic Topologies**

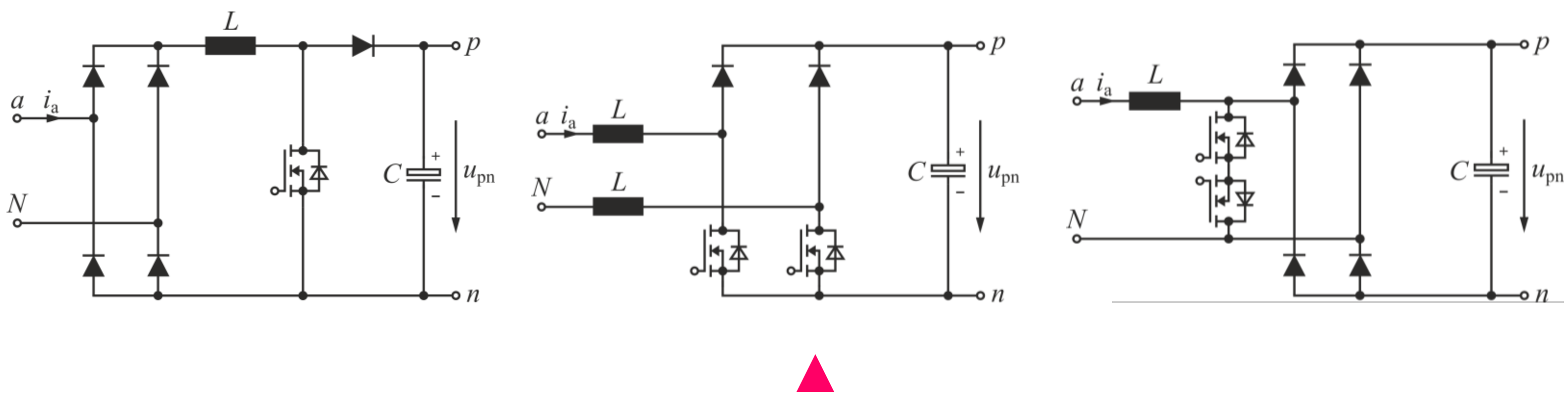


- **For High Efficiency Systems the "Bridgeless" Concept has been Paid High Attention**
- **Focus has Shifted to the *Extended* Bridgeless Converter featuring ZVS TCM Operation**

# Zero Voltage Switching – Triangular Current Mode (TCM) Operation

- Synchronous Rectification
- Negative Current Ensures ZVS

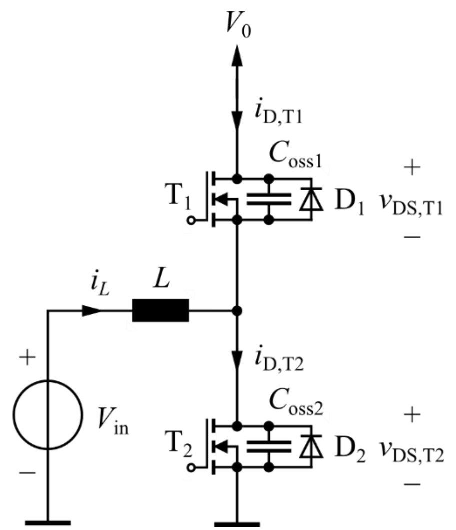


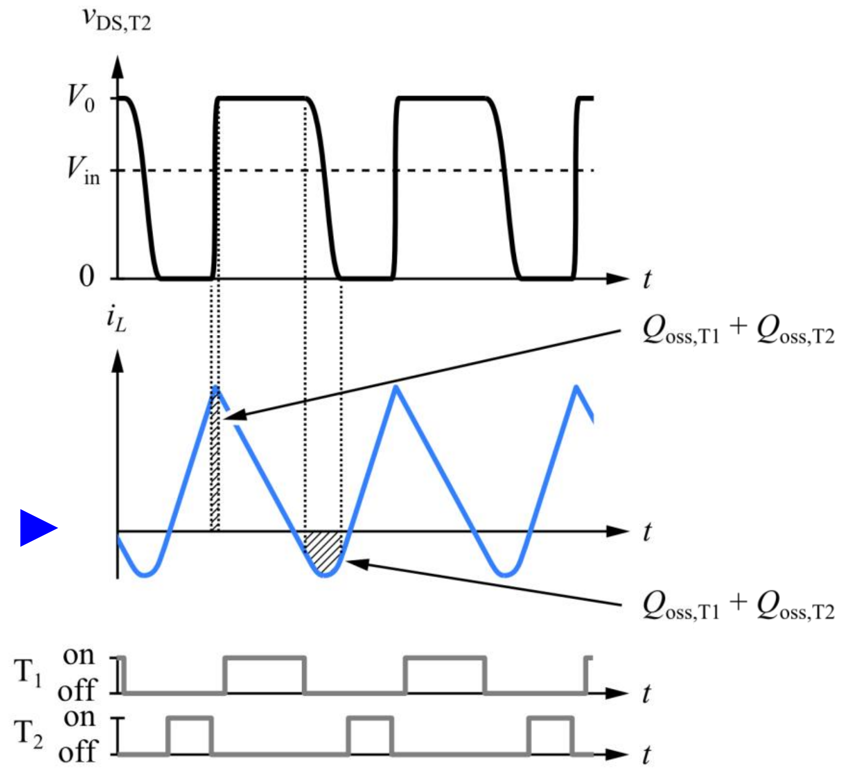

# ▶ Ultra-Efficient 1-Φ TCM Boost-Type PFC Rectifier

★ **99.36% @ 1.2kW/dm³**

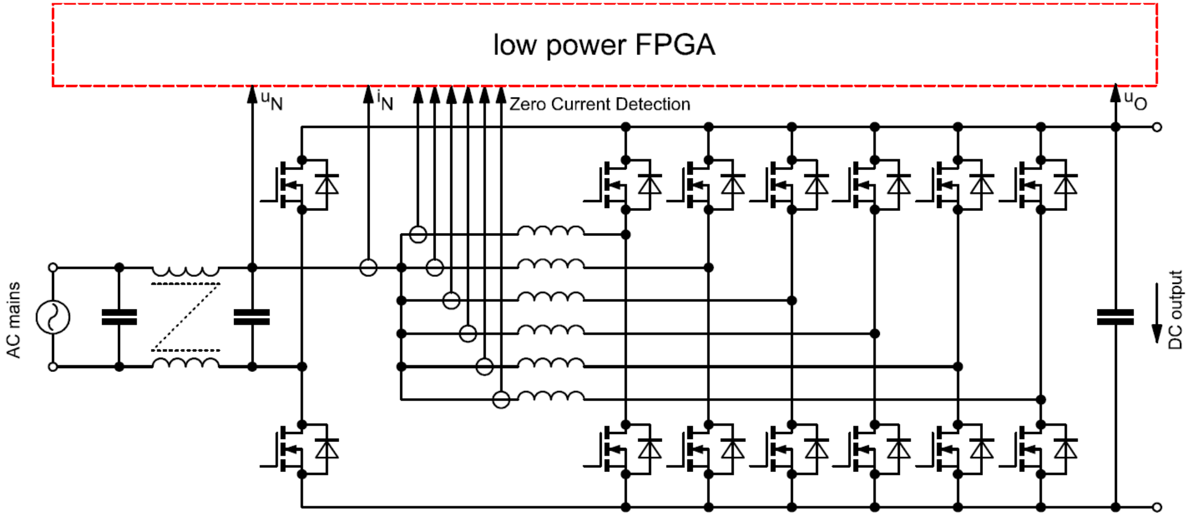


- **Bidirectional – Supports V2G Concepts**
- **Employs NO SiC Power Semiconductors -- Si SJ MOSFETs only**

# ▶ Ultra-Efficient 1-Φ TCM Boost-Type PFC Rectifier

★ **99.36% @ 1.2kW/dm³**

Research Project of ETH Zurich Supported
by European Center for Power Electronics

- **Bidirectional – Supports V2G Concepts**
- **Employs NO SiC Power Semiconductors -- Si SJ MOSFETs only**

# ► Ultra-Compact 1-Φ TCM Boost-Type PFC Rectifier

- Input Voltage 184...264$V_{AC}$
- Output Voltage 420$V_{DC}$
- Rated Power 3.3kW

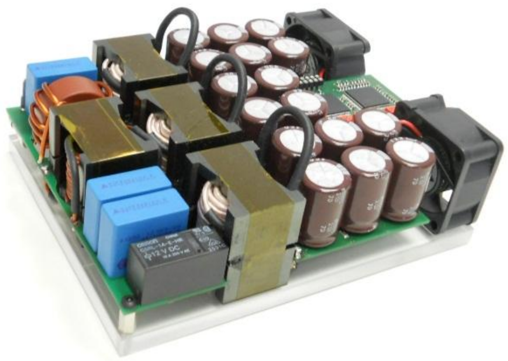

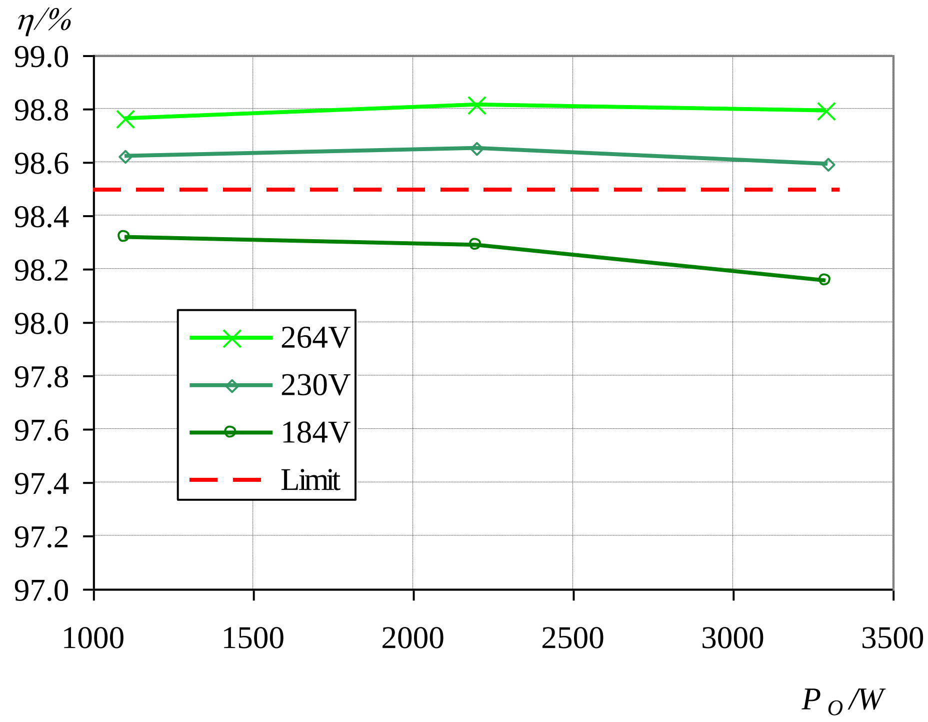


★ 98.6% @ 4.5kW/dm³

# ▶ KEYS Benefits of the TCM Concept

– Very High Performance Despite Using "Old" Si-Technology

- Only Basic Topology Employed
- ZVS Achieved by Only Modifying Operation Mode
- Active ZVS
- Triangular Current Mode (TCM)
- Variable Switching Frequency
- No Diode On-State Voltage Drop
- Continuously Guided u, i Waveforms
- Interleaving
- Utilization of Low Superjunct. $R_{DS,(on)}$
- Utilization of Digital Signal Processing

- Low Complexity
- No Aux. Circuits
- No (Low) Switching Losses
- No Direct Limit of # of Parallel Trans.
- Simple Symm. of Loading of Modules
- No Current Sensor (only i=0 Detection)
- Spread & Lower Ampl. EMI Noise
- Synchr. Rectification
- No Free Ringing → Low EMI Filter Vol.
- Low EMI Filter Vol. & Cap. Curr. Stress
- Low Cond. Losses despite TCM
- Low Control Effort despite 6x Interl.

... the Basic Concept is Known since 1989 (!)

# Y -Rectifier
# Δ-Rectifier

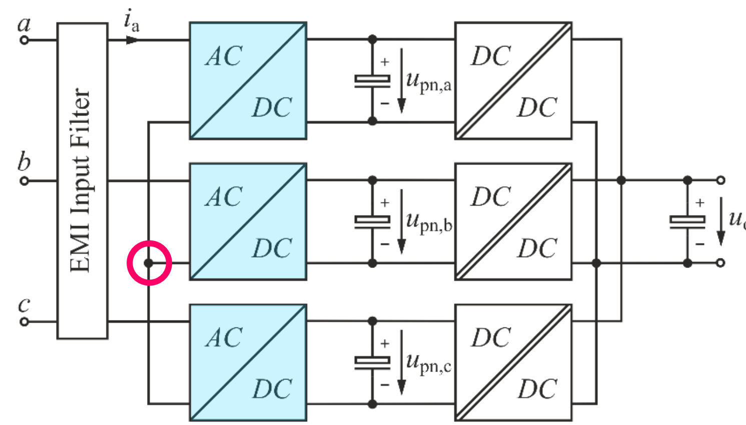


- Active Balancing of Phase Modules
- High Semiconductor Voltage Stress

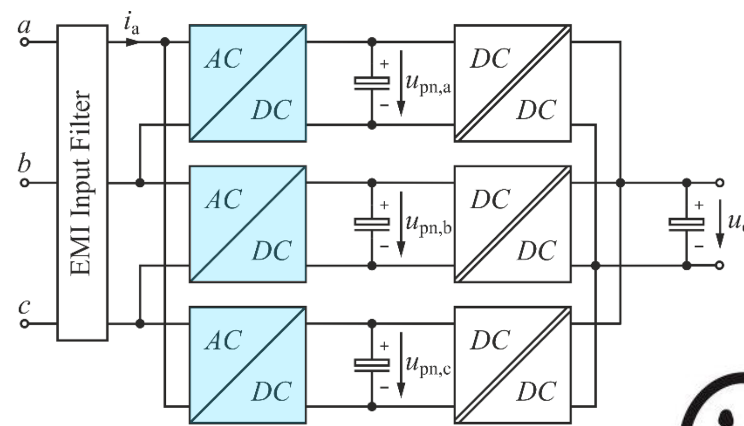


- Δ-Rectifier Clearly Preferable
- Y-Δ Reconfiguration allows to Cover Wide Input Voltage

# Y-Rectifier

## ■ 2/3-Control → Symm. AC Currents also for Unequal Loading of the DC Outputs

- Symmetric Loading $P_a = P_b = P_c = 1000$ W
- Asymmetric Loadng $P_a = 730$ W, $P_b = P_c = 1000$ W

Symm. Loading　　Asymm. Loading

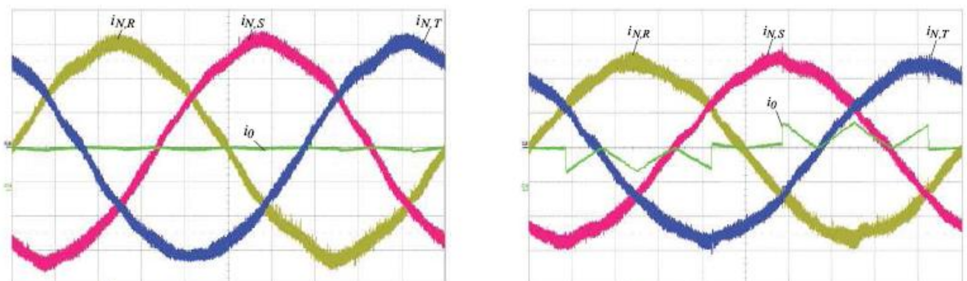


$U_N = 3 \times 230$ V (50 Hz)
$P_o = 3 \times 1$ kW
$U_o = 400$ V
$f_s = 58$ kHz
$L = 2.8$ mH (on AC-side)
$C = 660$ µF

Input Phase Currents, Control Signal $i_0$, Output Voltages

$i_{N,i}$: 1 A/div
$V_{DC,i}$: 100 V/div

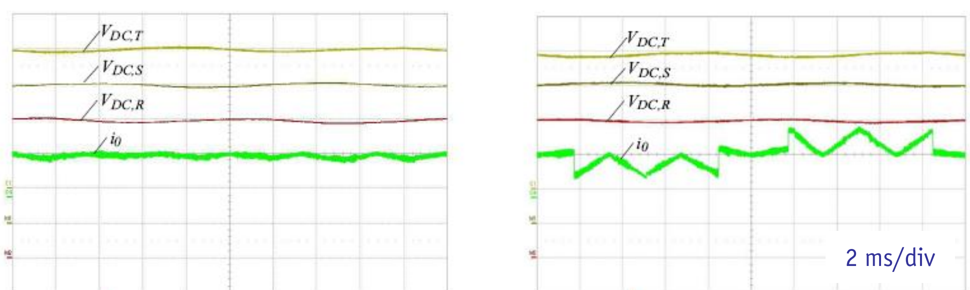

# Δ-Rectifier

## ■ Experimental Results

**$U_{LL}$ = 3 x 480 V (50 Hz)**
**$P_o$ = 5 kW**
**$U_o$ = 800 V**
**$f_s$ = 25 kHz**
**$L$ = 2.1 mH (on AC-Side)**

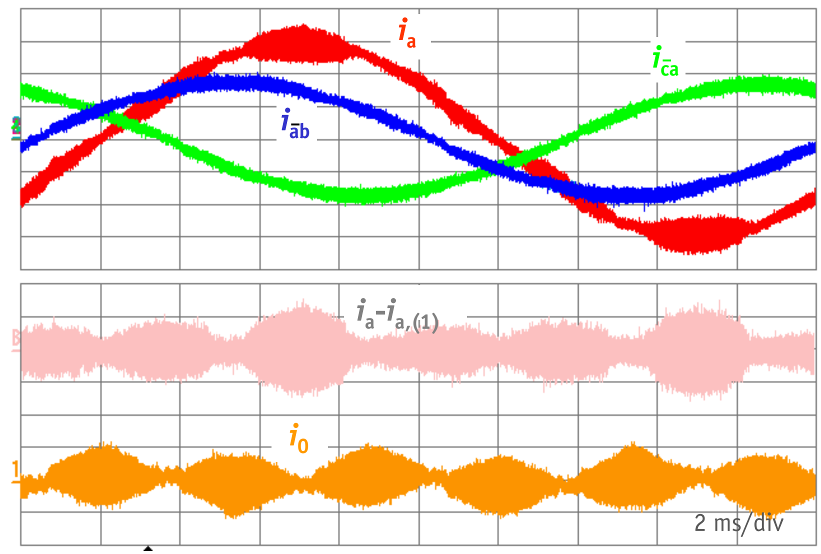


$i_a$, $i_{\bar{a}b}$, $i_{\bar{c}a}$: 5 A/div; $i_a - i_{a,(1)}$, $i_0$: 2 A/div

**- Formation of Input Phase Current** $i_a = i_{\bar{a}b} - i_{\bar{c}a}$
**- Circulating Zero Sequence Current** $i_0$

# Hybrid 3-Φ Boost-Type PFC Rectifier Systems

*3rd Harmonic Injection Rectifier*
*Active Filter-Type Rectifier*

# ▶ Classification of Unidirectional Rectifier Systems

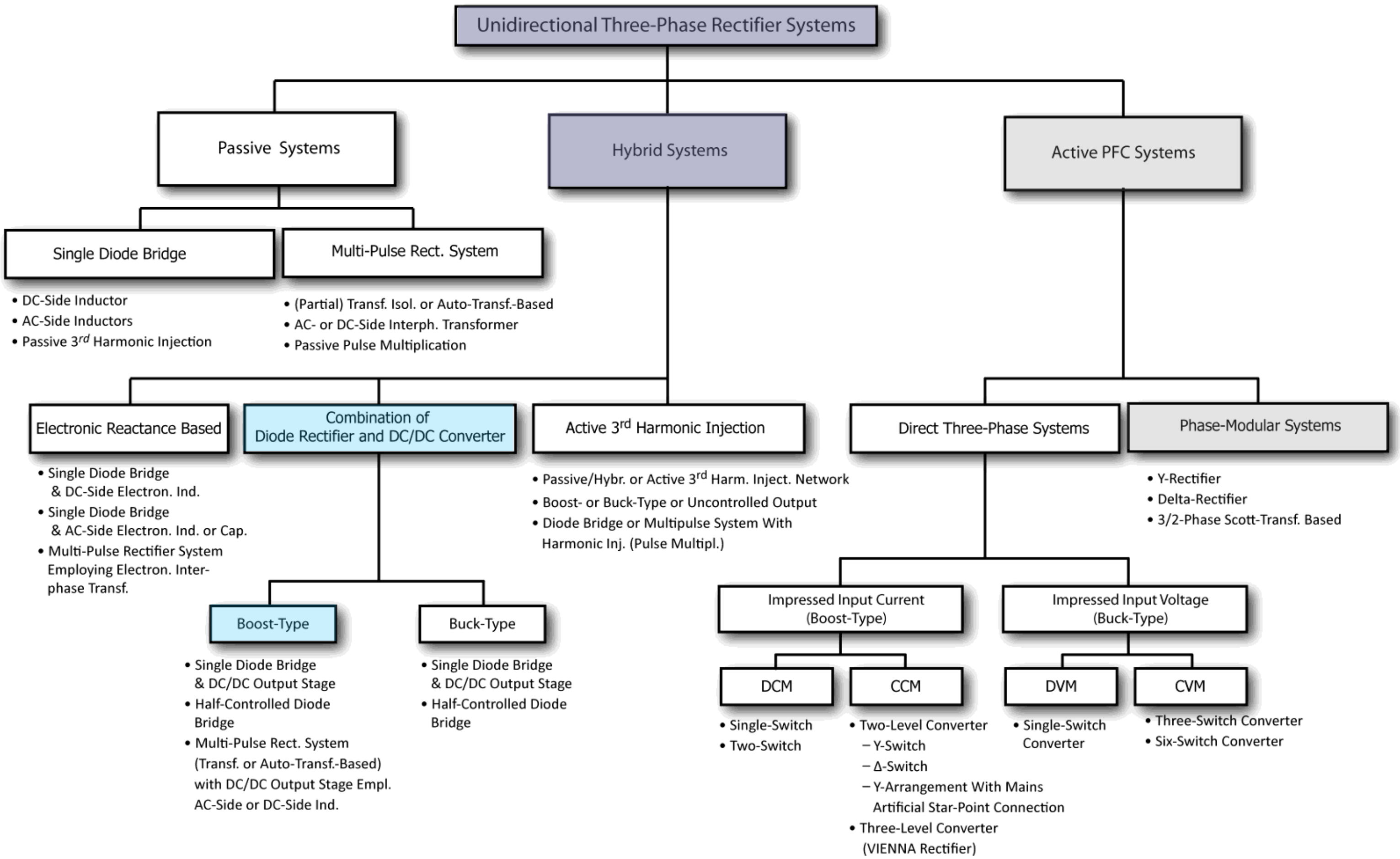

# Diode Bridge + DC/DC Boost Converter

- Controllable Output Voltage
- Low-Frequency Mains Current Distortion

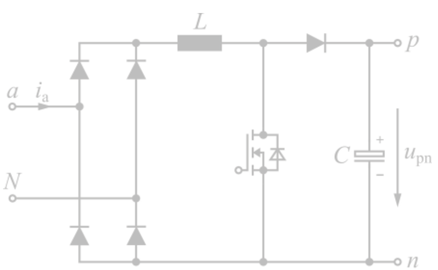


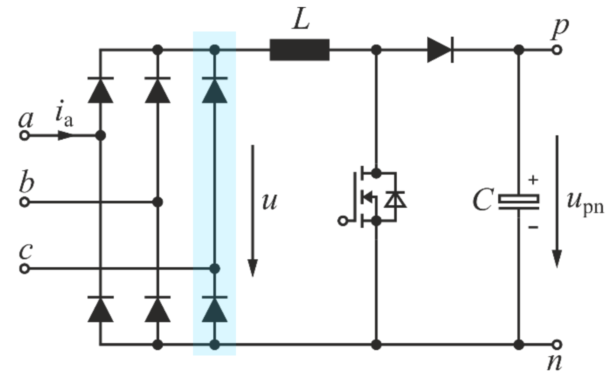


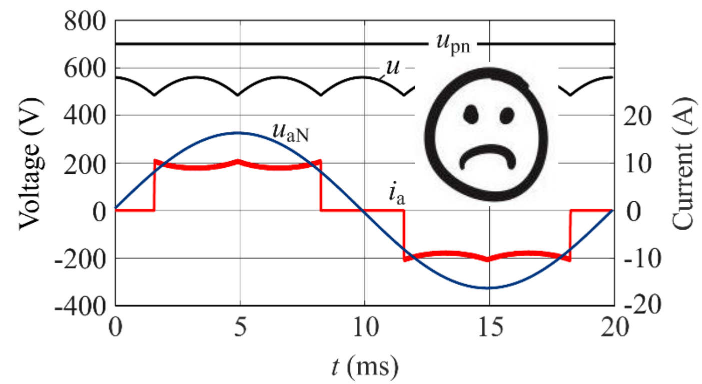

# 3-Φ DCM (PFC) Boost Rectifier

- Controllable Output Voltage
- Low-Frequency Mains Current Distortion

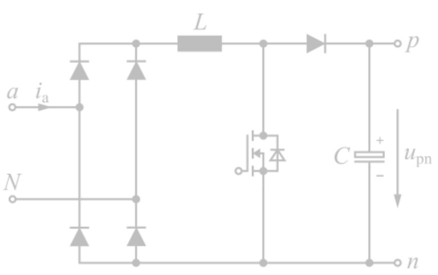


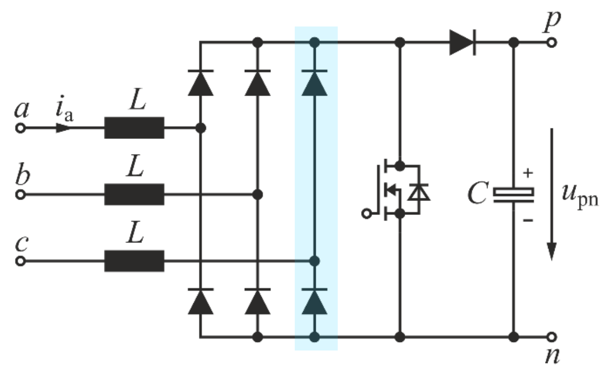


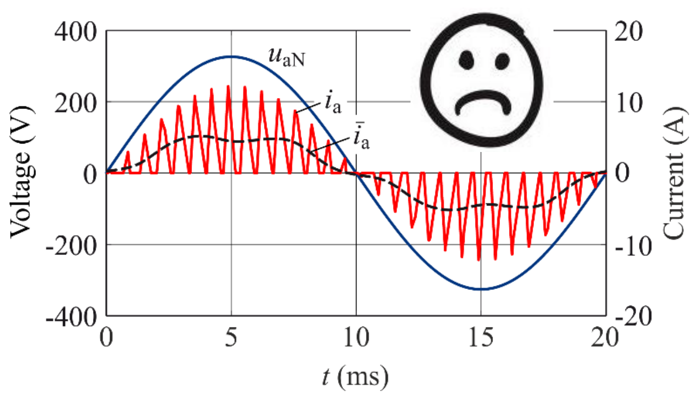

# ▶ Classification of Unidirectional Rectifier Systems

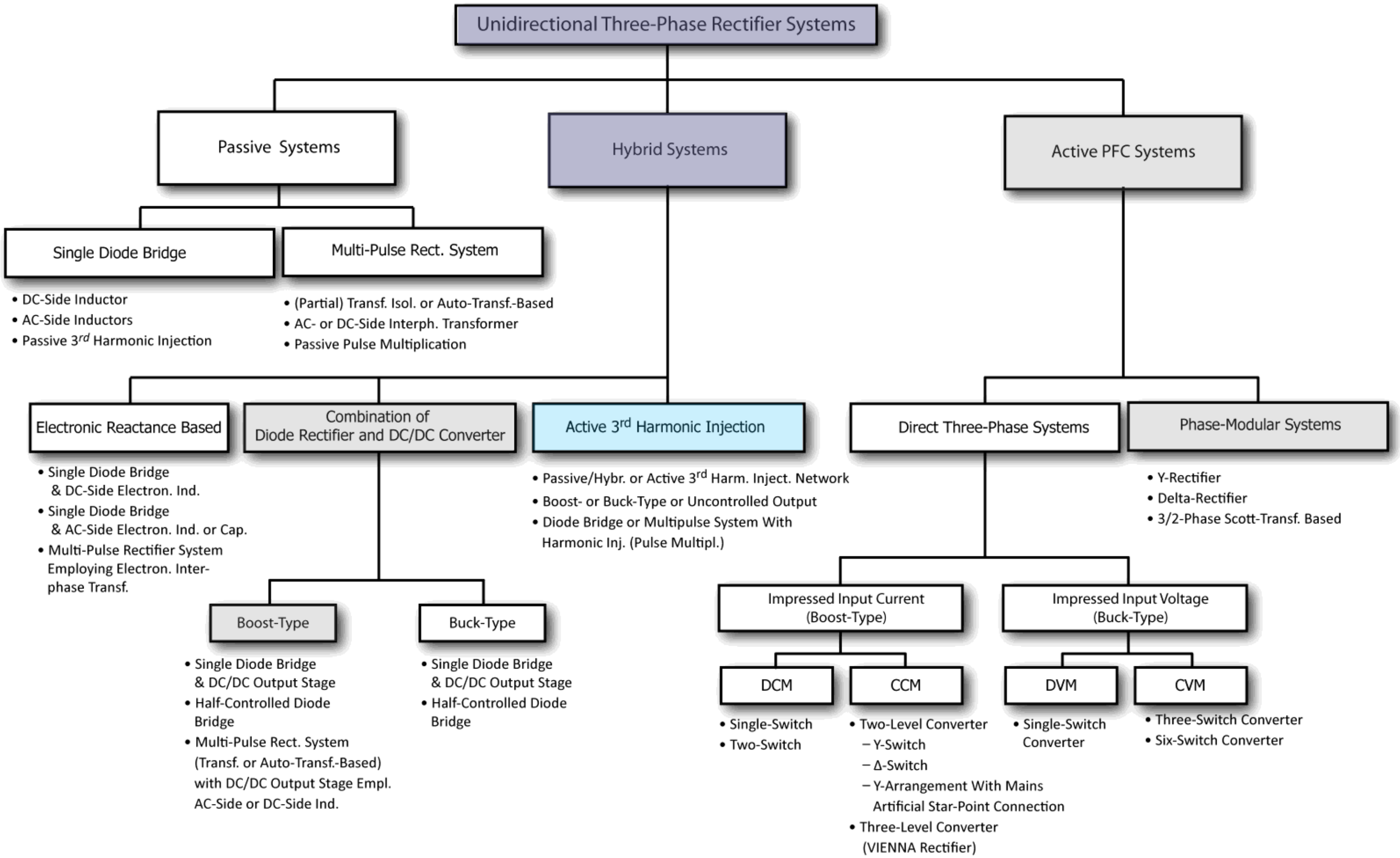

# 3-Φ Hybrid 3rd Harmonic Inj. PFC Boost-Rectifier

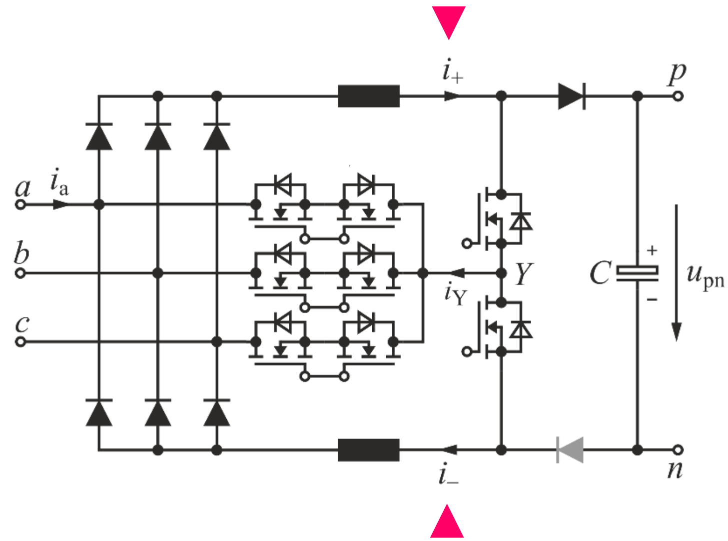


- **Independent Control of *i*+ and *i*-**

# 3-Φ Hybrid 3rd Harmonic Inj. PFC Boost-Rectifier

$i_+ = G \cdot u_a$

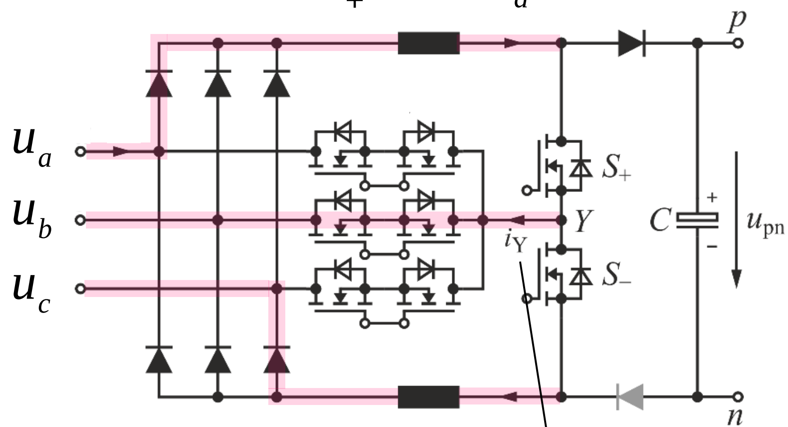


$i_- = G \cdot u_c$

$i_b = -G(u_a + u_c) = G \cdot u_b$

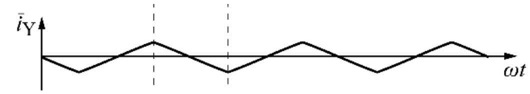


- **Sinusoidal Control of *i+* and *i-* and $i_Y$**

# 3-Φ Hybrid 3rd Harmonic Inj. PFC Boost-Rectifier

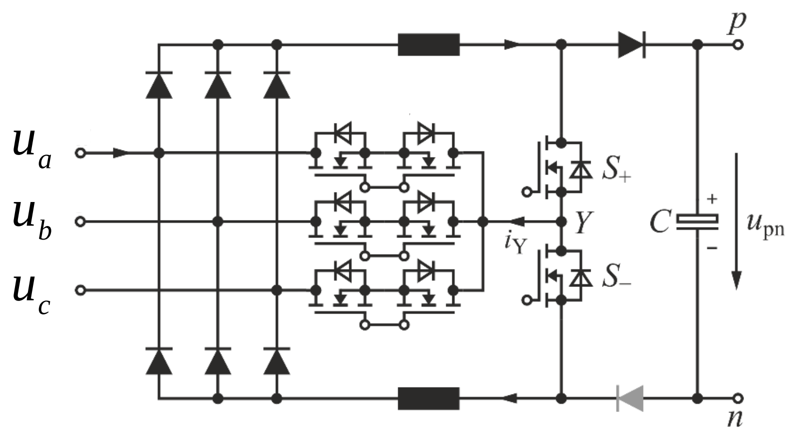


- Sinusoidal Mains Current Control → Limited to Ohmic Mains Behavior
- Output Voltage Control → High Minimum Output Voltage Level

# Remark #1 Alternative Active 3rd Harmonic Injection

- *No Output Voltage Control*
- Mains Current Close to Sinusoidal Shape

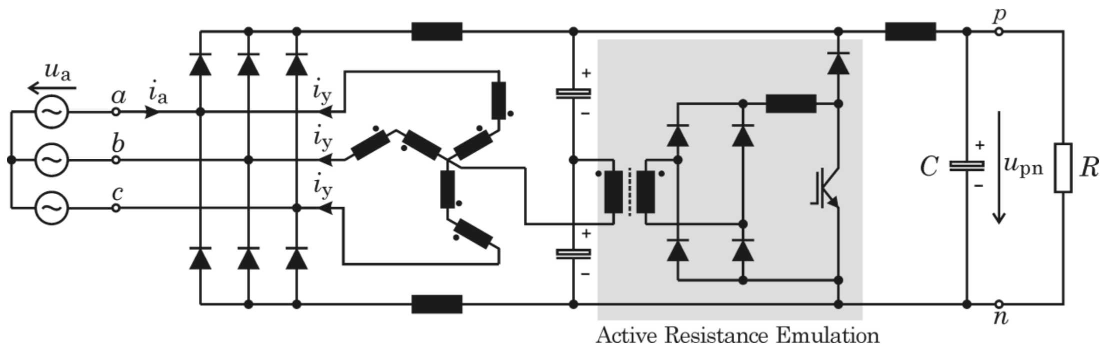


- Controlled Output Voltage
- Purely Sinusoidal Shape of Mains Current

e.g.: $i_1 = I + 3/2\, i_y$
$i_2 = I - 3/2\, i_y$

CCL: $3i_y = i_1 - i_2$

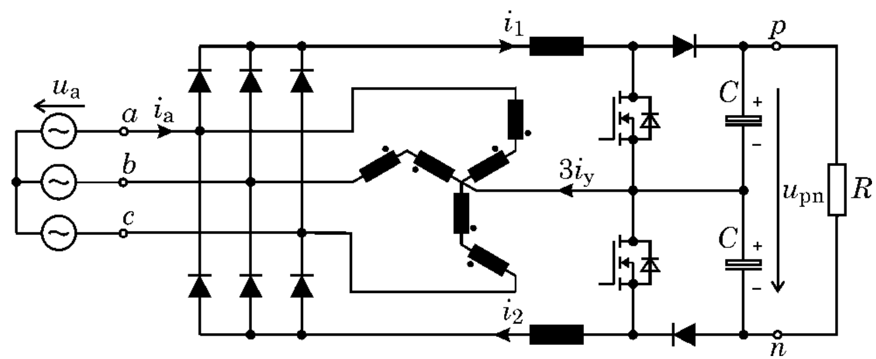


- Injection Into All Phases
- Bulky Passive (Low-Frequency) Injection Device

▲
*Minnesota Rectifier*

# – Active 3rd Harmonic Injection into All Phases

$\omega t \in \left[0, \frac{\pi}{3}\right]$

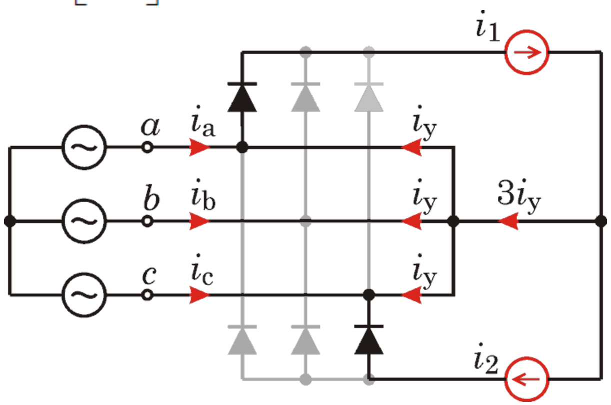


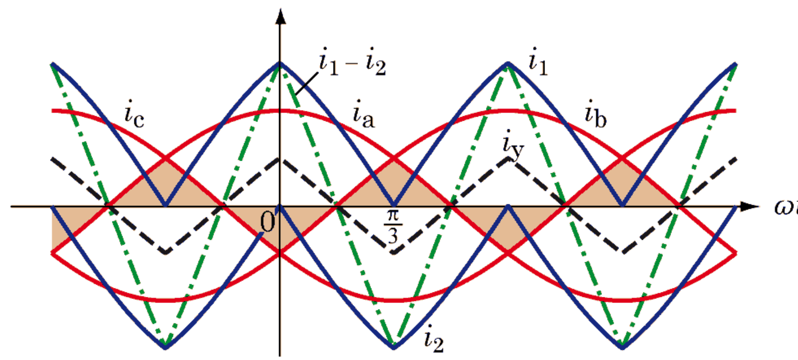


$$i_a = \hat{I}\cos(\omega t)$$
$$i_b = \hat{I}\cos\left(\omega t - \frac{2\pi}{3}\right)$$
$$i_c = \hat{I}\cos\left(\omega t + \frac{2\pi}{3}\right)$$

$$i_y = -i_b$$
$$i_1 = i_a + i_y$$
$$i_2 = -(i_c + i_y)$$

$$i_a + i_b + i_c = 0$$
$$i_1 - i_2 = i_a + i_y + i_c + i_y =$$
$$= -i_b + 2i_y = 3i_y$$

- **Current Control Implementation with Boost-Type DC/DC Converter (*Minnesota Rectifier*) or with Buck-Type Topology (!)**

# Remark #2 — Purely Passive 3rd Harmonic Injection

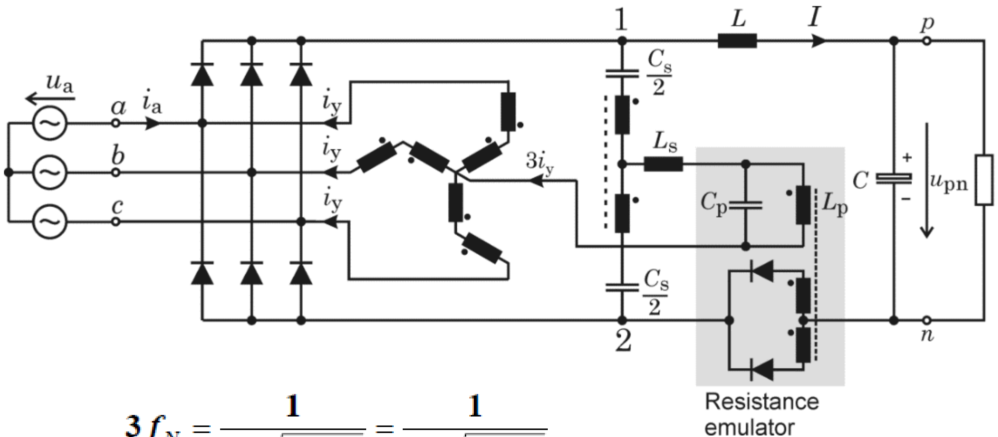


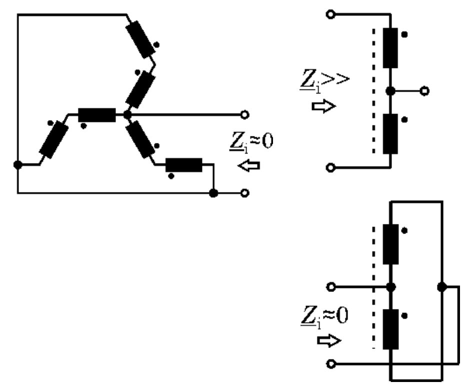


$$3 f_N = \frac{1}{2\pi\sqrt{L_S C_S}} = \frac{1}{2\pi\sqrt{L_p C_p}}$$

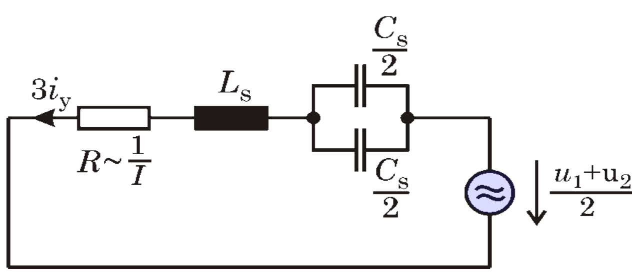


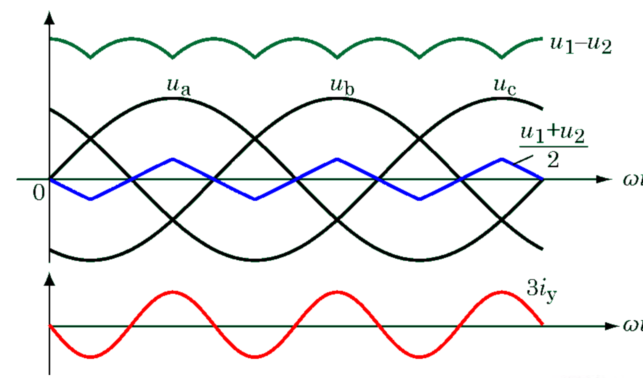


- No Output Voltage Control
- Bulky Passive (Low-Frequency) Injection Device

# Remark #2

# Purely Passive 3rd Harmonic Injection

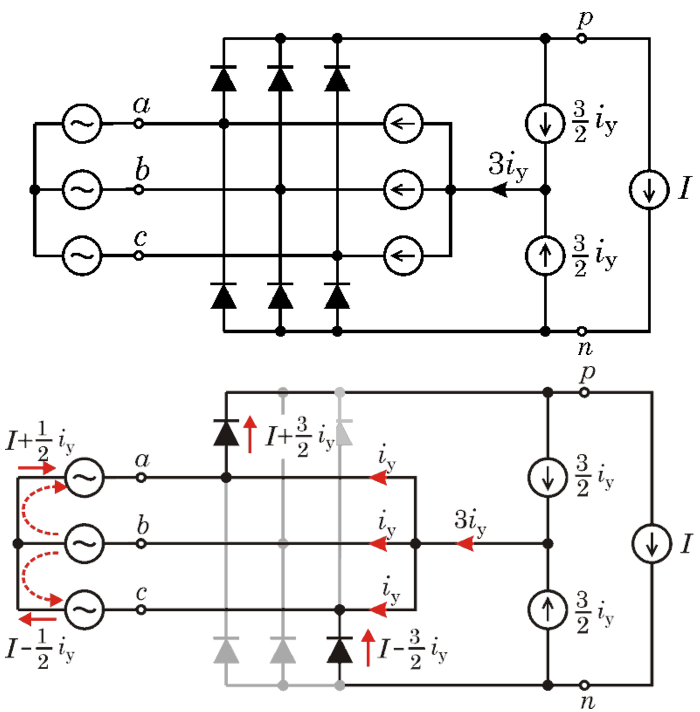


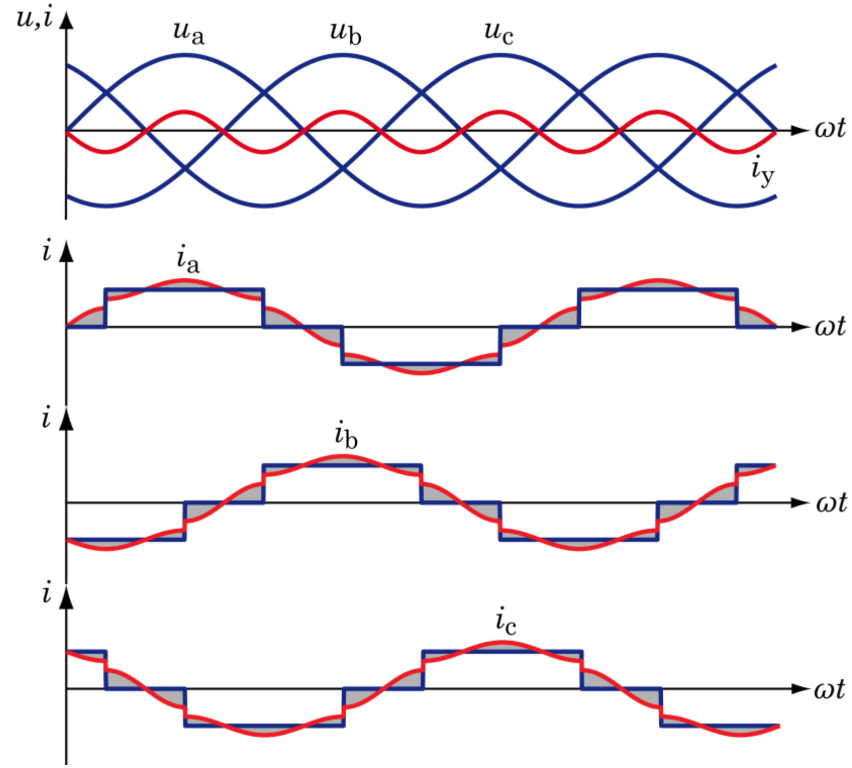


- **Minimum THD of Phase Current for $i_y = 1/2\ I$**
- **$THD_{min} = 5\ \%$**

# 3-Φ Active Filter Type PFC Rectifier

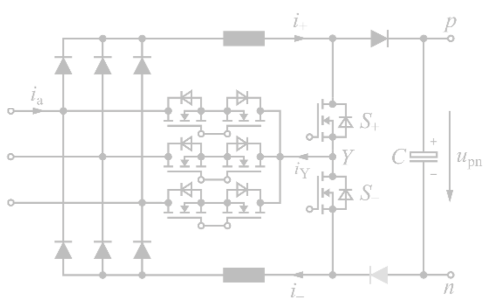


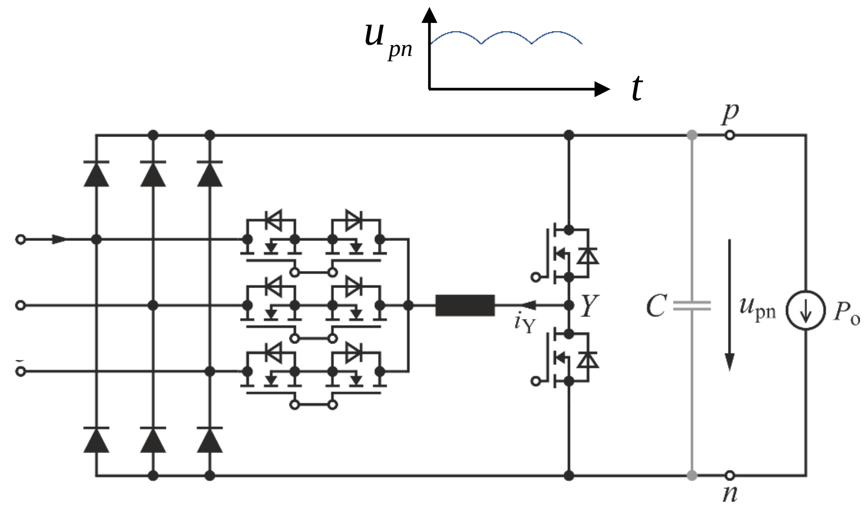


- Sinusoidal Mains Current

→ Requires Constant Power Load $P_0$= const.
→ *NO* (!) *Output Voltage Control*

# 3-Φ Active Filter Type PFC Rectifier

- ***$T_+$, $T_-$* Could be Replaced by Passive Network**

$$\omega t \in \left[0, \frac{\pi}{3}\right]$$

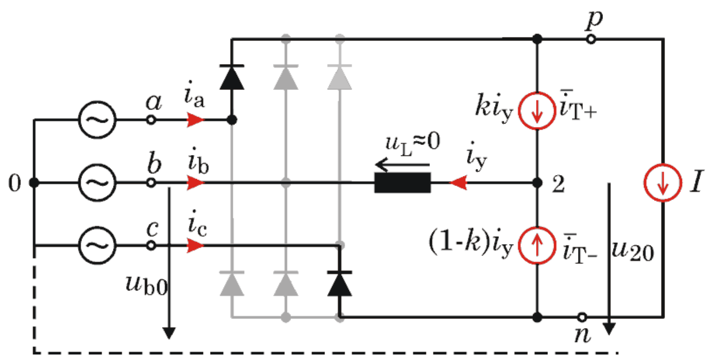


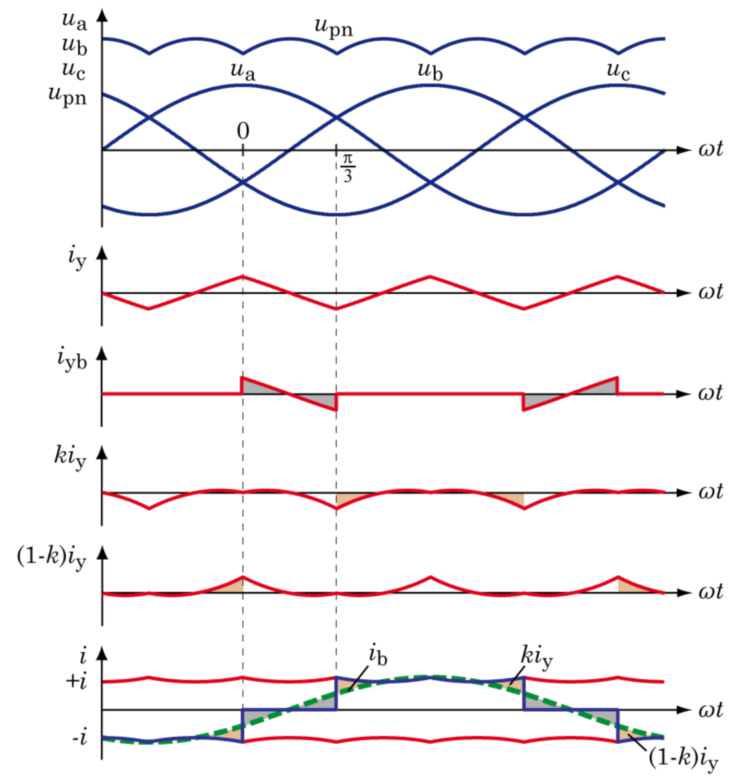

## Proof of Sinusoidal Mains Current Shape for $\omega t \in \left[0, \frac{\pi}{3}\right]$

$$i_a = G \cdot u_{a0}$$
$$i_b = G \cdot u_{b0}$$
$$i_c = G \cdot u_{c0}$$

- Current to be Inj. into Phase *b* $\quad i_y = -i_b$

- Local Avg. Ind. Voltage / Bridge Leg ($T_+$, $T_-$) Output Voltage $\quad \bar{u}_L \approx 0$ and/or $\bar{u}_{20} = u_{b0}$

- Bridge Leg Voltage Formation

$$\bar{u}_{20} = u_{b0} = k \cdot u_{a0} + (1-k)u_{c0}$$
$$u_{b0} = k \cdot u_{ac} + u_{c0}$$
$$k = \frac{u_{bc}}{u_{ac}}$$

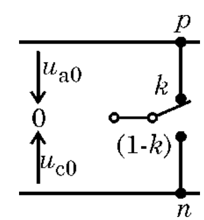


- Bridge Leg Current Formation

$$\bar{i}_{T_+} = k \cdot i_y = -k \cdot G \cdot u_{b0} = -G \cdot u_{b0} \frac{u_{bc}}{u_{ac}}$$

- Constant Power Load Current

$$i = \frac{P}{u_{ac}} = \frac{u_{ac} \cdot i_a + u_{bc} \cdot i_b}{u_{ac}}$$
$$= G \frac{u_a \cdot u_{ac} + u_b \cdot u_{bc}}{u_{ac}} = G\left( u_{a0} + u_{b0} \frac{u_{bc}}{u_{ac}} \right)$$

Condition

$$i_a + i_b + i_c = 0$$

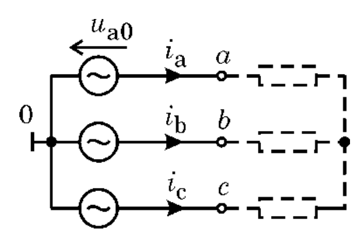


## Sinusoidal Mains Current

$$i + \bar{i}_{T_+} = G \cdot u_{a0} = i_a$$

# Remark Auto-XFRM-Based 12-Pulse Passive Rectifier Systems

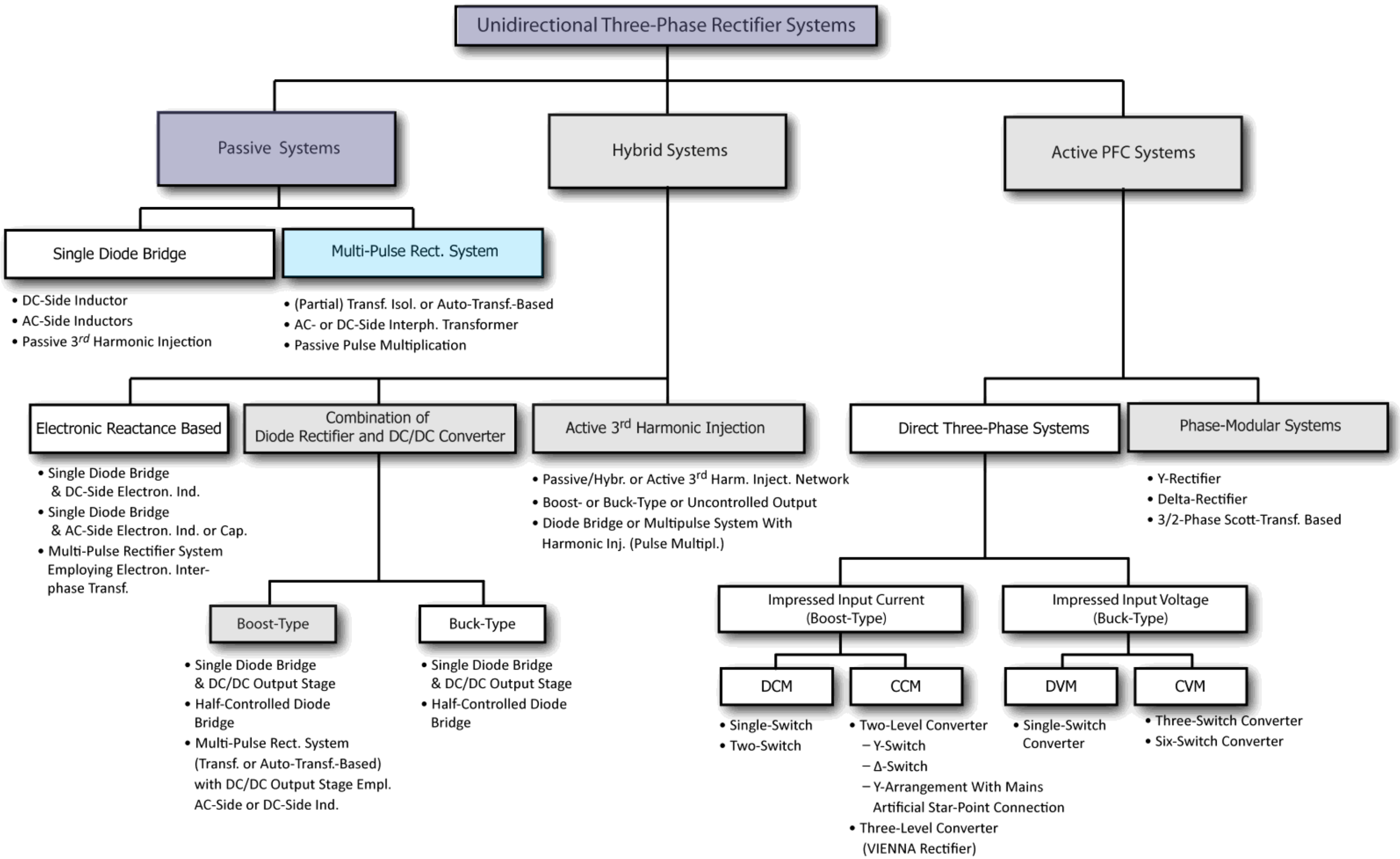

# Remark Auto-XFRM-Based 12-Pulse Passive Rectifier Systems

## ■ AC-Side Interphase-XFRM (Impr. DC Voltage)

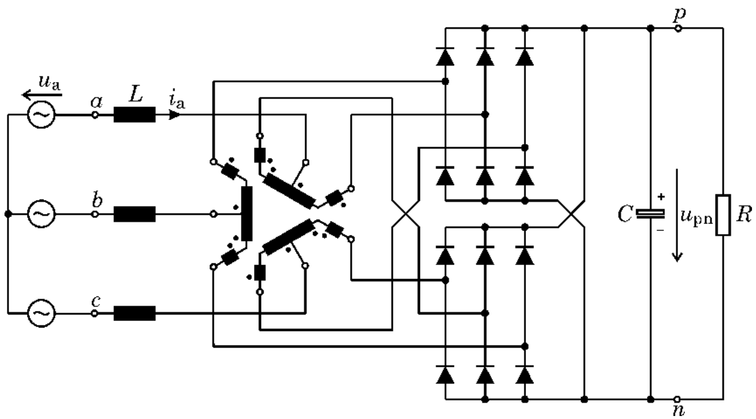


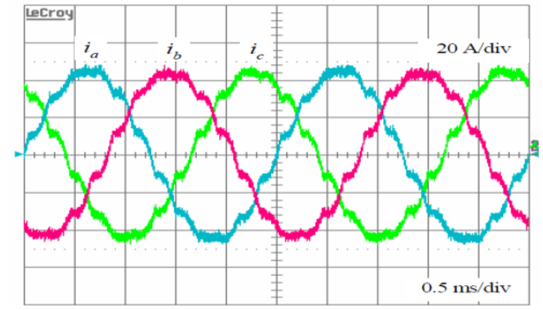


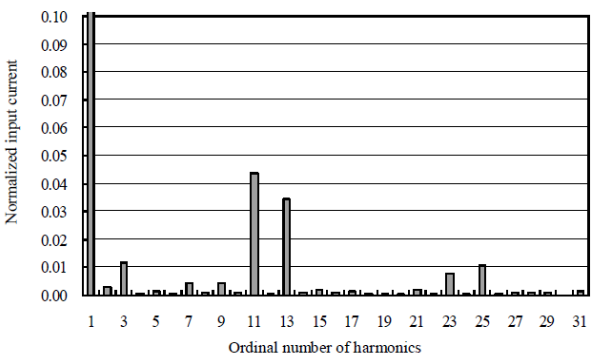


## ■ DC-Side Interphase-XFRM (Impr. DC Current)

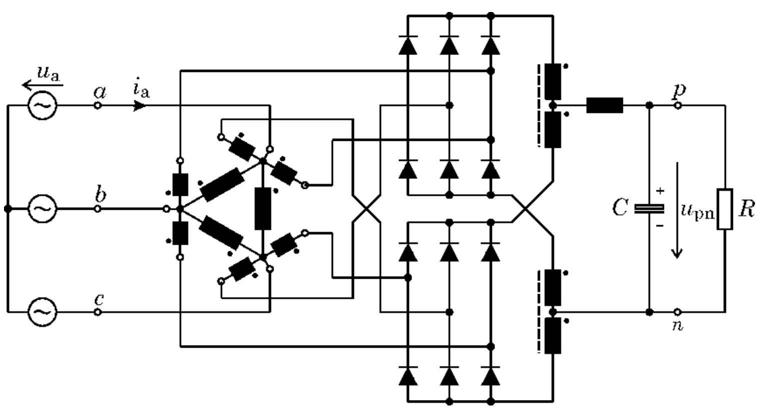


**DC-Side Interphase-XFRM can be omitted in Case of Full XFRM Isolation of Both Diode Bridges**

# Remark Auto-XFRM-Based 12-Pulse Hybrid Rectifier Systems

■ **Modulated Rectifier Output Current Impressed by DC/DC Boost Converter**

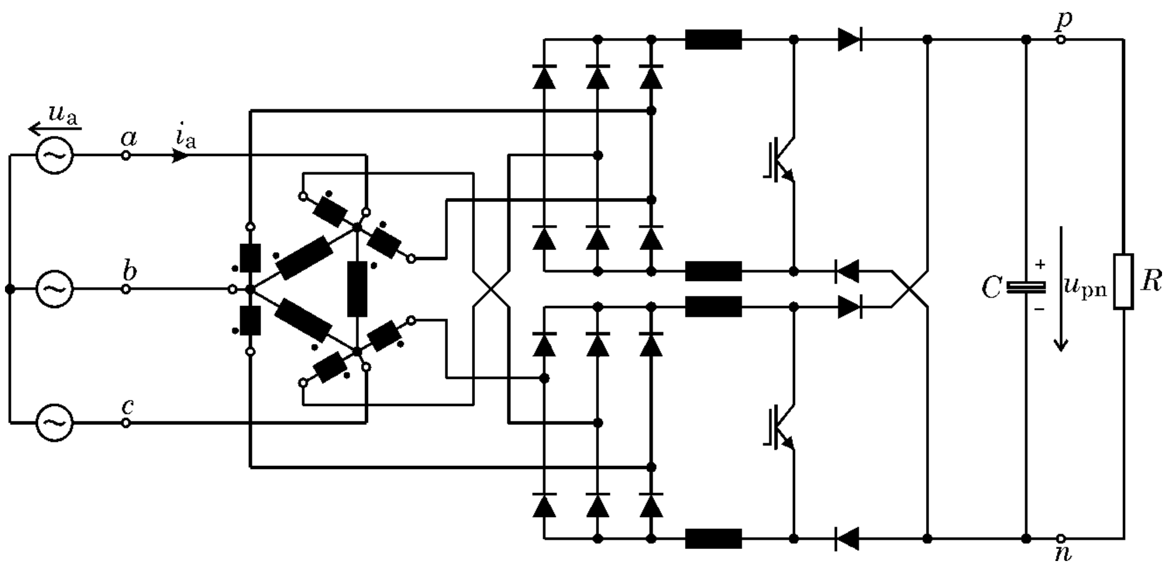


+ Output Voltage Controlled
+ Sinusoidal Mains Current Shaping Possible

- Active Converter Stage Processes Full Output Power
- Low Frequency Magnetics Employed

# Active 3-Φ Boost-Type PFC Rectifier Systems

*Δ-Switch Rectifier*
*Vienna-Rectifier*
*Six-Switch Rectifier*

# ▶ Classification of Unidirectional Rectifier Systems

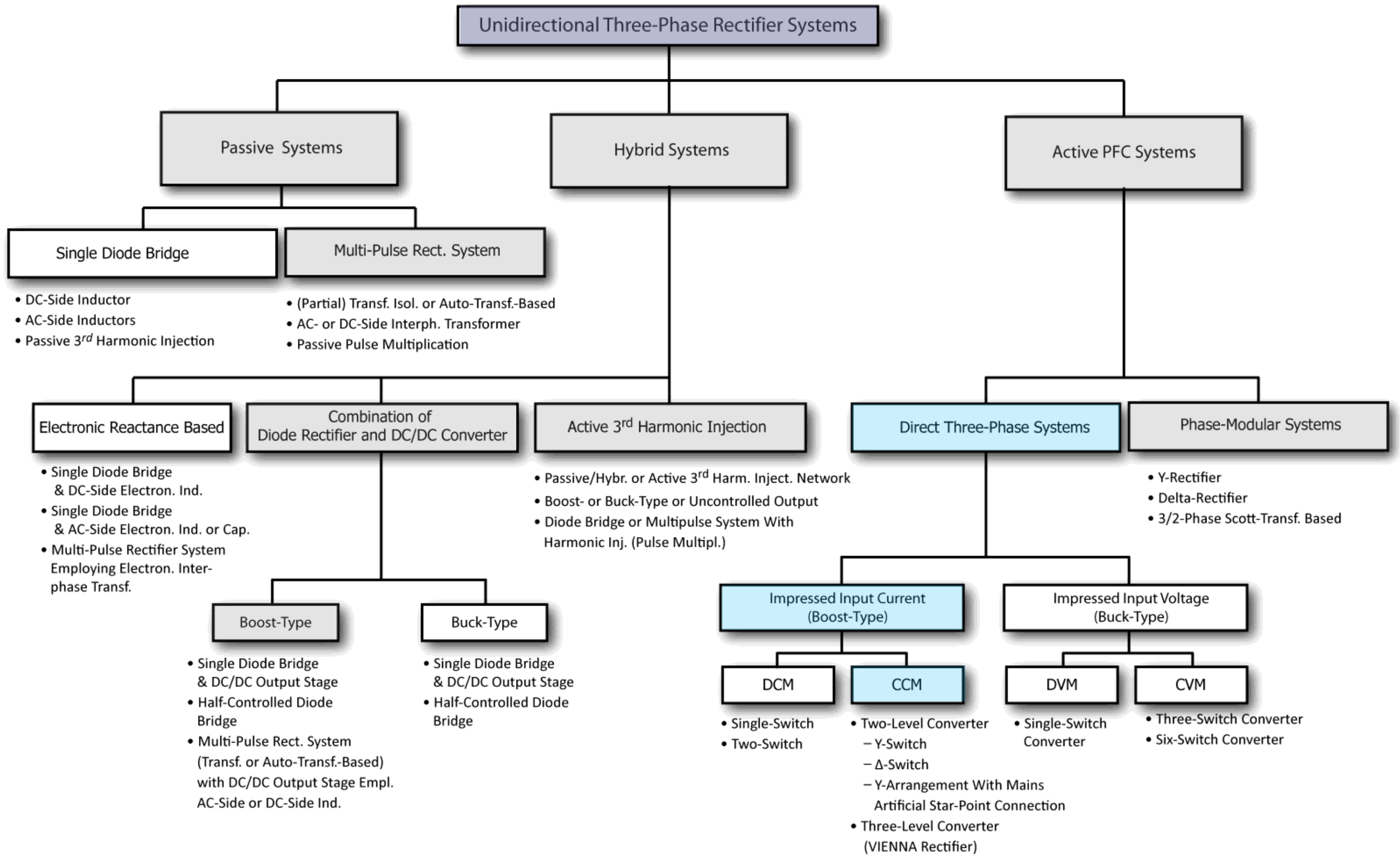

# Δ-Switch Rectifier

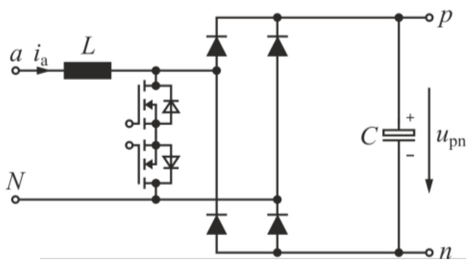


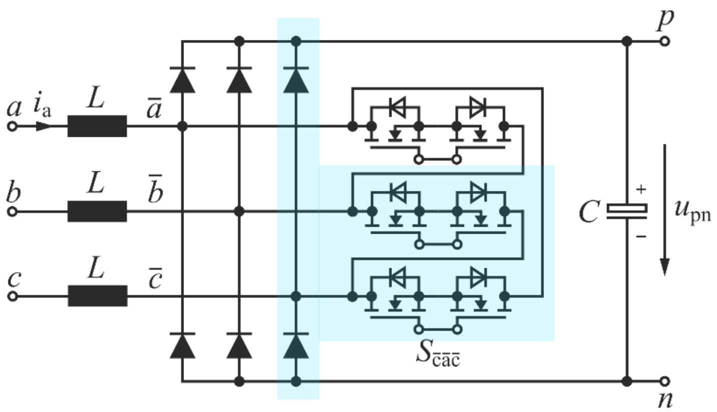


- **Derivation of 3-Φ Topology** → **Phase-Symmetry / Bridge-Symmetry**

# Δ-Switch Rectifier




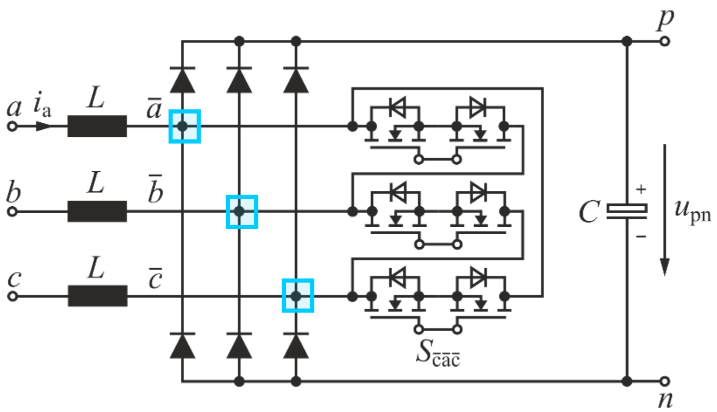


■ **Modulation of Diode Bridge Input Voltages / Conduction States**

# Δ-Switch Rectifier




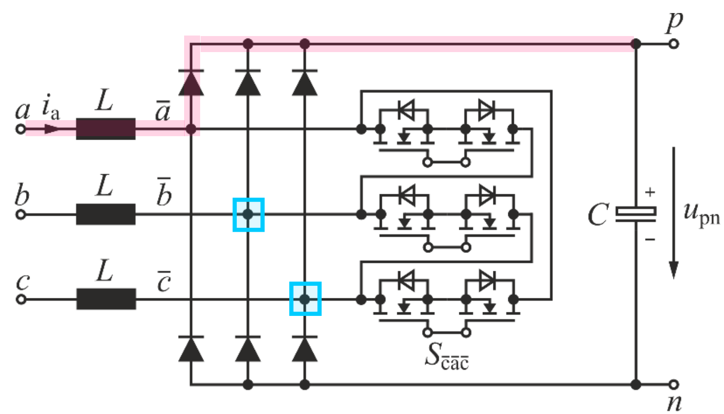


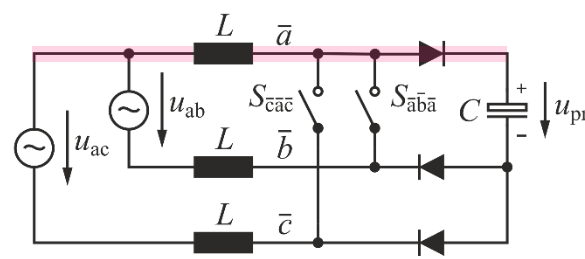


- **Output Voltage Control**
- **Sinusoidal Mains Current Control**
- **$\Phi$ = (-30°,+30°)**

# Δ-Switch Rectifier

## ▶ Experimental Analysis

$U_{LL}$ = 115 V (400Hz)
$P_o$ = 5 kW
$U_o$ = 400 V
$f_S$ = 72 kHz

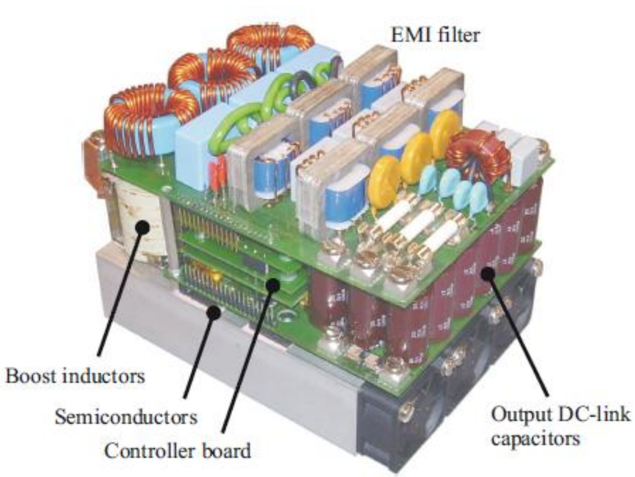


2.4 kW/dm$^3$

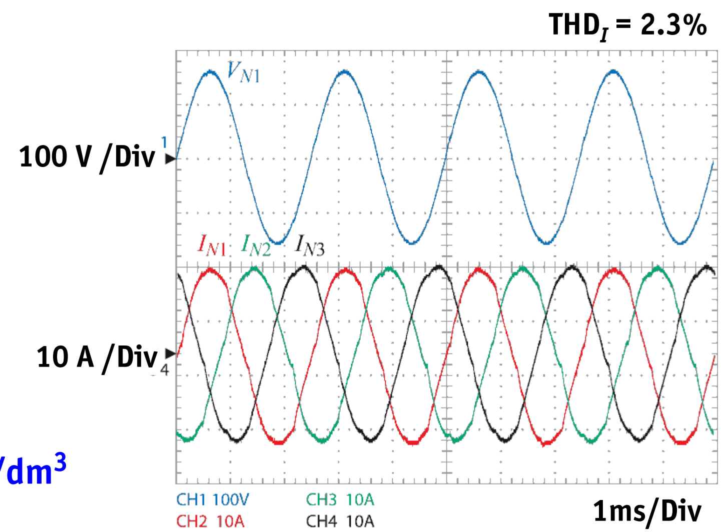


■ Advanced Control for Low Common-Mode Output Voltage

# Vienna Rectifier

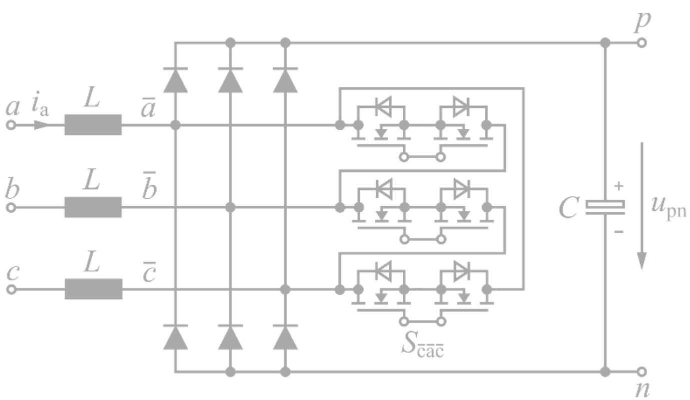


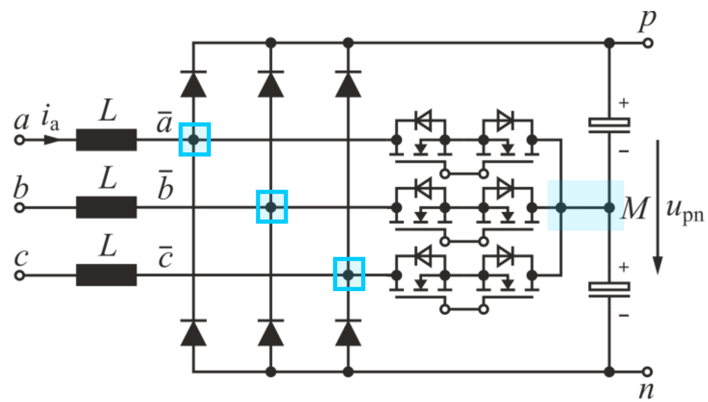


- Replace Δ-Switch by Y-Switch
- Connect Y-Switch to Output Center Point
- Maximum Phase/Bridge Symmetry

# Vienna Rectifier

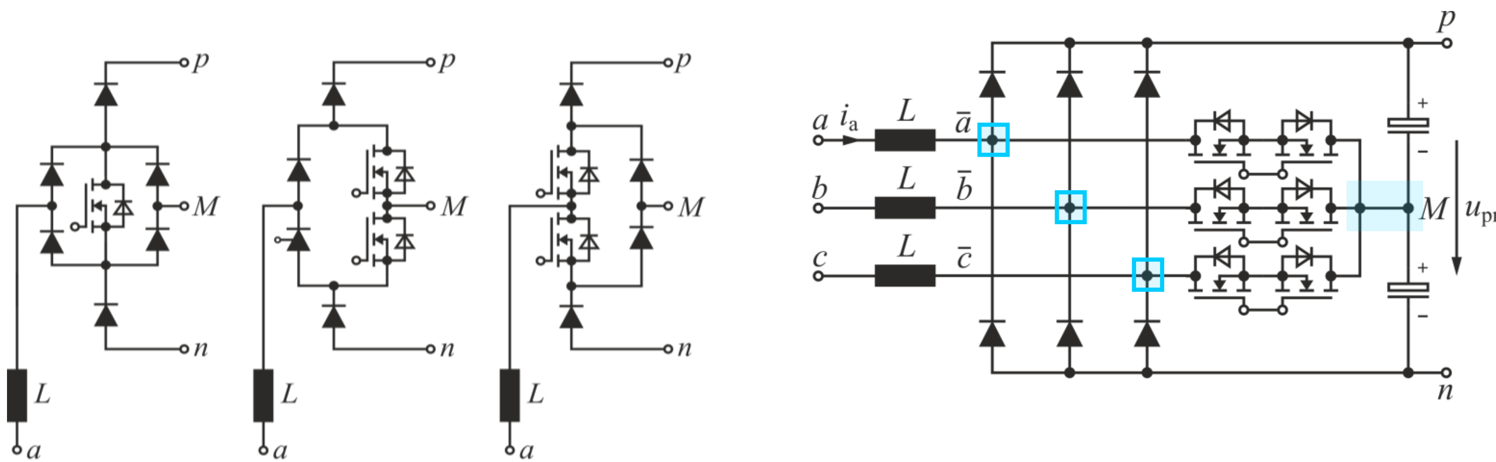


- Output Voltage Control
- Sinusoidal Mains Current Control
- $\Phi$ = (-30°,+30°)

# Vienna Rectifier

▶ Three-Level Characteristic

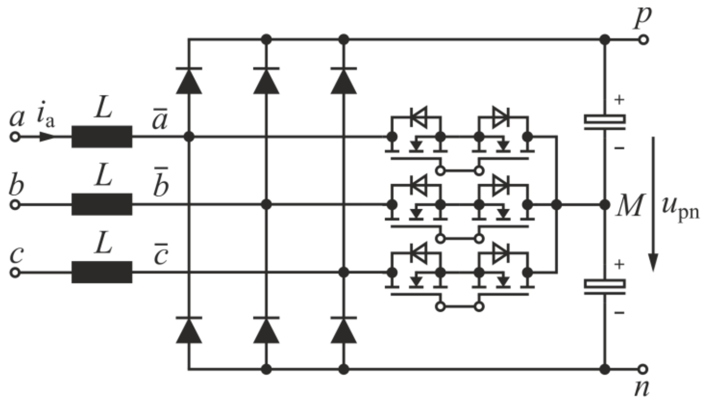


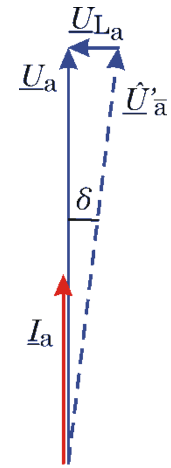


- \+ Low Input Inductance Requ.
- \+ Low Switching Losses,
- \+ Low EMI

- − Higher Circuit Complexity
- − Control of Output Voltage Center Point Required

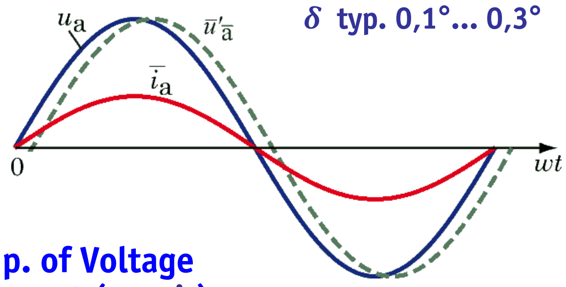


δ typ. 0,1°... 0,3°

▶ Difference of Mains Voltage (e.g. $u_a$) and Mains Frequency Comp. of Voltage Formed at Rectifier Bridge Input (e.g. $\bar{u}'_{\bar{a}}$) Impresses Mains Current (e.g. $i_a$)

# Time Behavior of the Components of Voltages $u_{\bar{a}}, u_{\bar{b}}, u_{\bar{c}}$

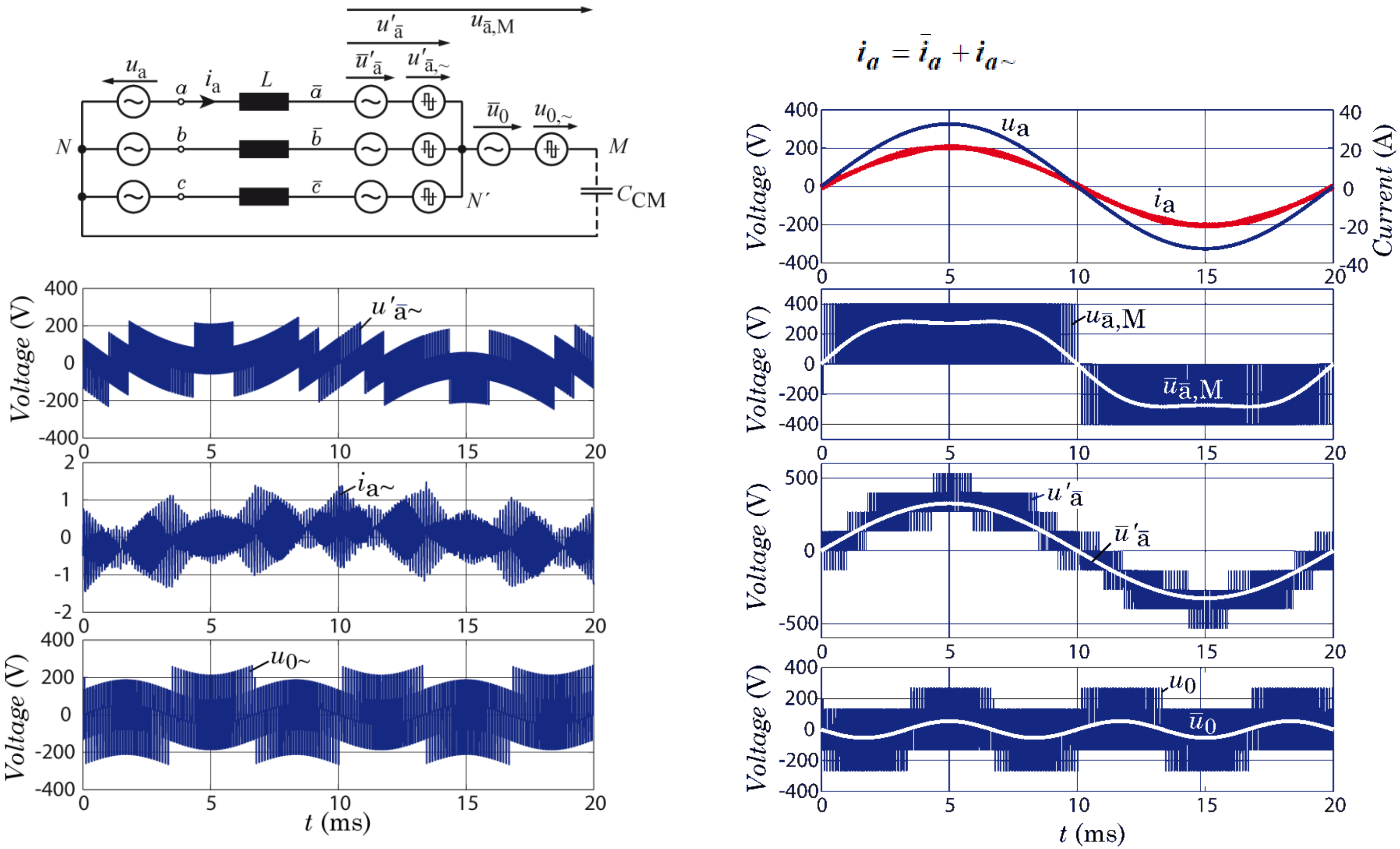

# Control Structure

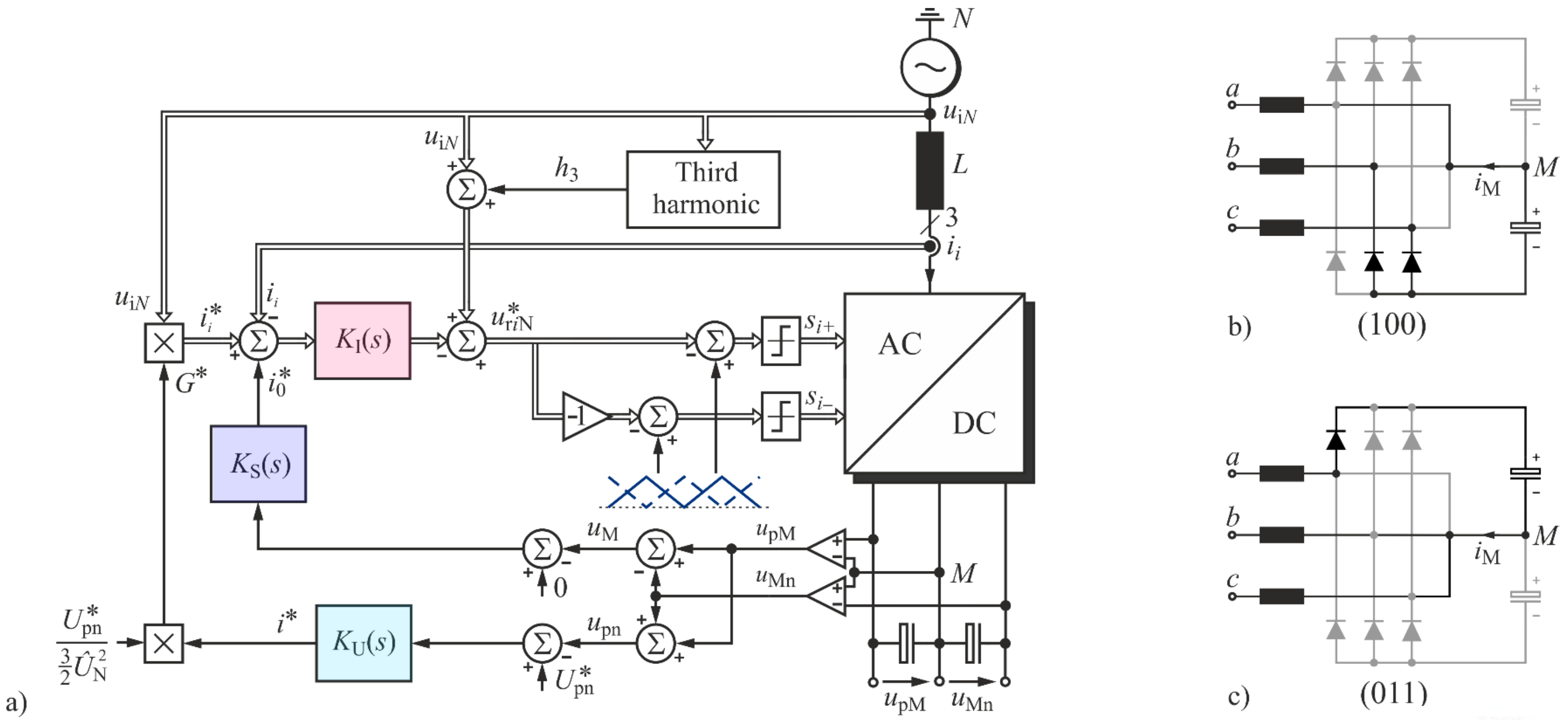


- **Output Voltage Control & Inner Mains Current Control & *NPP* Control**

# Experimental Results

$P_0$ = 10kW
$U_N$ = 230V
$f_N$ = 800Hz
$U_0$ = 800V
$THD_i$ = 1.6%

★ 10kW/dm³

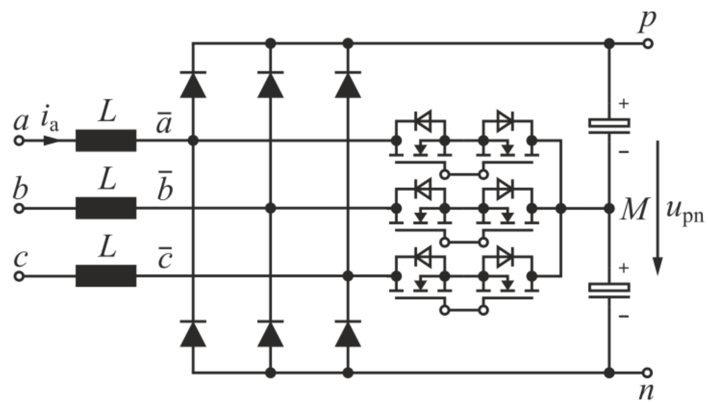


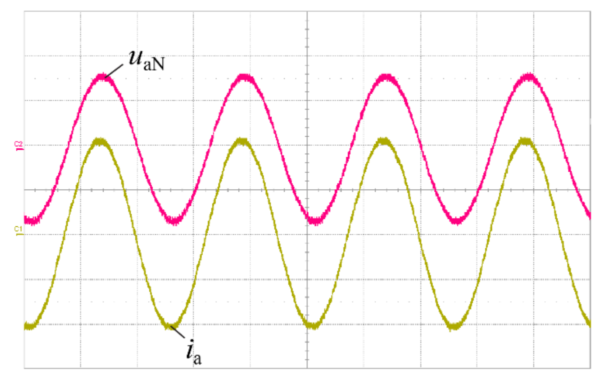


10A/Div
200V/Div
0.5ms/Div

✓

# Half-Controlled Bridge Rectifier

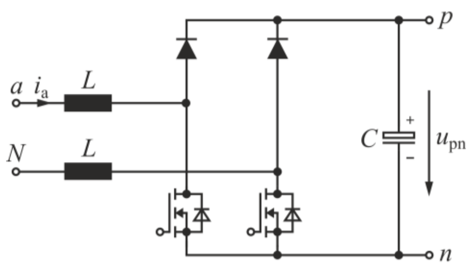


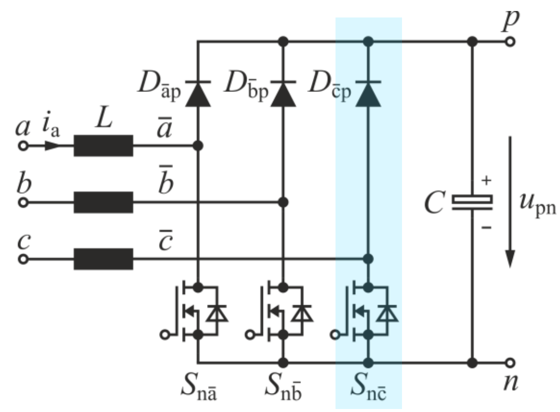


- **Derivation starting from 1-Φ Bridgeless PFC Rectifier**

# Half-Controlled Bridge Rectifier




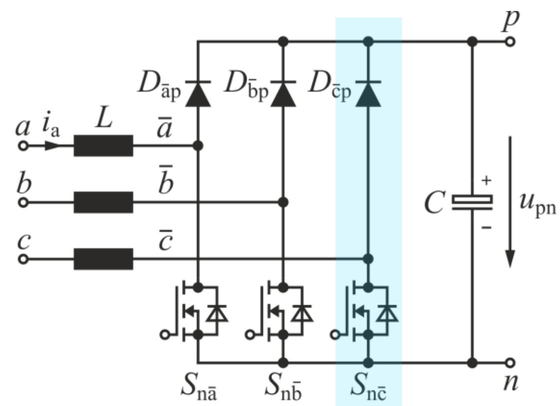


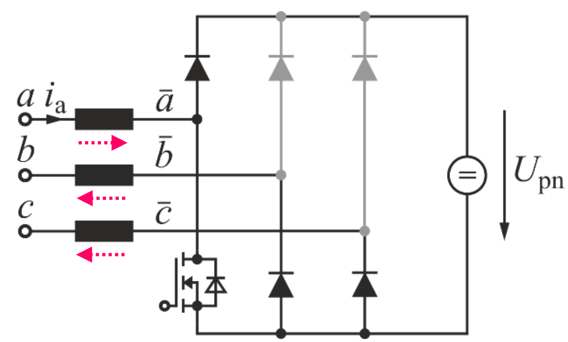


- **Output Voltage Control**

→ **Phase- but *NO Bridge-Symmetry***
→ ***NO Sinusoidal Mains Current Control***

# Fully-Controlled (Six-Switch) Bridge Rectifier

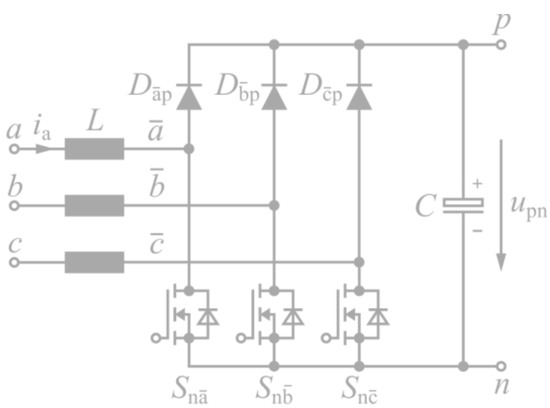


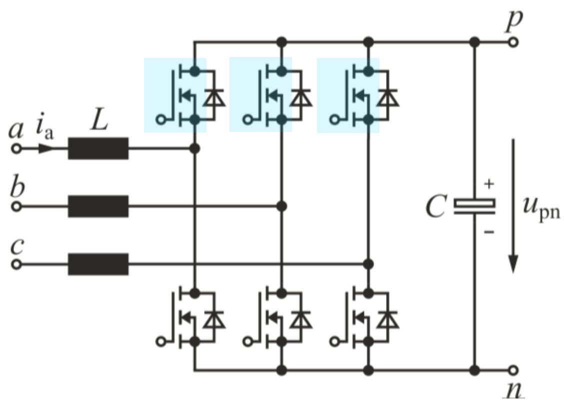


- **Output Voltage Control**

→ Phase- & *Bridge-Symmetry*
→ *Sinusoidal Mains Current Control*
→ $\Phi$ = *(-180°,+180°) – Bidirectional (!)*

# Evaluation of Boost-Type Systems

*3rd Harmonic Inj. Rectifier*
*Δ-Switch Rectifier*
*Vienna-Rectifier*
*Six-Switch Rectifier*

# Boost-Type PFC Rectifiers

- 3rd Harmonic Inj. Type
- Diode Bridge Conduction Modulation

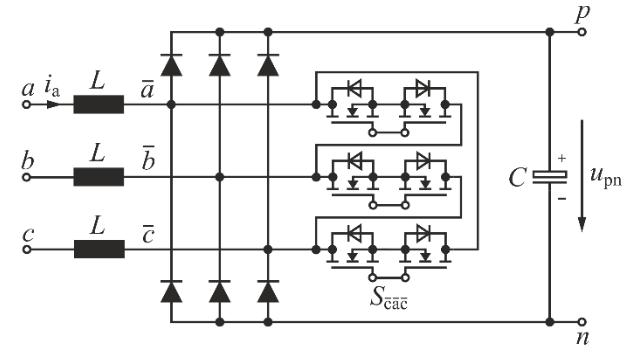


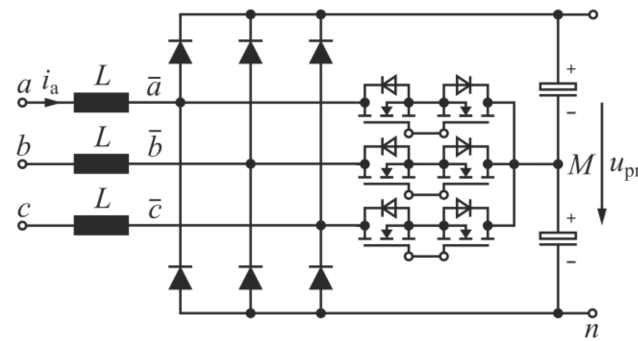


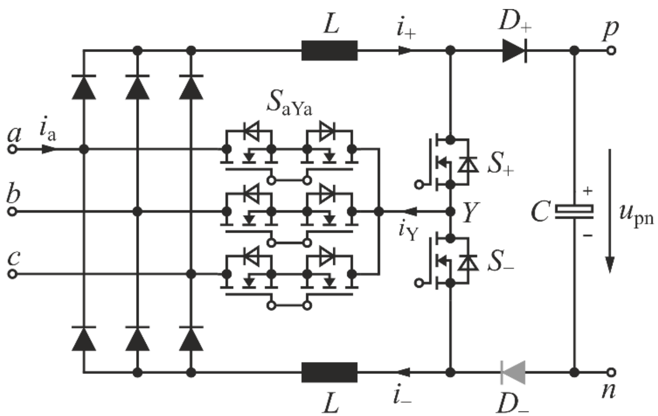


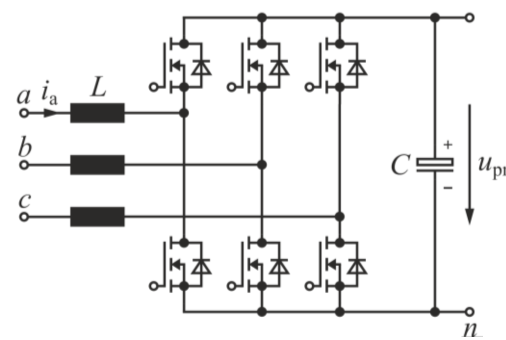

# Boost-Type PFC Rectifiers

- 3rd Harmonic Inj. Type
  → **Limited Operating Range**

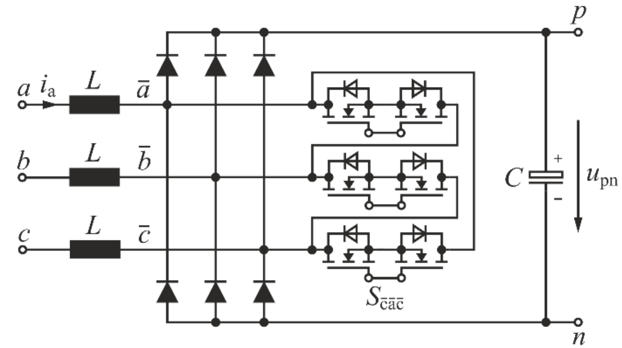


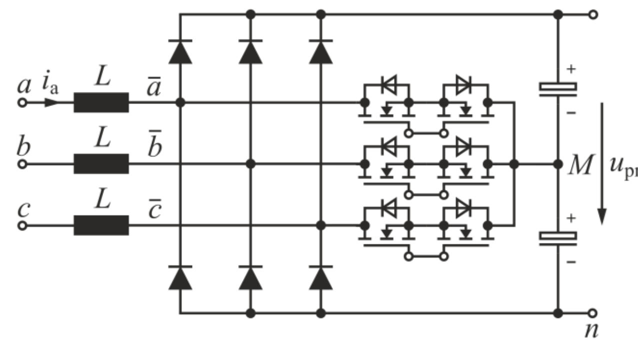


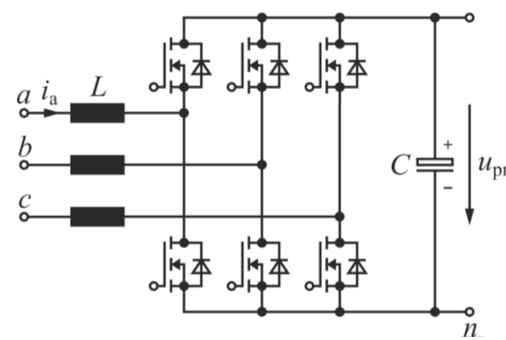


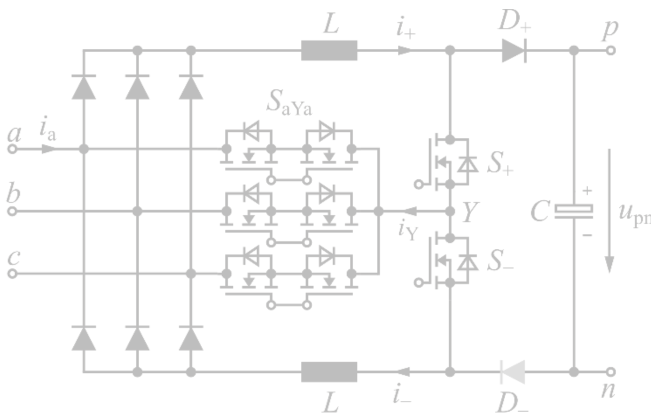

# Boost-Type PFC Rectifiers

- Δ-Switch Rectifier
  → System Complexity

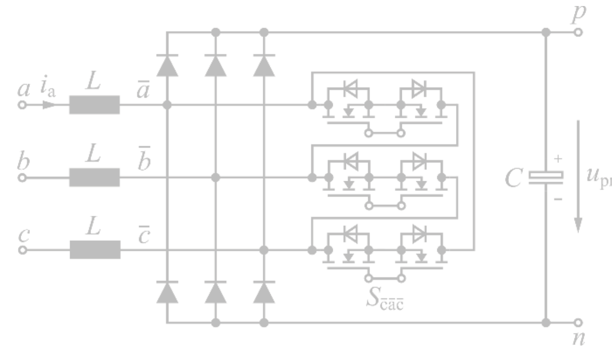


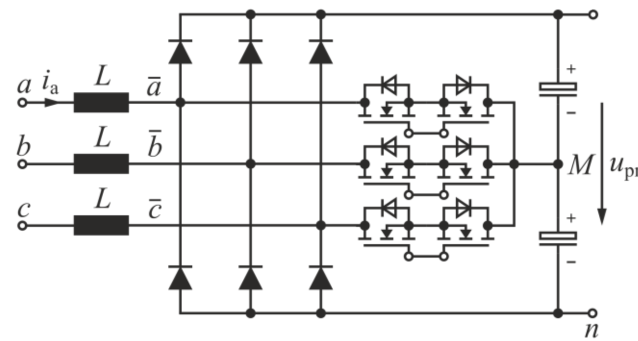


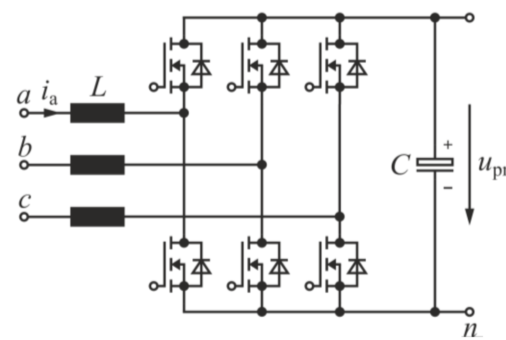


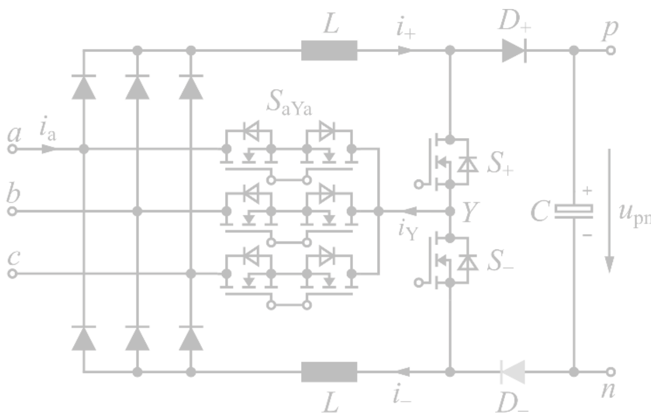

# Vienna Rectifier vs. Six-Switch Rectifier

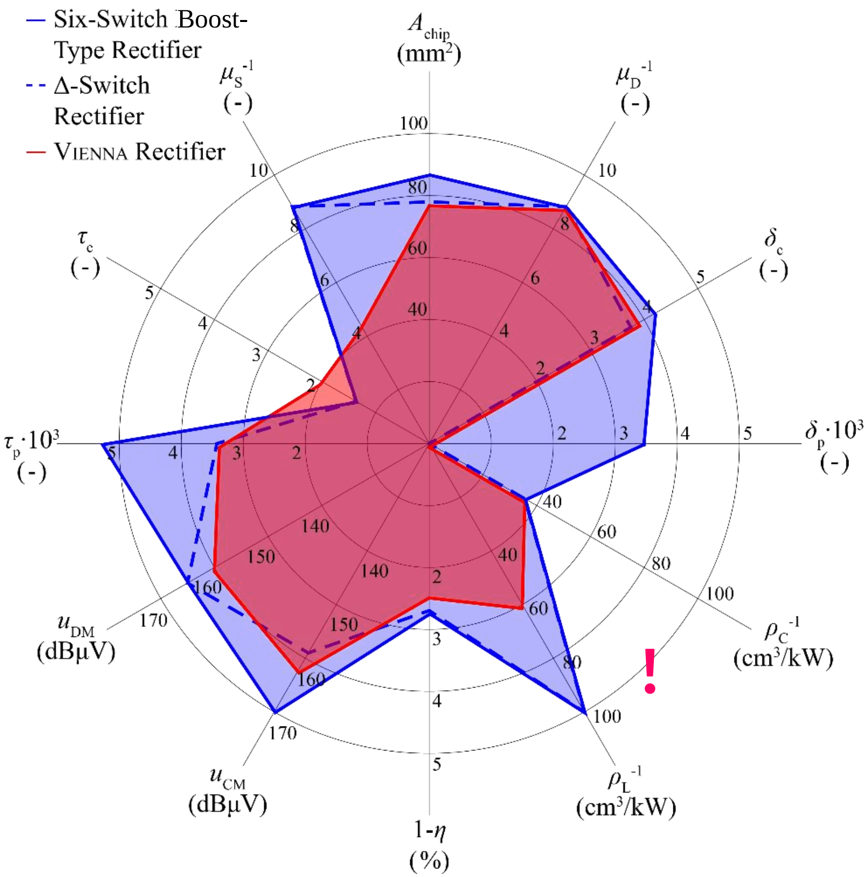


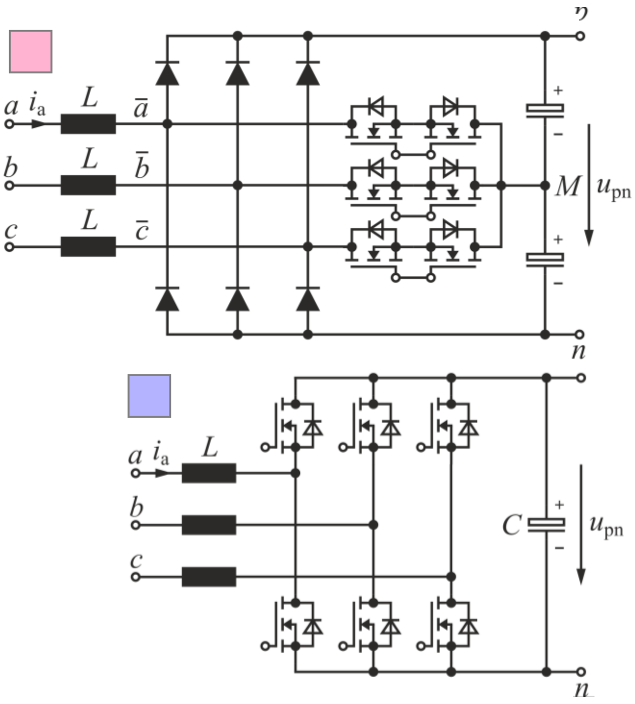

# Performance Indices

## ▶ Diodes

$$\text{Diode VA - Rating} = \frac{1}{\mu_D} = \frac{\sum_n V_{D,\max,n} I_{D,\max,n}}{P_o}$$

$$\text{Diode Conduction Losses} = \frac{\sum_n I_{D,avg,n}}{I_o}$$

## ▶ Power Passives

$$\text{Percentage Reactance} = \frac{2\pi f_N I_N L_N}{V_N}$$

$$\text{Rated Inductor Power} = \frac{I_L \Delta I_{L,pkpk} L f_s}{P_o}$$

$$\text{Capacitive Current Stress} = \frac{\sum_n I_{C,rms,n}}{I_o}$$

## ▶ Transistors

$$\text{Transistor VA - Rating} = \frac{1}{\mu_T} = \frac{\sum_n V_{T,\max,n} I_{T,\max,n}}{P_o}$$

$$\text{Transistor Conduction Losses} = \frac{\sum_n I_{T,rms,n}}{I_o}$$

$$\text{Transistor Sw. Losses Boost} = \frac{\sum_n I_{T,avg,n} V_{T,n}}{P_o}$$

$$\text{Transistor Sw. Losses Buck} = \frac{\sum_n I_{T,n} V_{T,avg,n}}{P_o}$$

## ▶ Conducted Noise (DM, CM)

$$V_{Noise} = V_{DM} + V_{CM}$$

$$V_{CM} = \frac{V_a + V_b + V_c}{3}$$

$$V_{DM}^2 = V_{DM,tot}^2 - V_{N,rms}^2$$

$$V_{CM}^2 = V_{CM,tot}^2 - V_{CM,LF}^2$$

# EV Charging
# DC/DC Power Transfer

**– Isolation Transformer**
**– IPT (WPT)**

**ACKNOWLEDGEMENT**

The authors would like to express their sincere appreciation to ABB Switzerland Ltd. for the support of research on IPT whose results are partly presented in this Tutorial

# EV Charging – Power Electronics Topologies

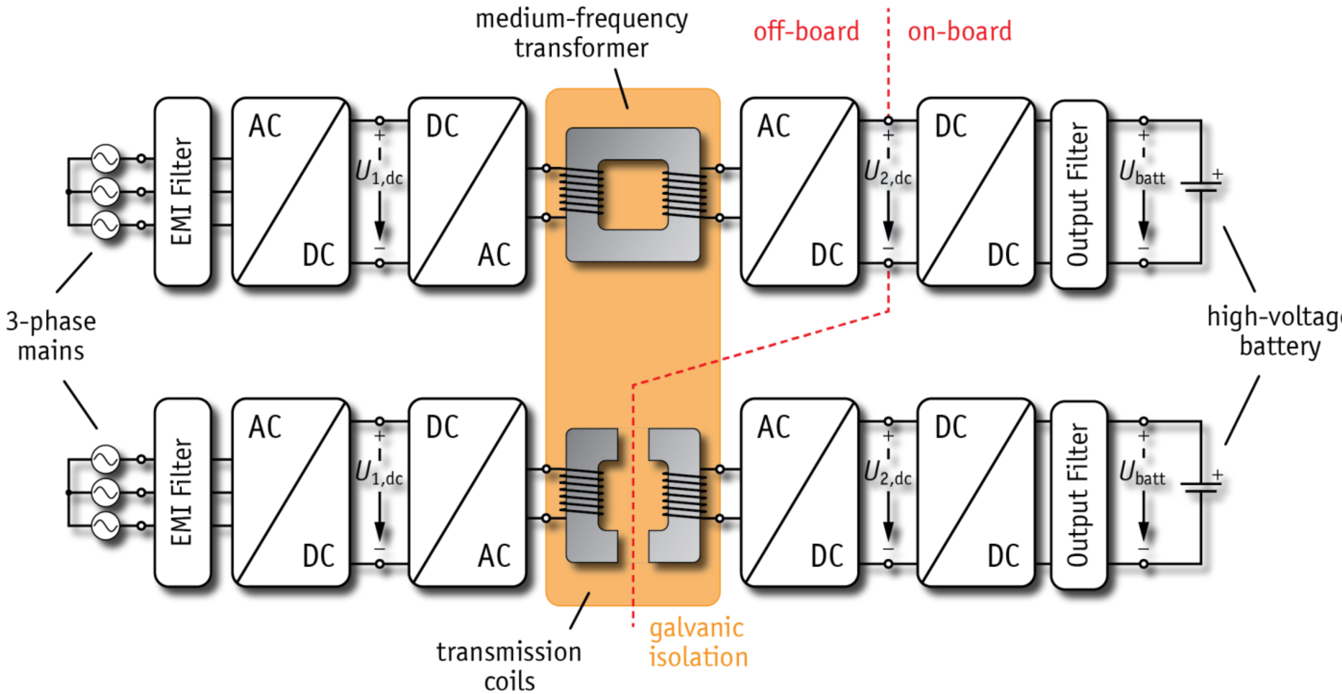


▲ **Structure of a 3-Φ Isolated 2-Stage High-Power Battery Charging System with MF XFRM or IPT Transmission Coils**

# EV Charging – Wireless / Inductive Power Transfer

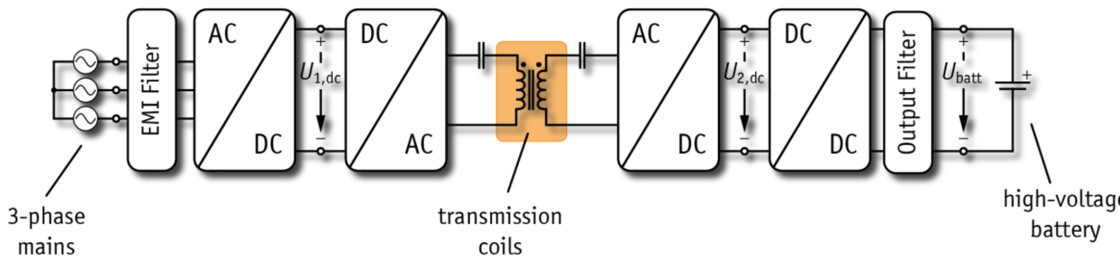


▲ Structure of a 3-Φ 2-stage IPT charging system

Image: James Provost for IEEE Spectrum

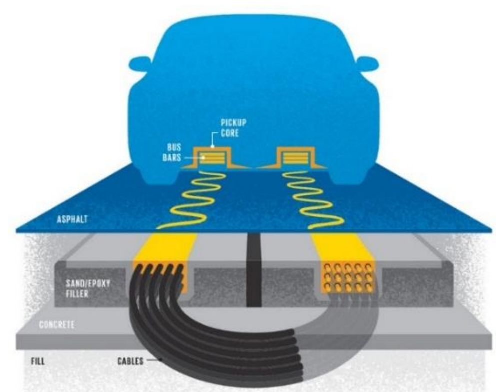


- Inherent Galvanic Isolation
- High Convenience, Usability & Safety
  - High Market Potential
  - Driver for Future Development
- More Frequent Recharging
  - Reduced Battery Stress
  - Long Lifetime/Small Volume

# IPT Worldwide Demonstration / Research Activities

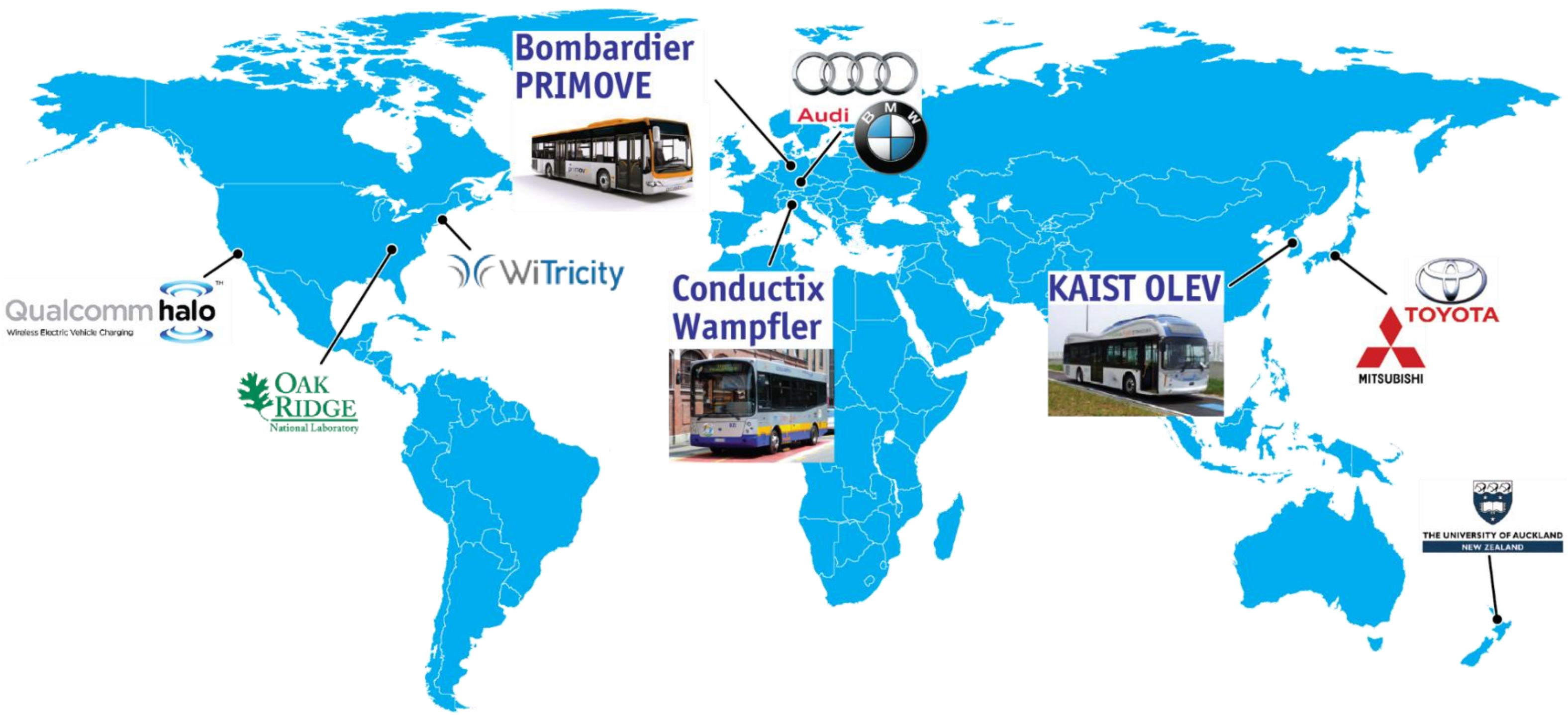

# Realization Examples

# Bombardier: PRIMOVE

Source: Bombardier PRIMOVE Website, http://primove.bombardier.com, 2.6.2014 /
D. Dilba, «Die Tram oben ohne», in *Technology Review*, Heise Online, 8.6.2011.

## Light Rail w/o Overhead Line


- Elimination of Cables and Posts
- Simplified Installation, e.g. in Public Areas
- Increased Reliability, Less Maintenance

Test Track Augsburg (2010): 150 kW, 10 cm, 20 kHz

## Wireless Electric Bus


- Wireless Charging at Bus Stops
- Extended Battery Life, Lower Battery Weight
- No Battery Exchange, No Additional Dwell Time
- Fewer Fleet Vehicles
- Lower Total Cost of Ownership

Test Track Braunschweig (2014): 200 kW, (?) cm

# Bombardier: PRIMOVE

Source: Bombardier PRIMOVE Website, http://primove.bombardier.com, 2.6.2014 / D. Dilba, «Die Tram oben ohne», in *Technology Review*, Heise Online, 8.6.2011.

## Light Rail w/o Overhead Line

- Elimination of Cables and Posts
- Simplified Installation, e.g. in Public Areas
- Increased Reliability, Less Maintenance

Test Track Augsburg (2010): 150 kW, 10 cm, 20 kHz

## Wireless Electric Bus


- Wireless Charging at Bus Stops
- Extended Battery Life, Lower Battery Weight
- No Battery Exchange, No Additional Dwell Time
- Fewer Fleet Vehicles
- Lower Total Cost of Ownership

Test Track Braunschweig (2014): 200 kW, (?) cm

# KAIST: On-line Electric Vehicle (OLEV)

***J. Kim et al.,*** «Coil design and shielding methods for a magnetic resonant wireless power transfer system," *Proc. IEEE*, vol. 101, no. 5, pp. 1332 – 1342, 2013.

## Wireless Electric Bus

- 30% Reduced Battery Weight
- Fewer Fleet Vehicles
- Compliance with ICNRIP 1998
- 5-15% of Round-Trip Track Electrified

**Test Track Gumi (South Korea): 100 kW, 20 kHz, 17 cm**

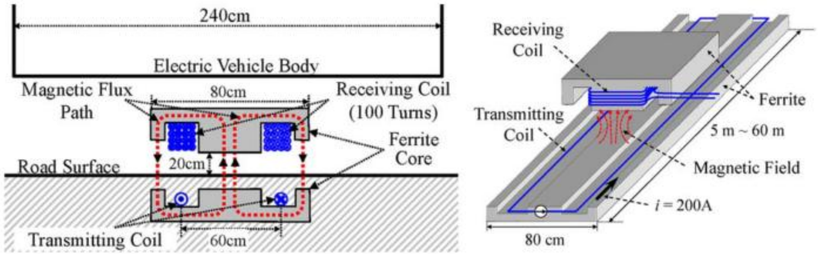

# Dynamic EV Charging on Highways

- **Electrified IPT Lanes on Highways allow Charging In-Motion**
  - No More «Fuel Stops» Needed
  - No Time Lost during Charging
  - No «Range Anxiety»

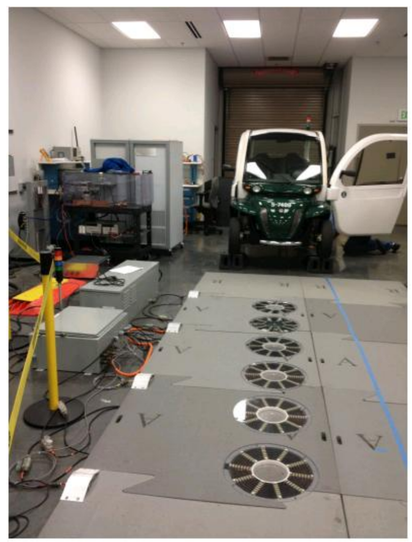

▲ Dynamic IPT Demonstration Track @ ORNL

Image: James Provost for IEEE Spectrum

# But, Realization is Challenging

## Simplified Calculation (1)

- 20 km of Highway @ avg. 25 kW [1], 120 km/h
  → 20/120 h x 25 kW = 4.2 kWh used

- 200 m IPT-Lane per 20 km of Highway (=1%)
- Speed while Charging 50 km/h
  → 14 s for Charging

- Charging 4.2 kWh in 14 s:

  → 1 MW / Vehicle
  Required Charging Power !

  – Slowing Down to 50 km/h every 20 km?
  – High Cost for Infrastructure
  – Medium Voltage Supply
  – Battery that Handles 1 MW?

Image: James Provost for IEEE Spectrum

[1] **T. Bütler and H. Winkler,** «Energy consumption of battery electric vehicles (BEV),» EMPA, Dübendorf, Switzerland, 2013.

# But, Realization is Challenging

Image: James Provost for IEEE Spectrum

## Simplified Calculation (2)

- 1 MW / Vehicle at an Ultra-Fast Charging Station
- Re-Charging in 10 min

→ 167 kWh Delivered Energy
→ 6.6 h Driving Possible

- Stopping for 10 min every 7 h?
- Large Cost for Infrastructure
- Medium Voltage Supply
- Battery that Handles 1 MW?

# Dynamic (EV) Charging: Possible Applications

- **Electrify Spots where Vehicles Stop, e.g. Traffic Lights, Bus Stop,..**

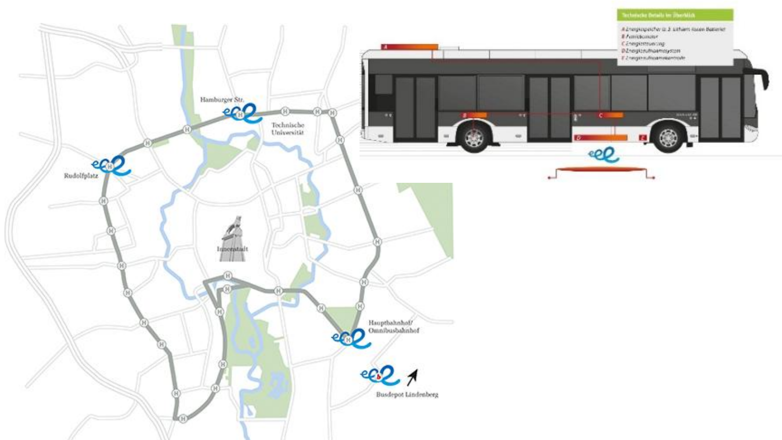

Source: Braunschweig Verkehrs AG

Source: Qualcomm

- **Power Supply of Moving Transportation Carts / Vehicles @ Industrial Sites**

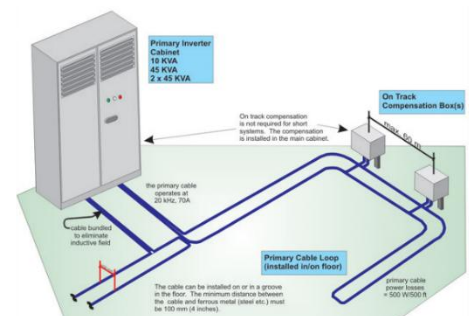


Source: VAHLE

▲ **Contatless power supply of automatic guided vehicles in industrial sites**

# Main Design Challenges

# Inductive Power Transfer for EV

- **Magnetic Coupling**
  - Physical Efficiency Limit
  - Sensitivity to Coil Misalignment
- Magnetic Stray Field
  - Limited by Standards
    (e.g. 27 µT @ 100 kHz)
- Power Density
  - Coil Size / Air Gap - Ratio
  - Weight of Shielding & Core

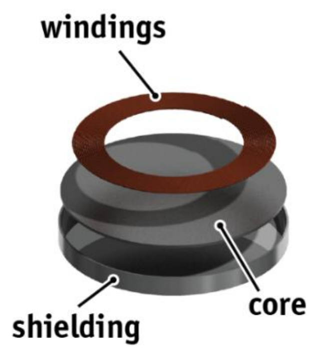


Image: J. Kim *et al.* (KAIST)

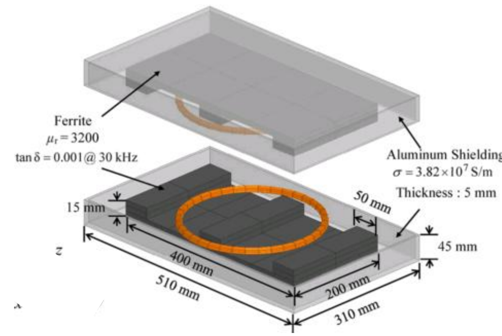


Source: Brusa Elektronik AG

# Inductive Power Transfer for EV

- **Magnetic Coupling**
  - Physical Efficiency Limit
  - Sensitivity to Coil Misalignment

- **Magnetic Stray Field**
  - Limited by Standards (e.g. 27 µT @ 100 kHz)

- **Power Density**
  - Coil Size / Air Gap - Ratio
  - Weight of Shielding & Core

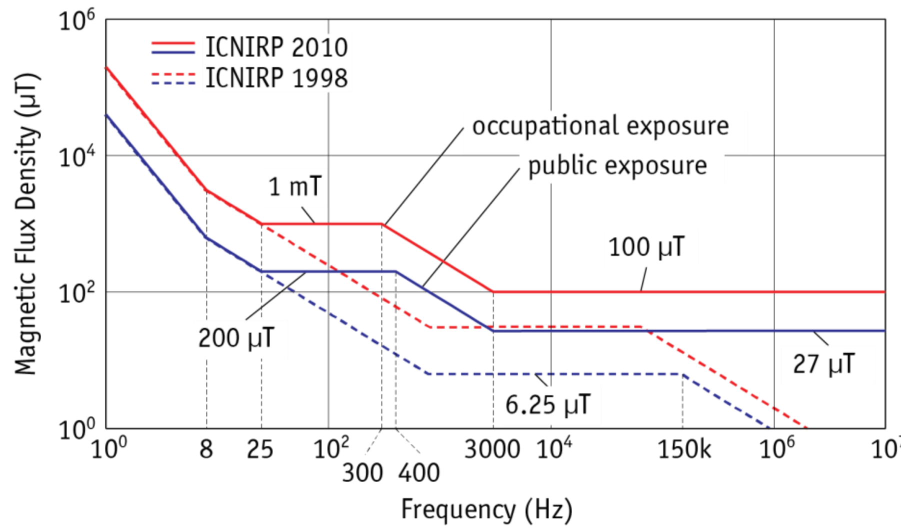


▲ ICNIRP 1998 & 2010 reference values for mag. fields

# Inductive Power Transfer for EV

- ▶ **Magnetic Coupling**
  - Physical Efficiency Limit
  - Sensitivity to Coil Misalignment
- ▶ **Magnetic Stray Field**
  - Limited by Standards
    (e.g. 27 μT @ 100 kHz)
- ▶ **Power Density**
  - Coil Size / Air Gap - Ratio
  - Weight of Shielding & Core


▲ PRIMOVE bus lowers receiver coil to road surface

- Increased Coupling / Efficiency
- Reduced Magnetic Stray Field
- Mechanical Positioning Aids

# Inductive Power Transfer for EV

- **Magnetic Coupling**
  - **Physical Efficiency Limit**
  - **Sensitivity to Coil Misalignment**
- **Magnetic Stray Field**
  - **Limited by Standards (e.g. 27 µT @ 100 kHz)**
- **Power Density**
  - **Coil Size / Air Gap - Ratio**
  - **Weight of Shielding & Core**

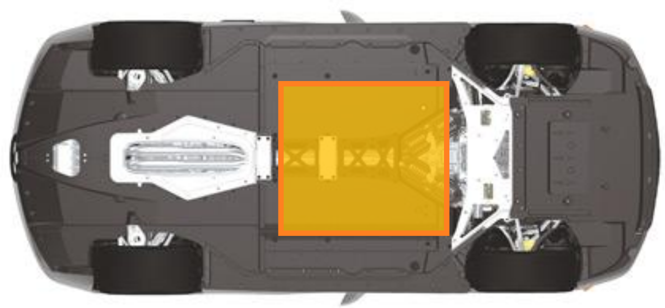

Source: Lexus

# Σ Inductive Power Transfer

- **Requirements & Interface**
  - Charging Power + Air Gap
  - Electrical Interface

- **Coil Design**
  - Low **Stray Field** → Despite High Power Transmission
  - High **Misalignment Tolerance** → Limited Parking Accuracy
  - Small **Size**, Low **Weight** → Incl. Core and Shielding Materials

- **Optimization**
  - High Transmission **Efficiency** → Thermal Limitations / Energy Cost
  - High **Power Density** → Automotive Application!
  - Cost, Reliability, ...

# Σ Inductive Power Transfer

- **Requirements & Interface**
  - Charging Power + Air Gap
  - Electrical Interface
- **Coil Design**
  - Low Stray Field
  - High Misalignment Tolerance
  - Small Size, Low Weight
- **Optimization**
  - High Transmission Efficiency
  - High Power Density
  - Cost, Reliability, ...

***Multi-Objective Optimization!***

# IPT System Components

*Basic Design Principles*
*Transmission Coil Design*
*Stray Field & Shielding*
*Coil Modeling & Power Loss Estimation*

# Inductive Power Transfer – Working Principle (1)

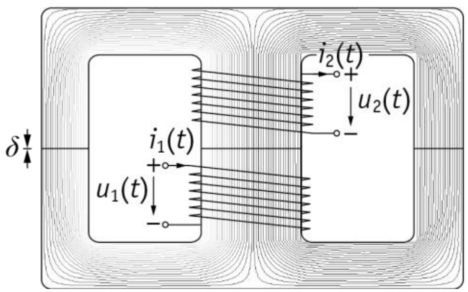


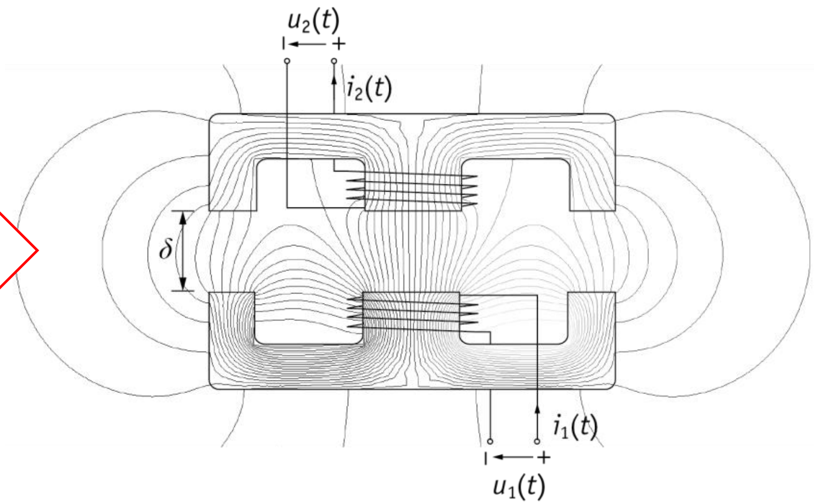


- **1-Phase E-core Transformer**
  - Flux Concentrated in Low Reluctance Iron-Path
  - Magnetic Coupling $k > 95\%$
  - Efficiency $\eta > 99\%$
- **Transformer with Large Air Gap**
  - Flux not Concentrated, due to High Reluctance of Air Gap
  - Magnetic Coupling $k \approx 10\,..\,35\%$

# Inductive Power Transfer – Working Principle (2)

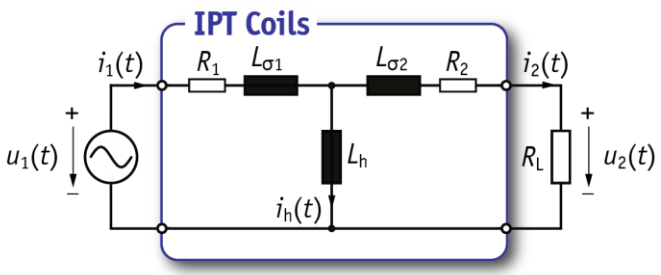


▲ Transformer equivalent circuit diagram

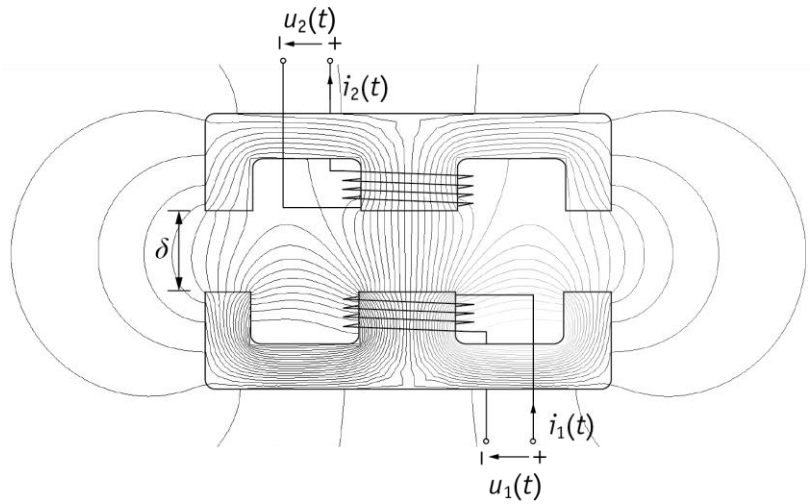


- **Mutual Inductance Approx. 10 .. 35% of Self-Inductance**
- **Losses Modeled as Parasitic Winding Resistances**

- **Transformer with Large Air Gap**
  - **Flux not Concentrated, due to High Reluctance of Air Gap**
  - **Magnetic Coupling $k \approx 10\,..\,35\%$**

# Inductive Power Transfer – Working Principle (3)

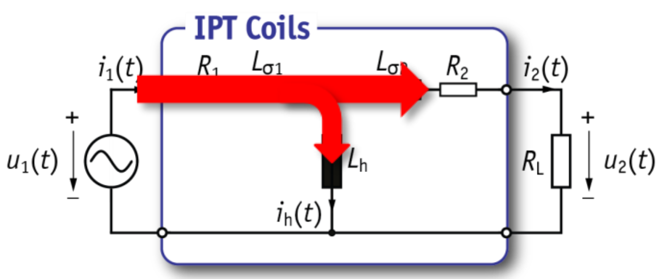


▲ Transformer equivalent circuit diagram

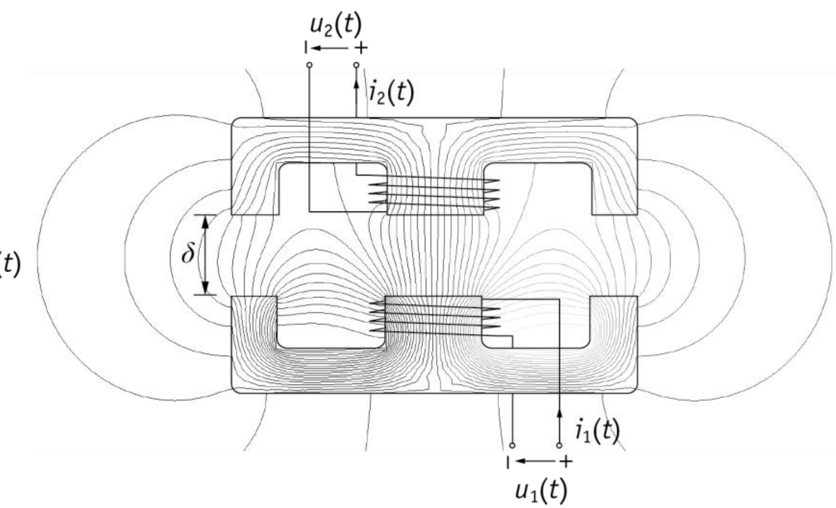


- High Magnetization Current, Delivers Zero Output Power
- High Copper Losses in Transmitter Coil (+ Losses in Core Material)

- Transformer with Large Air Gap
  - Flux not Concentrated, due to High Reluctance of Air Gap
  - Magnetic Coupling $k \approx 10\,..\,35\%$

# *Series* Compensation of Receiver

Resonant Compensation
of $L_2$ at $\omega_0 = 1/(L_2 C_2)^{½}$

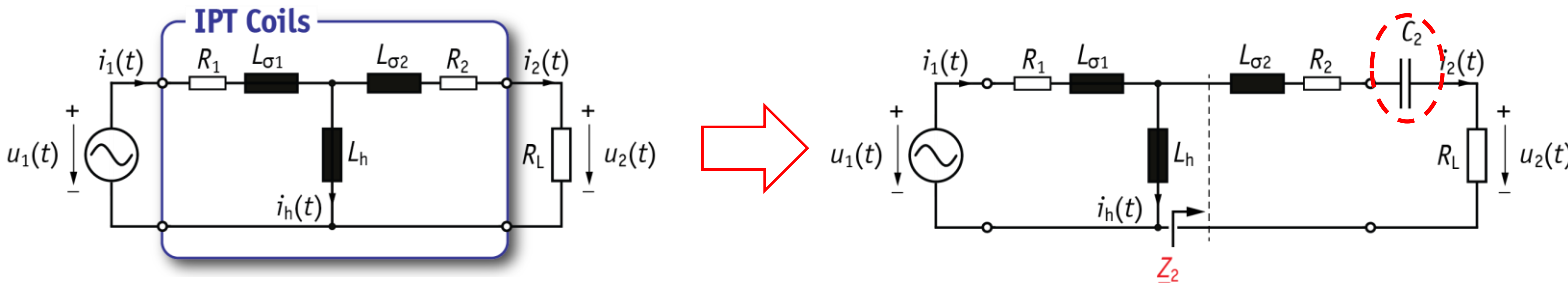


▲ Series compensated receiver - equivalent circuit

- Reduce Receiver Impedance
- Reduced Magnetization Current
  → More Current in Receiver Circuit

- Current Source: Best for
  Low Impedance Loads
  (e.g. High Power Level)

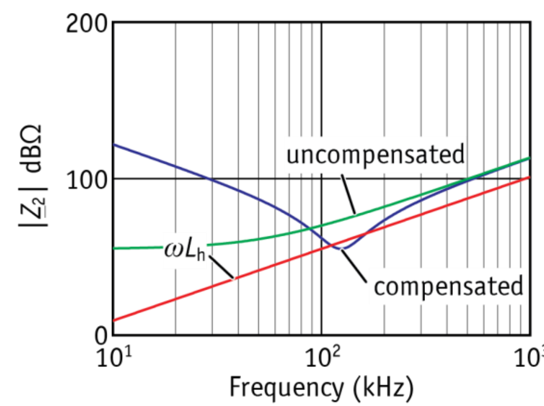


▲ Impedance of the receiver circuit

# Power Converter – Topology

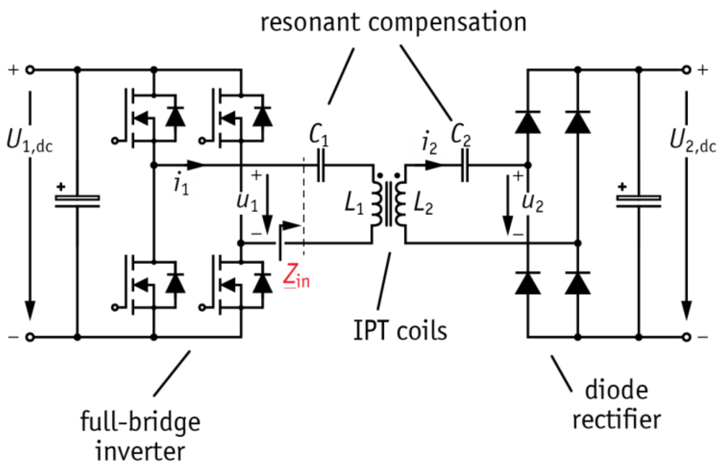


▲ Series compensated resonant converter topology

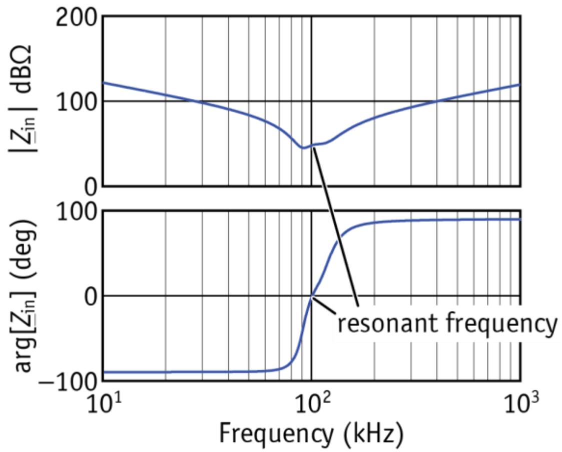


▲ Bode diagram of input impedance

- **Resonant Capacitor at Transmitter to Reduce Inverter Current**
- **Tuned to Same Frequency** $\omega_0 = 1/(L_1 C_1)^{1/2}$

- **Switching above Resonance**
  - **Minimum Conduction Losses**
  - **Zero Voltage Switching of MOSFETs**

# Power Converter – Prototype System

**R. Bosshard, J. W. Kolar et al.,** "Modeling and $\eta$-$\alpha$-Pareto optimization of inductive power transfer coils for electric vehicles," *IEEE J. Emerg. Sel. Topics Power Electron.* (accepted for publication), 2014.

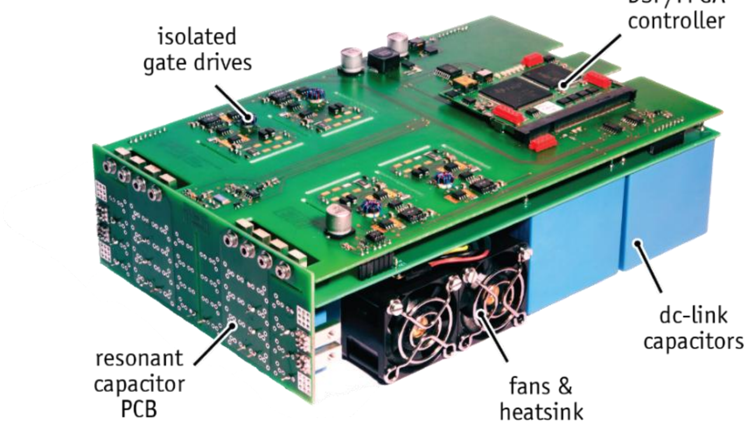


▲ 5 kW prototype power converter

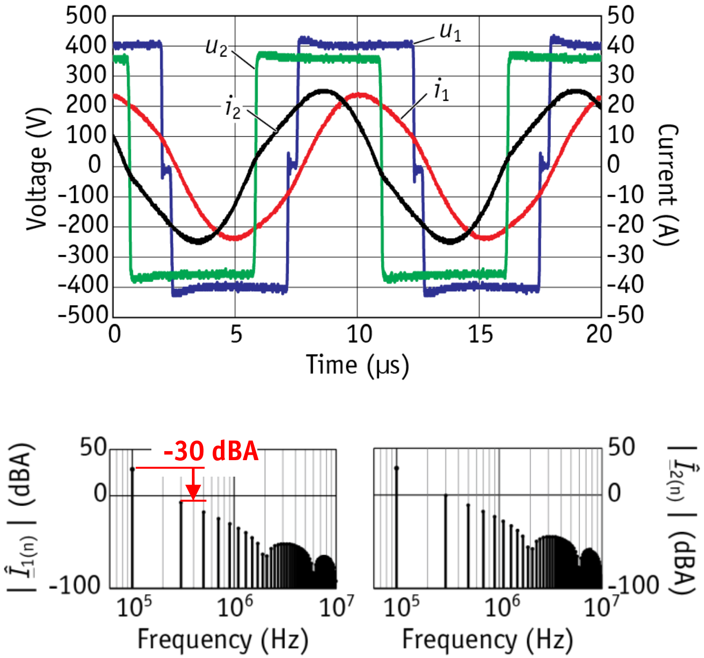


▲ Measured waveform & spectrum

- ▶ Full-Bridge Inverter 5 kW @ 100 kHz
- ▶ Cree 1.2 kV SiC MOSFETs (42 A)
- ▶ DSP/FPGA-based Control

# Power Converter – Load Model

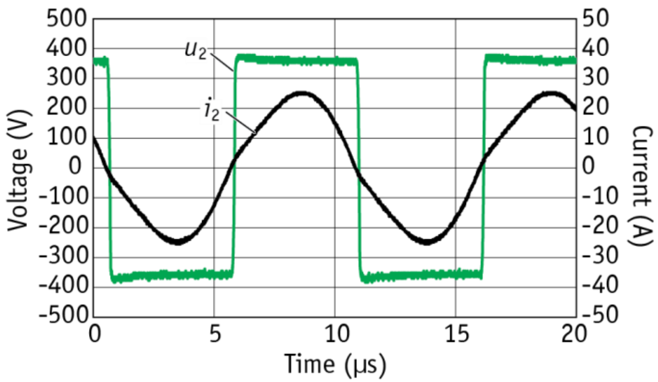


▲ Current and voltage waveforms at resonant circuit output / diode rectifier input

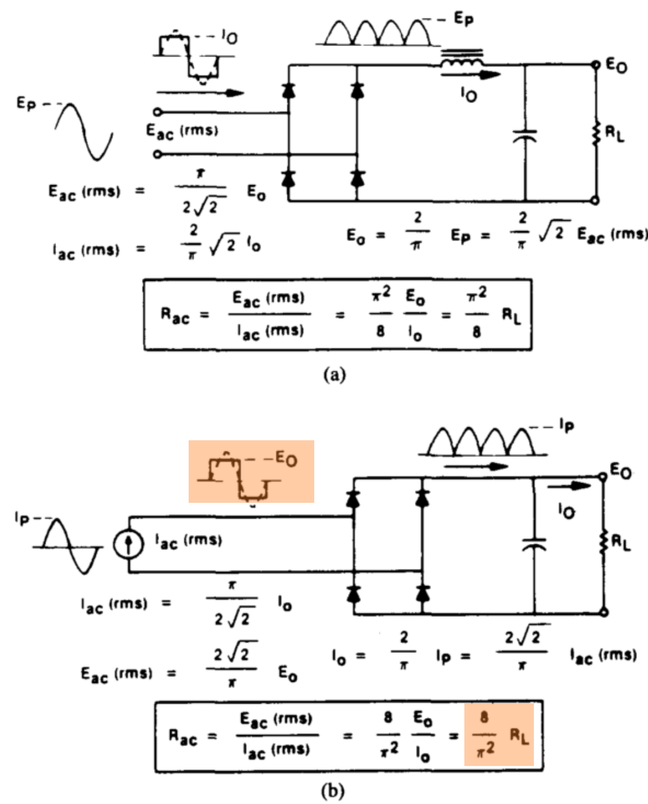

Fig. 3. Equivalent ac resistors as presented by rectifier loads. (a) Voltage source drive (applies to parallel and series-parallel converters). (b) Current source drive (applies to series converter).

► **Fundamental-Frequency Model of Load:**

**(Valid at a Single Operating Point)**

$$R_L = \frac{8}{\pi^2}\frac{U_{2,dc}^2}{P_2}$$

R. Steigerwald, "A comparison of half-bridge resonant converter topologies," IEEE *Trans. Power Electron.*, vol. 3, no. 2, pp. 174-182.

# Effect of *High* Equivalent Load Resistance

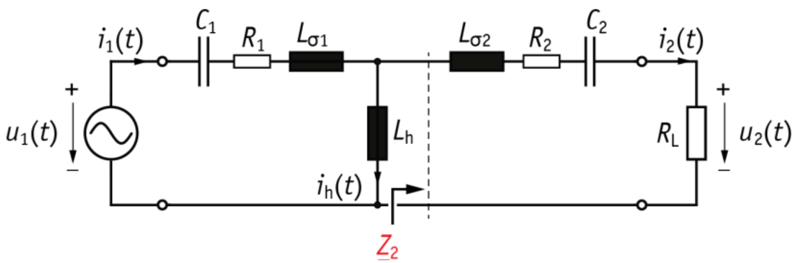


▲ Series compensated receiver - equivalent circuit

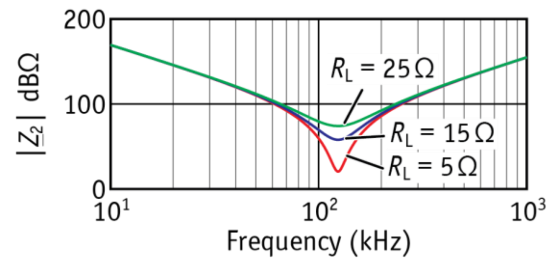


▲ Influence of the load resistance on receiver impedance

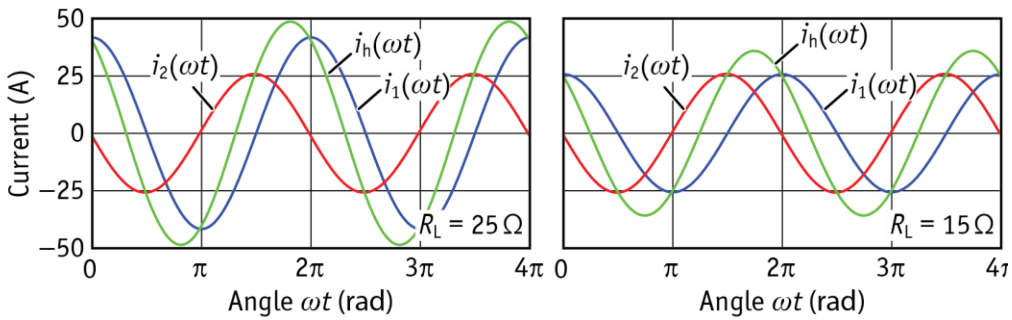


▶ High Load Resistance Leads to decoupling of the Receiver
→ High Transmitter Current $i_1(t)$

▲ Calculated waveforms of transmitter, mutual and receiver currents for different load resistances

# Effect of *Low* Equivalent Load Resistance

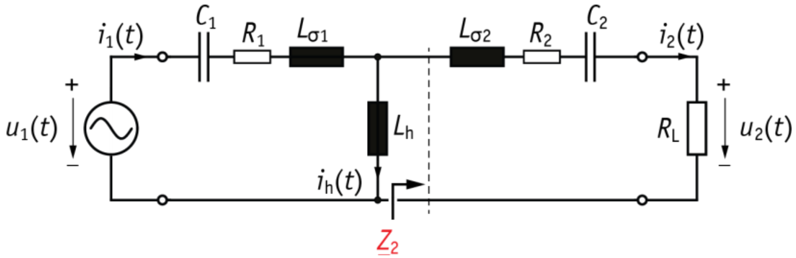


▲ Series compensated receiver - equivalent circuit

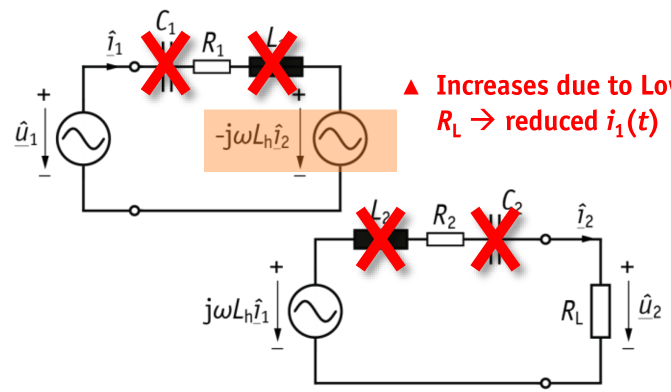


▲ Increases due to Low $R_L$ → reduced $i_1(t)$

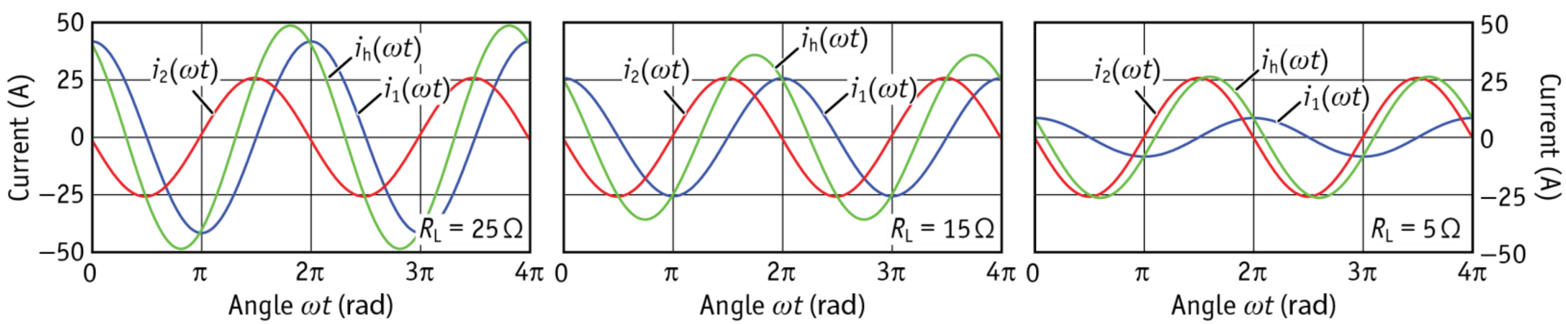


▲ Calculated waveforms of transmitter, mutual and receiver currents for different load resistances

# Load Matching Condition (1)

- Converter Characteristic Exhibit an Loss Minimum / Efficiency Maximum
- Minimum is given by «Matching» of Receiver Coil Reactance $\omega_0 L_2$ and Load $R_L$

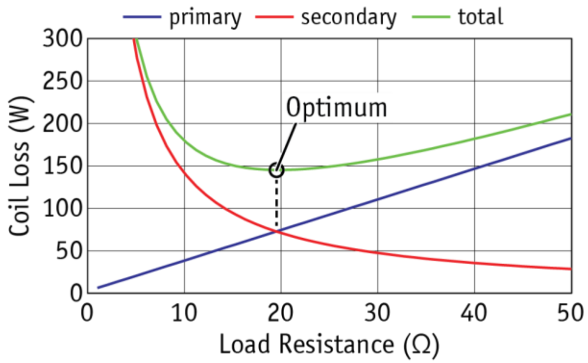


▲ Power losses for given power, frequency, inductance and $k$ = 0.35

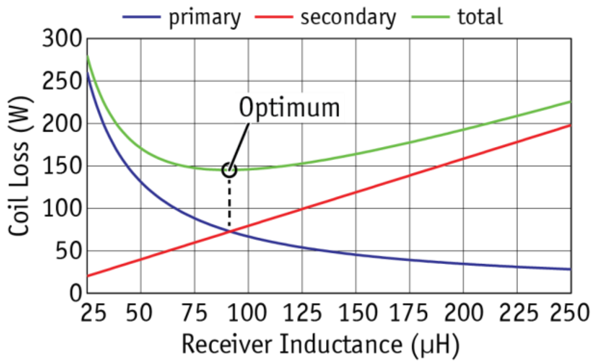


▲ Power losses for given power, frequency, load resistance and $k$ = 0.35

# Load Matching Condition (2)

- Can be Calculated Analytically
- Simple Approximation for $Q > 100$:
  - Series Comp. Receiver: $\left(\frac{R_L}{\omega_0 L_2}\right)_{opt,SS} \approx k$
  - Parallel Comp. Receiver: $\left(\frac{R_L}{\omega_0 L_2}\right)_{opt,SP} \approx \frac{1}{k}\sqrt{1+k^2}$
- Whenever Possible, Design $\omega_0 L_2$ According to «Matching Condition»

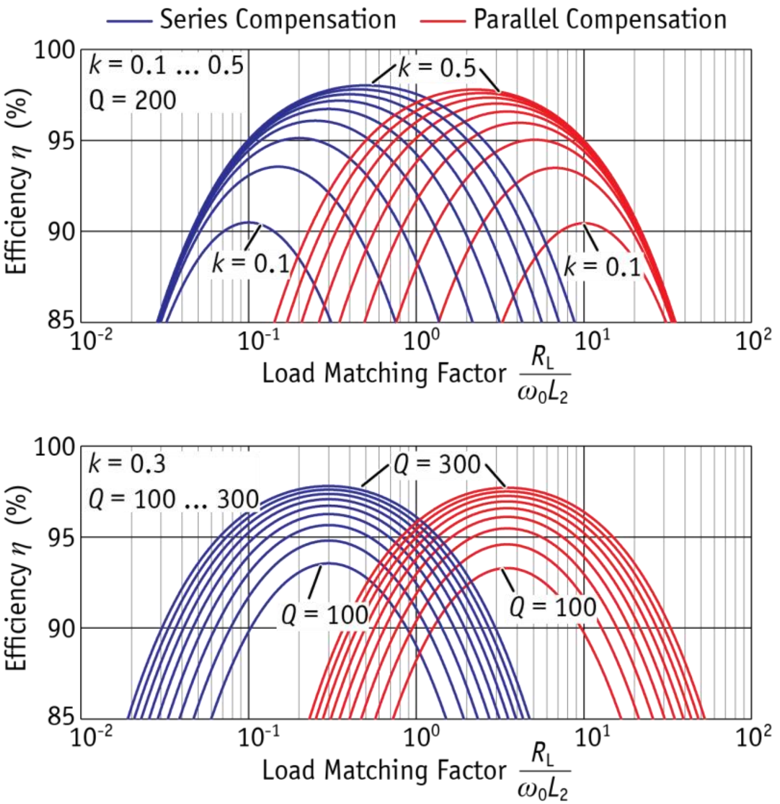

# Maximum Transmission Efficiency

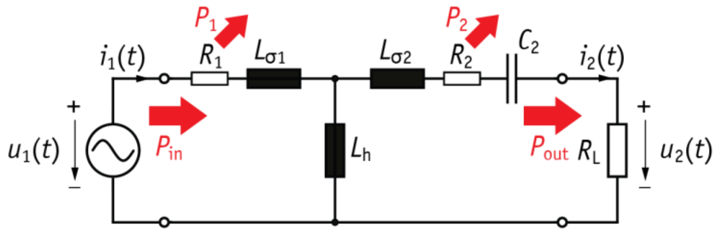


▲ **Power losses mainly occur in coil windings (core losses are neglected here)**

▶ **Physical Limit on Transmission Efficiency**

$$\eta_{max} = \frac{k^2 Q_1 Q_2}{\left(1+\sqrt{1+k^2 Q_1 Q_2}\right)^2}$$

**Figure-of-Merit:** $k\sqrt{Q_1 Q_2} = kQ$

- **Magnetic Coupling** $k \approx 10..35\%$
- **Coil Quality Factors** $Q_1, Q_2$
- **Matching is Needed to Reach** $\eta_{max}$

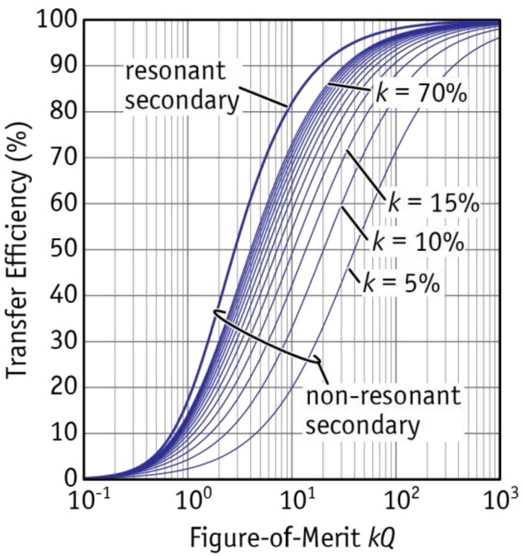


▲ **Efficiency vs. FOM for resonant and non-resonant receiver circuits**

**K. van Schuylenbergh and R. Puers,** *Inductive Powering: Basic Theory and Application to Biomedical Systems*, 1st ed., Springer-Verlag, 2009.

# Alternative Options: Parallel Circuit Topologies

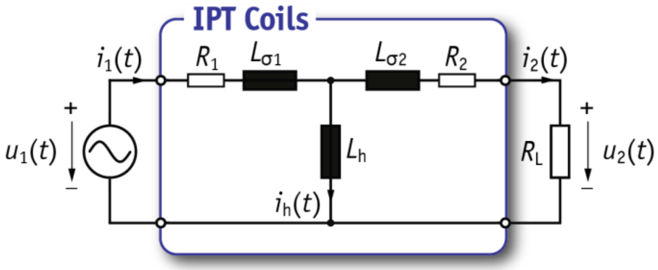


**Possible Compensation Topologies:**

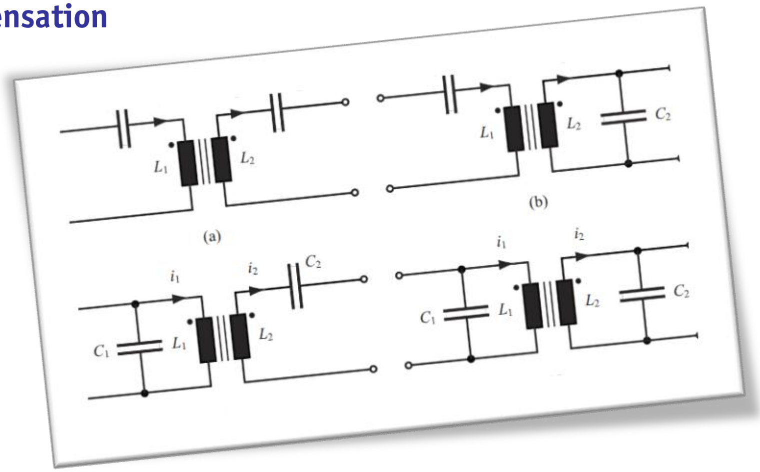


▲ Further possible topologies for the resonant tank

- ▶ **Large Number of Alternative Topologies Exist**
- ▶ **Same Figure-of-Merit and Performance Criteria Apply!**

# Alternative Options: Unity-Gain Resonant Circuit

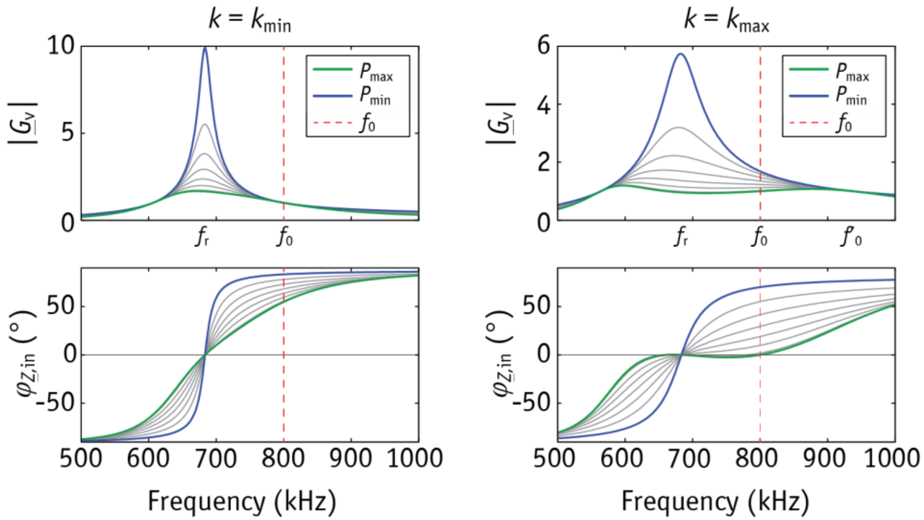


**O. Knecht, R. Bosshard, and J. W. Kolar,** "Optimization of Transcutaneous Energy Transfer Coils for High Power Medical Applications," in *Proc. Workshop on Control and Modeling for Power Electron. (COMPEL)*, 2014.

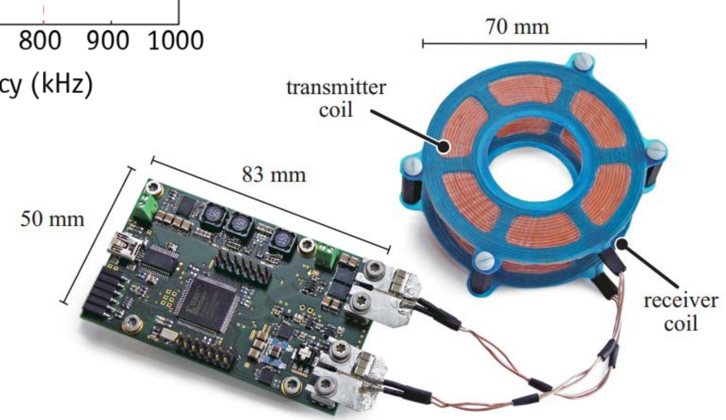


- **Load-Independent Transfer Ratio**
  **(at Cost of Higher RMS Coil Currents)**
- **Useful for Applications, where..**
  - **Reduced Control Effort is Desired**
  - **Transmission Coils have Fixed Positions, e.g. Contactless Gate Drive Supply**

# Σ Inductive Power Transfer

- **Resonant Circuit Design**
  - Series/Series Resonance
  - Load Matching

- **Coil Modeling**
  - Power Loss Estimation
  - Calculation of Stray Field

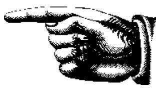

- **Optimization**
  - High Transmission Efficiency
  - High Power Density
  - Cost, Reliability, ...

# Coffee Break

**until 15:30**

# IPT Transmission Coil Design

# Structures of Single-Phase Transformers

▲ Available ferrite parts for power transformers

Source: Huigao Megnetics

- E- and Pot-Core Transformer
- U-Core Transformer
- Toroidal Transformer
  not Suitable for IPT

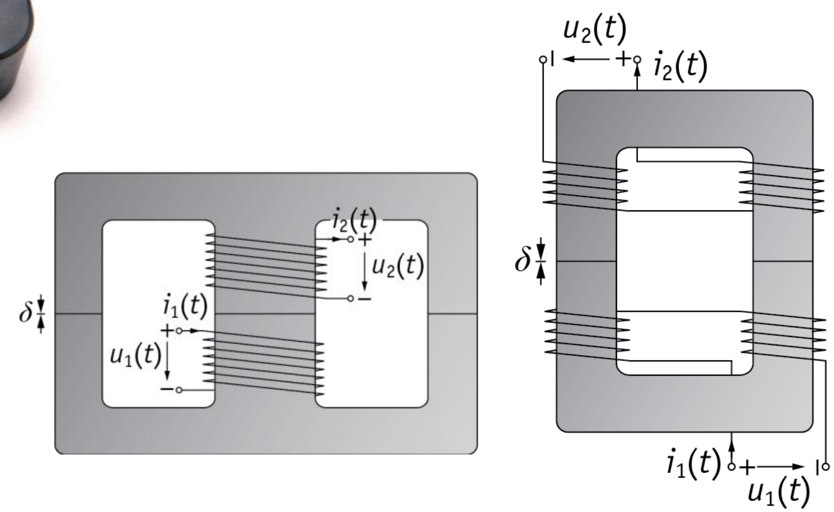


▲ Common structures for single-phase transformers

# Structures for IPT Coils (1)

## E-Type IPT Coils

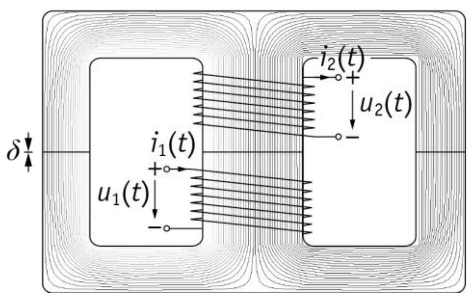


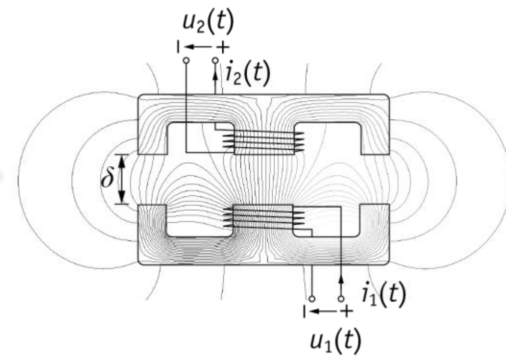


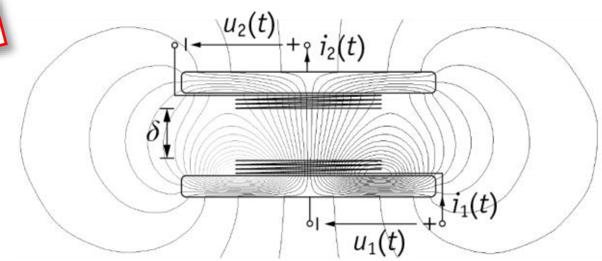


- E- and Pot-Core Transformer
- Flux Follows 2 Loops, E-Shaped Path

# Structures for IPT Coils (2)

## E-Type IPT Coils

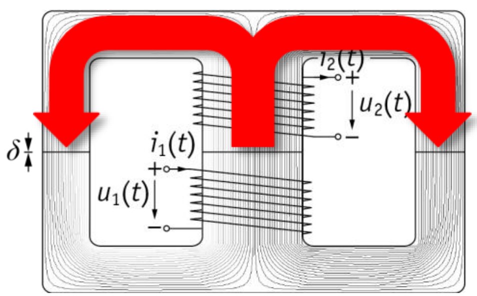


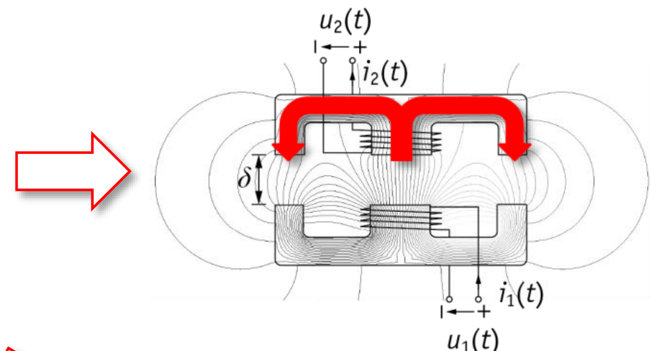


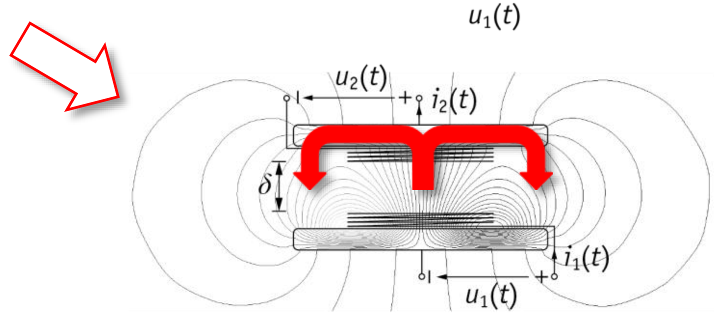


- E- and Pot-Core Transformer
- Flux Follows 2 Loops, E-Shaped Path

# E-Type IPT Coils - Examples

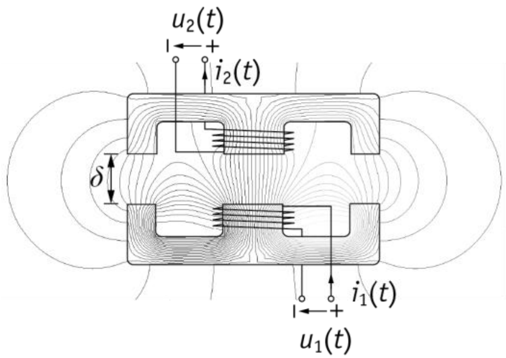


Image: J. Kim *et al.* (KAIST)

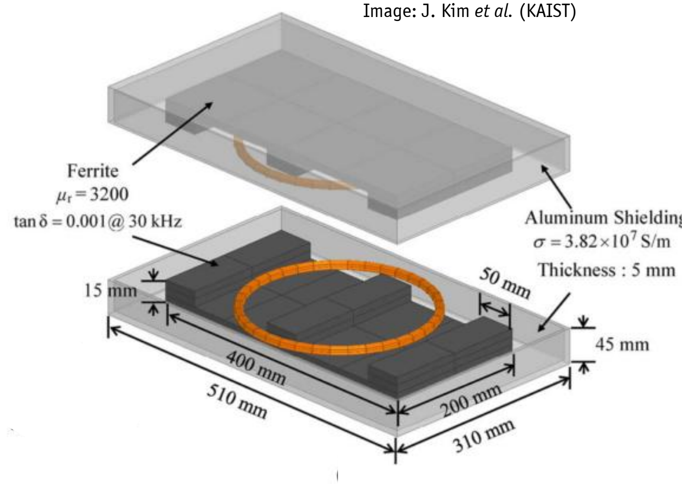


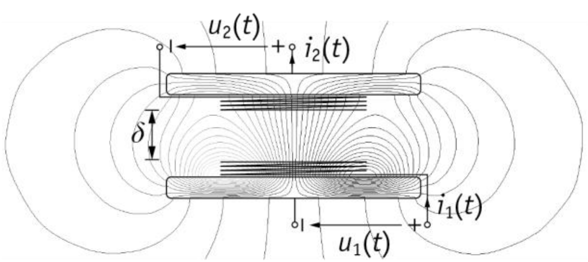


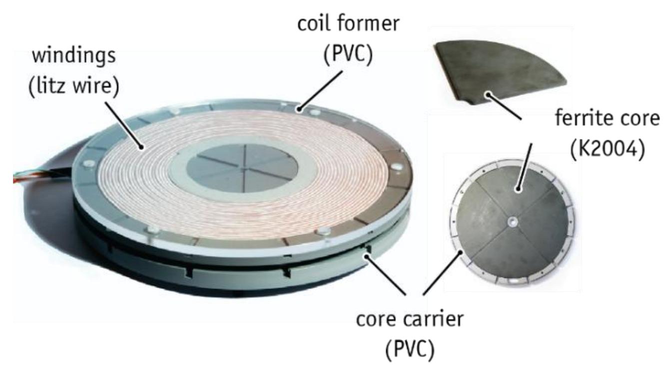

# Structures for IPT Coils (3)

## U-Type IPT Coils

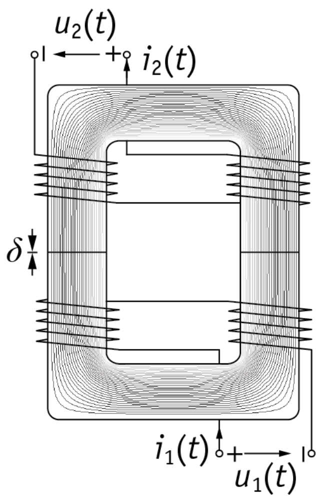


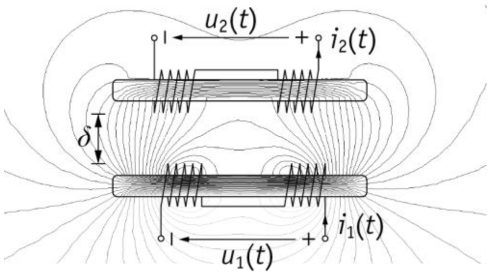


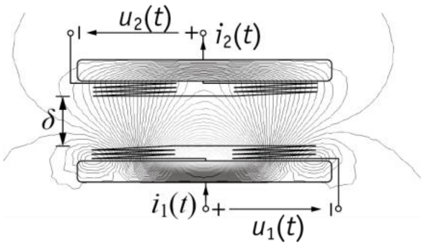


- U-Core Transformer
- Flux Follows 1 Loop, U-Shaped Path

# Structures for IPT Coils (4)

## U-Type IPT Coils

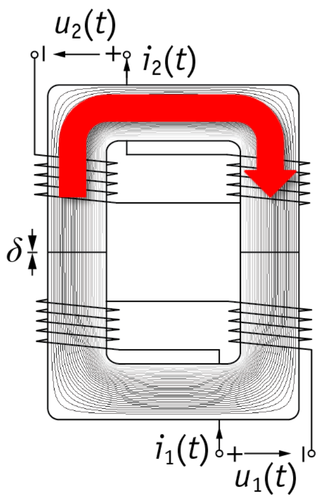


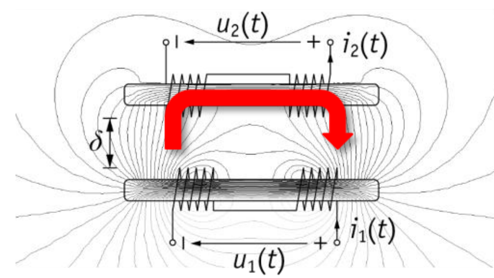


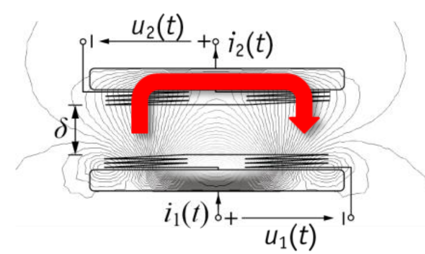


- U-Core Transformer
- Flux Follows 1 Loop, U-Shaped Path

# U-Type IPT Coils - Examples

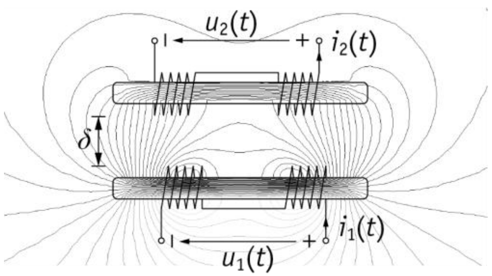


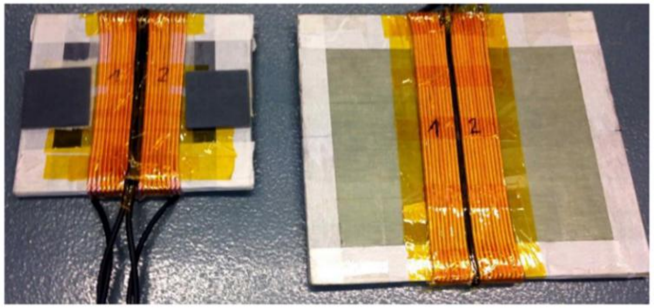

**F. Turki et al.**, "Impact of the working frequency on wireless power transfer systems," in *Proc. Int. Exhibition and Conf. for Power Electronics (PCIM Europe)*, pp. 1378-1383, 2014.

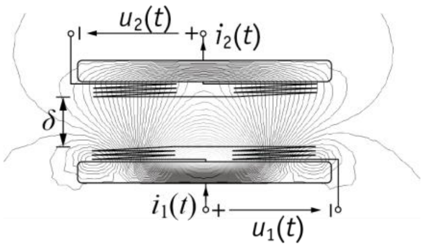


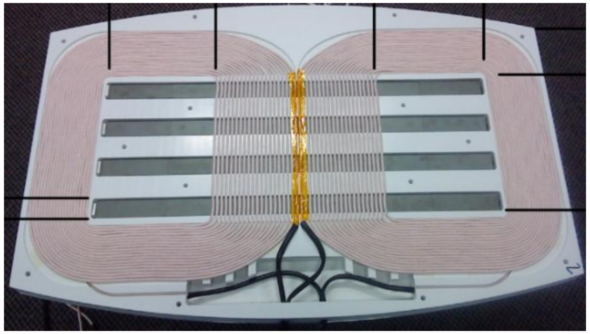

**C.-Y. Huang**, "Design of IPT EV Battery Charging Systems for Variable Coupling Applications," PhD Dissertation, Univ. of Auckland, 2011.

# Performance Comparison of Typical Coil Structures

## Required Performance

- Efficiency → *FOM = kQ*
  - Magnetic Coupling
  - Quality Factor
- Coil Misalignment / Freedom-of-Position
- Coil Size / Power Density
  - Area-related Power Density: $\alpha = P_{out}/A_{coil}$
- Stray Field Compliance
- Material / Manufacturing Cost

# Comparison of Basic Coil Geometries

- Almost Equal Coupling for Circular, Square, Rectangular coil
- Main Factor is the Enclosed Area of the Coil → Maximize!

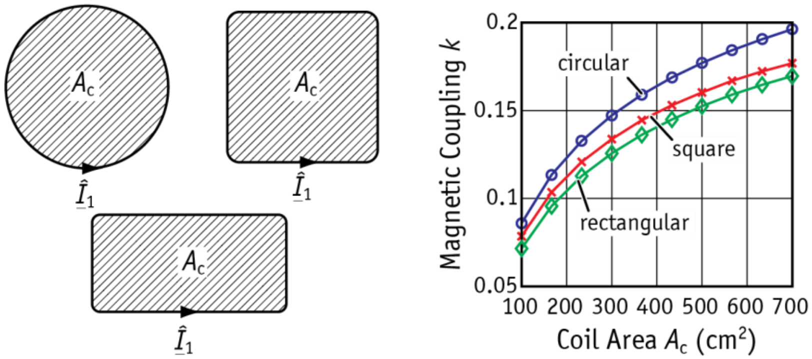


- Area Covered by Winding Determines Coupling of Circular Spiral Coils

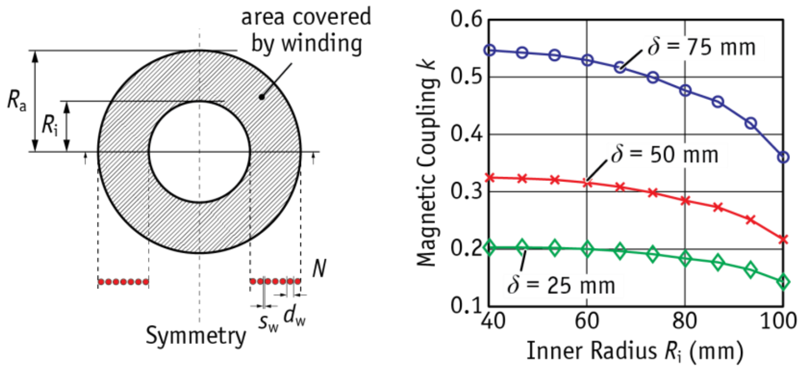

# Coupling - Advanced Designs

- ***The*** **Best Besign … does not Exist.**
  **Main Factor for Coupling:**
  **Enclosed Area of the Coil!**

- **Cooling Capability of Power Electronics and Coil Determine «Misalignment Performance»**

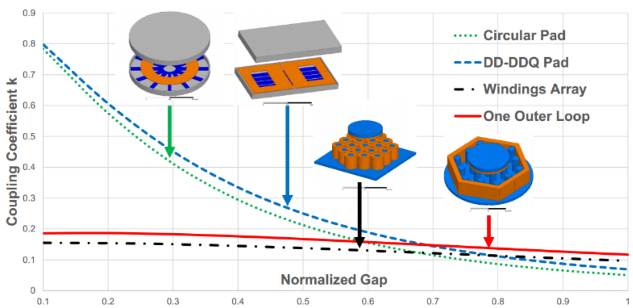


▲ **Magnetic coupling vs. air gap for 4 coil geometries**
**M. Lu and K. D. T. Ngo,** "Comparison of coil designs for wireless inductive power transfer," in *Proc. CPES Power Electron. Conf.*, 2011.

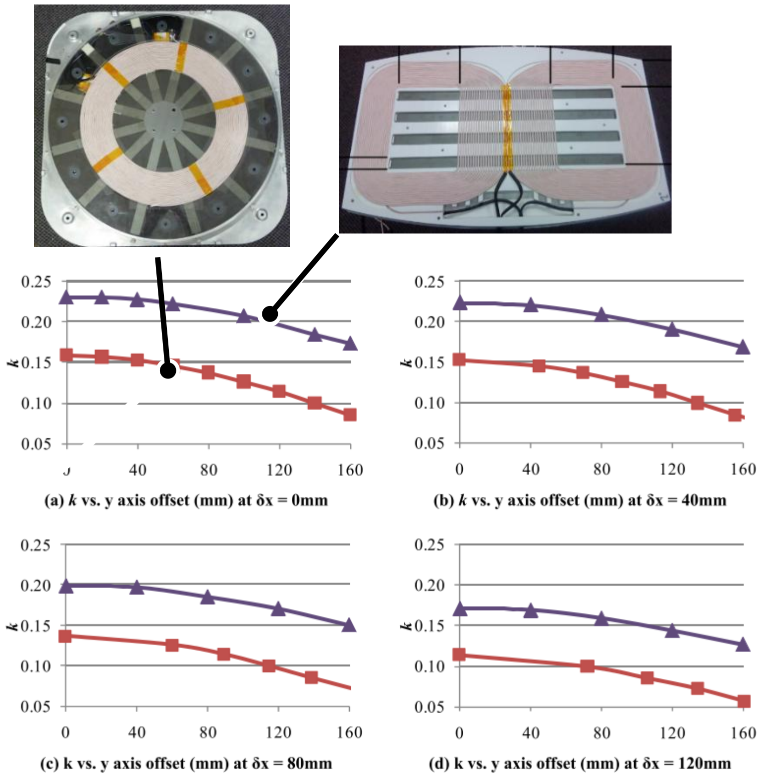


▲ **Measured coupling of a circular pad (700 mm diam.) and a double-D charging pad (740 x 400 mm)**
**C.-Y. Huang,** "Design of IPT EV Battery Charging Systems for Variable Coupling Applications," PhD Dissertation, Univ. of Auckland, 2011.

# Freedom-of-Position: Multiple Coils

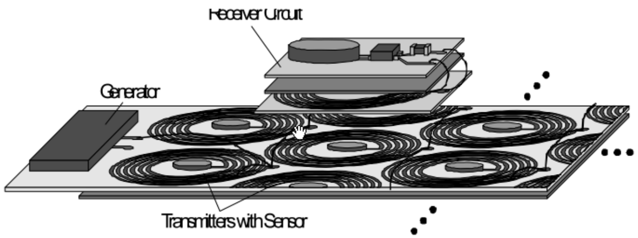


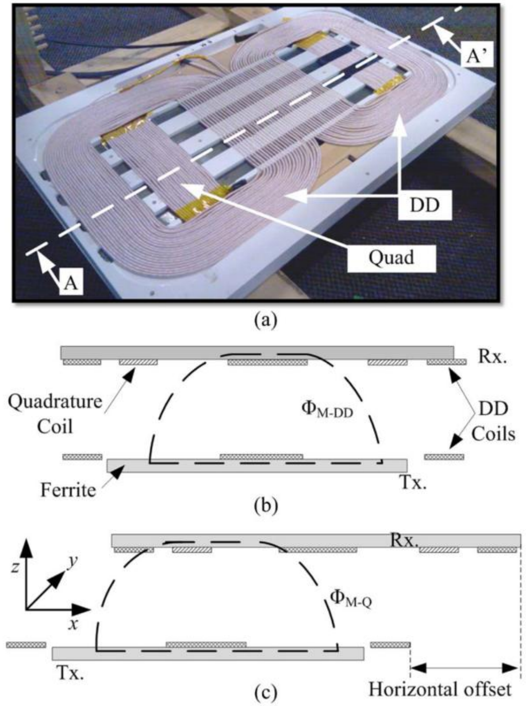


▲ **Array of overlapping transmitter coils improve freedom-of-position of the Philips inductive charging pad**

**E. Waffenschmidt and T. Staring,** "Limitation of inductive power transfer for consumer applications," in *Proc. 13th European Conf. on Power Electron. and Applications (EPE Europe)*, pp. 1-10, 2009.

▲ **Improvement of the double-D with additional coil which is used only in «misaligned» position**

**M. Budhia, J. Boys, G. Covic et al.,** "Development of a single-sided flux magnetic coupler for electric vehicle IPT charging systems," *IEEE Trans. Ind. Electron.*, vol. 60, no. 1, pp. 318-328, 2011.

# Freedom-of-Position: Parking Assistant

▲ IPT charging station with parking guides


▲ Parking assistant with image recognition

Source: Toyota

- **Latest Assistants Achieve 5 cm Parking Accuracy**
- **Dimensioning of Electronics for Worst-Case Parking Position**
- **Control must Provide Compensation**

# Freedom-of-Position: High-$Q$ Coils

- **Physical Limit on Transmission Efficiency**

$$\eta_{\max} = \frac{k^2 Q_1 Q_2}{\left(1 + \sqrt{1 + k^2 Q_1 Q_2}\right)^2}$$

**Figure-of-Merit:** $k\sqrt{Q_1 Q_2} = kQ$

- **Freedom-of-Position:**
  **Compensation of Low $k$ with High $Q$**

- **High-$Q$ Systems: no Fundamental Difference!**

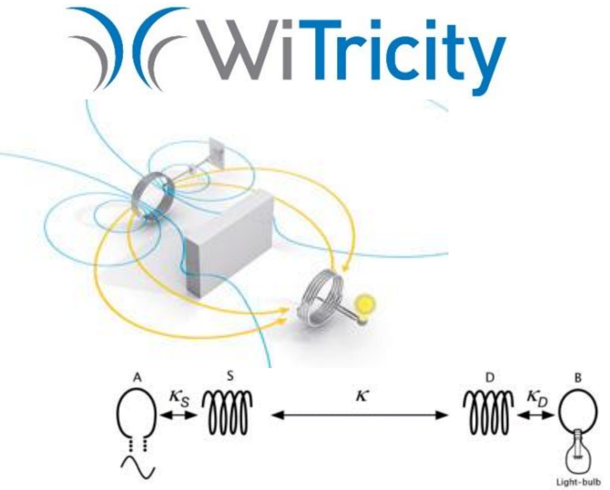


- ***«Highly Resonant Wireless Power Transfer»***
  - Operation of «High-$Q$ Coils» at Self-Resonance (Maximum of $Q$)
  - High Frequency Operation (kHz ... MHz)

# Stray Field & Shielding

# Magnetic Shielding with *Magnetic* Materials (1)

- **Low Reluctance / High Permeability** Materials Allow Guiding Magnetic Field
- **Careful: Frequency Dependency!**

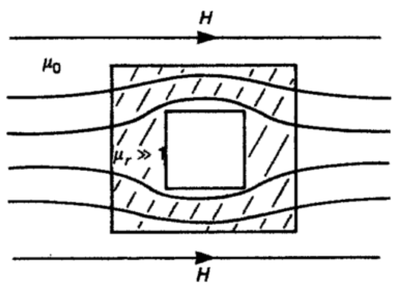


▲ **High permeability material diverts magnetic field**

**C. Paul,** "Shielding," in *Introduction to Electromagnetic Compatibility*, 2nd ed., Jon Wiley & Sons, Hoboken, 2006, ch. 10, sec. 4, pp. 742-749.

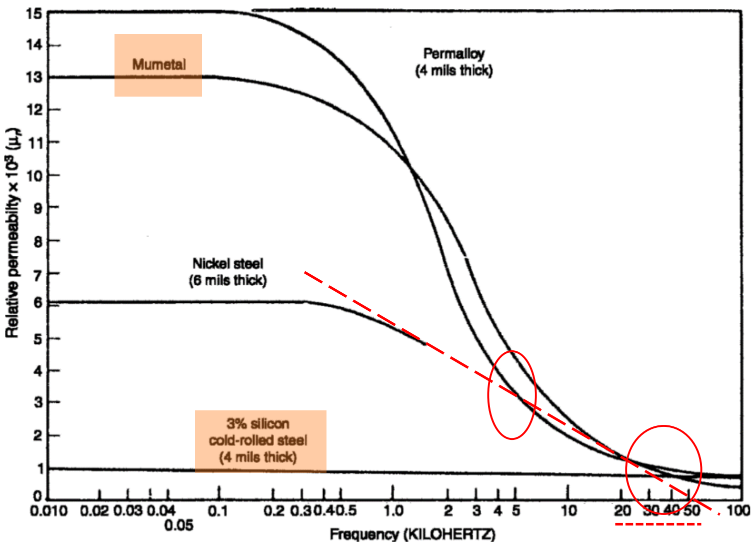


▲ **Frequency dependency of ferromagnetic materials**

**H. W. Ott,** *Noise Reduction Techniques in Electronic Systems,* 2nd ed., Wiley- Interscience, New York, 1988.

# Magnetic Shielding with *Magnetic* Materials (2)

- **Low Reluctance / High Permeability**
  **Materials Allow Guiding Magnetic Field**

- **Not Possible in the Air Gap!**

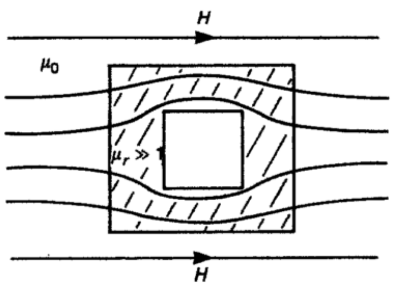


▲ **High permeability material diverts magnetic field**

**C. Paul,** "Shielding," in *Introduction to Electromagnetic Compatibility*, 2nd ed., Jon Wiley & Sons, Hoboken, 2006, ch. 10, sec. 4, pp. 742-749.

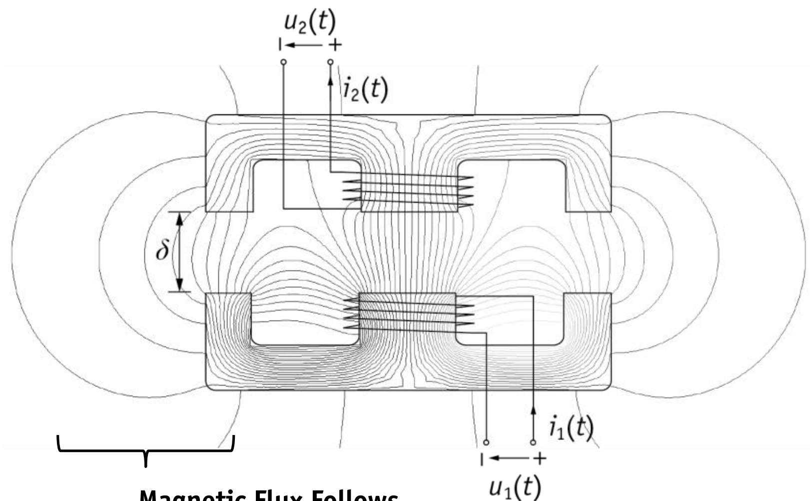


**Magnetic Flux Follows Low Reluctance Path:**

$$R_{\text{mag}} = \frac{l}{\mu_0 A}$$

- **Flux Must Spread out to Sides to Increase Effective *A*!**

# Magnetic Shielding with *Magnetic* Materials (3)

- **Coil Design Must Provide a Return Path for the Flux:**

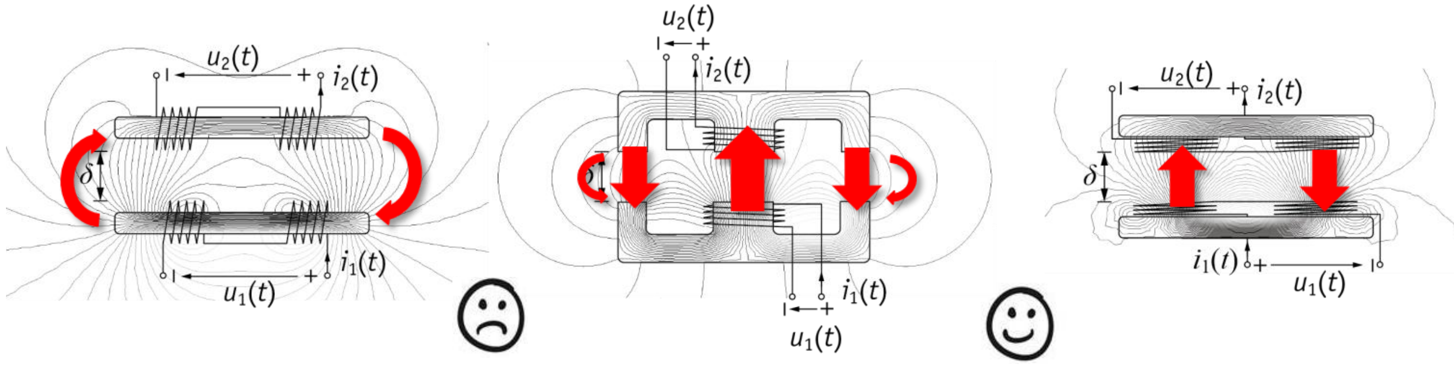


- **Alternative Methods:**
  - **Higher Frequency for Same Power allows Lower Flux in Air Gap** (shown later)
  - **Smaller Coils, Field follows approx. $1/r^2$**
  - **But: Reduces Magnetic Coupling** → **Trade-Off with Efficiency!**

# Magnetic Shielding with *Conductive* Materials

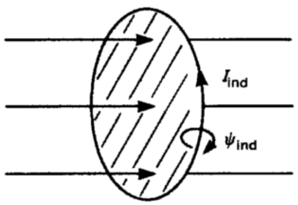


◀ **Current in conductor produces opposing magnetic field**

**C. Paul,** "Shielding," in *Introduction to Electromagnetic Compatibility*, 2nd ed., Jon Wiley & Sons, Hoboken, 2006, ch. 10, sec. 4, pp. 742-749.

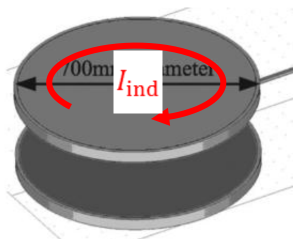


Image: M. Budhia *et al.*

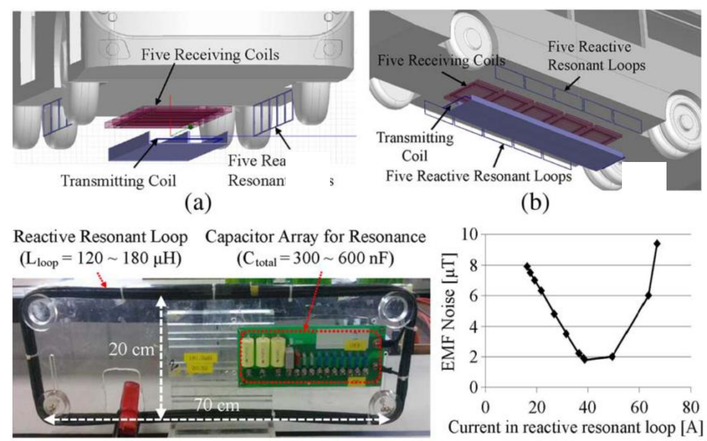


▲ **Selective shielding with additional resonant circuit**

- May Cancel Coupled Flux
- Reduces Magnetic Coupling
- High Eddy Current Losses!

**J. Kim et al.,** «Coil design and shielding methods for a magnetic resonant wireless power transfer system," *Proc. IEEE*, vol. 101, no. 5, pp. 1332 – 1342, 2013.

# Coil Modeling & Power Loss Estimation

# Finite-Element Modeling of IPT Coils

- ▶ **Circular Spiral Coil**
  - **High Coupling / Area Ratio**
  - **Simplified Modeling & Verification**

- ▶ **Axis-Symmetric Design**
- ▶ **Frequency Domain Model at Resonant Frequency**

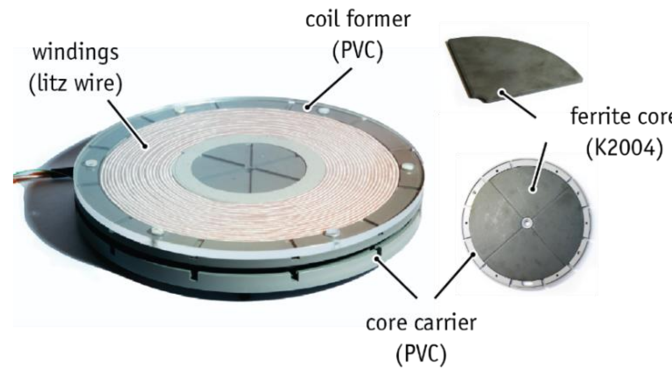


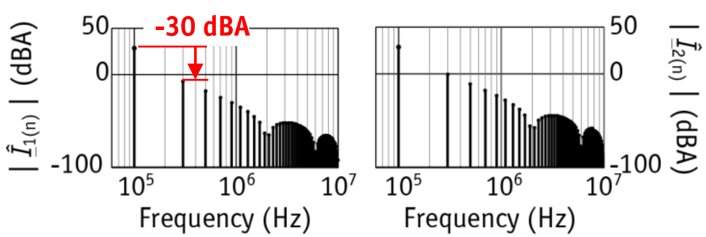


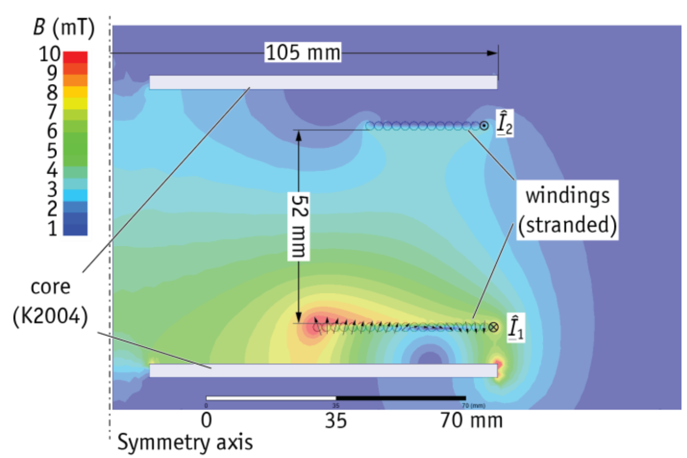


- ▶ **2D-Finite Element Solvers:**
  - **FEMM (free, www.femm.info)**
  - **Ansys Maxwell, COMSOL, ...**

# FE-Assisted Winding Loss Calculation

**J. Mühlethaler,** "Modeling and multi-objective optimization of inductive power components," Ph.D. dissertation, Swiss Federal Insititute of Technology (ETH) Zurich, 2012.

- **Skin-Effect Calculated Analytically**

$$p_{\mathrm{skin}} = n \cdot R_{\mathrm{dc}} \cdot F_{\mathrm{R}}(f_0) \cdot \left(\frac{\hat{I}}{n}\right)^2$$

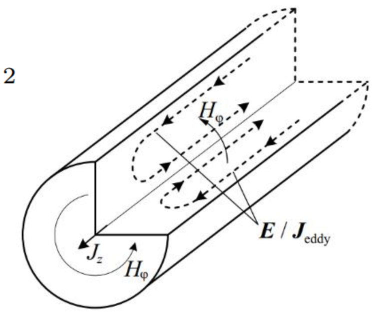


- **Proximity-Effect Calculation Requires External Field**

$$p_{\mathrm{prox}} = n \cdot R_{\mathrm{dc}} \cdot G_{\mathrm{R}}(f_0) \cdot \left(\hat{H}_{\mathrm{e}}^2 + \frac{\hat{I}^2}{2\pi^2 d_{\mathrm{a}}^2}\right)$$

from FE

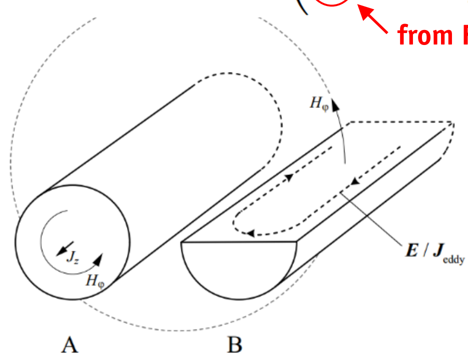


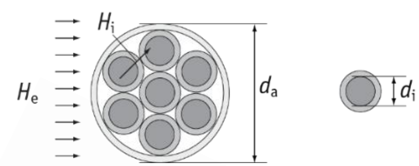


# FE-Assisted Core Loss Calculation

▲ Ferrite core segment (Kaschke K2004)

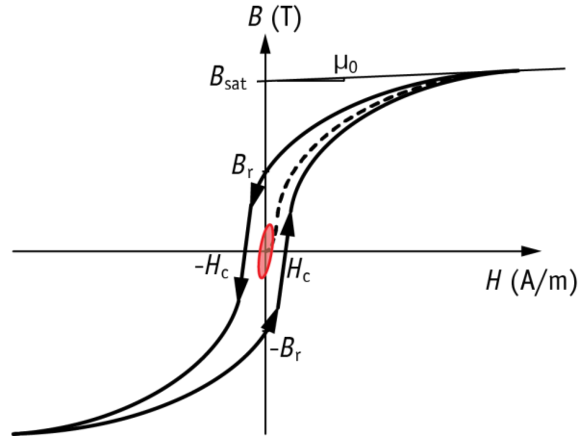


▲ Schematic drawing of BH-loop

- **Core Loss Integration with FE-Tool**
  - Assumption: Sinusoidal Current, Calculation with Steinmetz Equation

$$p_{\mathrm{core}} = \kappa \cdot f_0^{\alpha} \cdot \hat{B}^{\beta}$$

- **Flux Density Low,** due to High Air Gap Reluctance
- **Core Losses have Minor Effect,** 24% Core Losses @ 100 kHz

# Verification of
# FEM Field Calculations

# Verification of FEM Field Calculations

▲ Commercial field probe Narda ELT-400

- Commercial Field Probe
  - 12 cm Probe-Head Diameter
  - High Bandwidth
  - High Cost

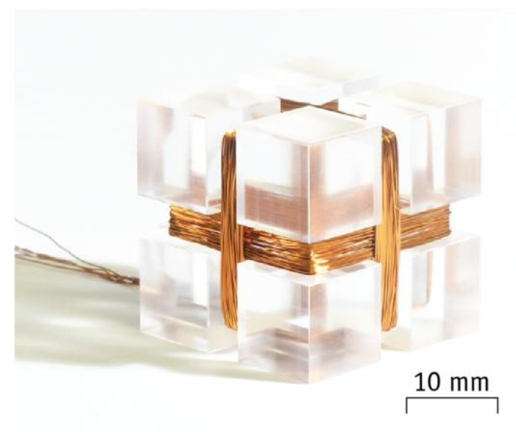


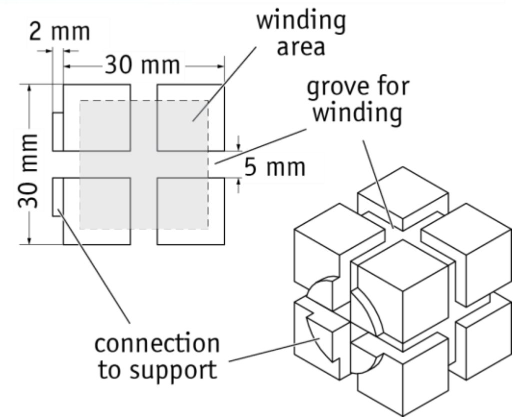

# Design of Custom Field Probe

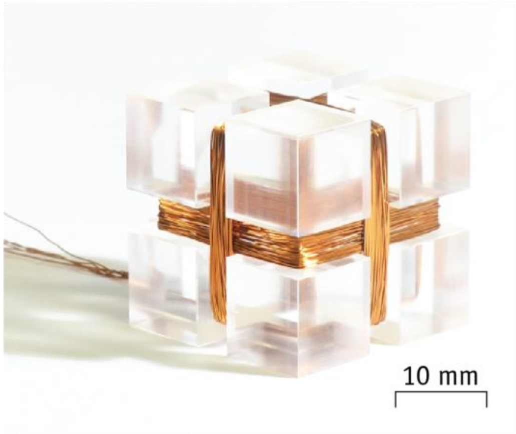


▲ Custom field probe for verification

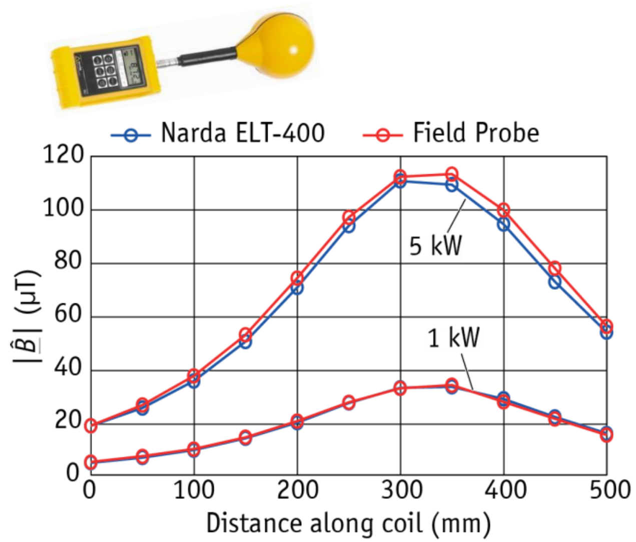


▲ Comparison to commercial product

- **Probe for Magnetic Field Measurements**
  - Optimized for 100 kHz, High Accuracy
  - Sensitivity: 14.5 mV/μT @ 100 kHz
  - Accuracy: < 5% Error (Compared to Narda ELT-400)
  - Size: 30x30x30 mm

# Measurement of the Stray Field @ 5 kW

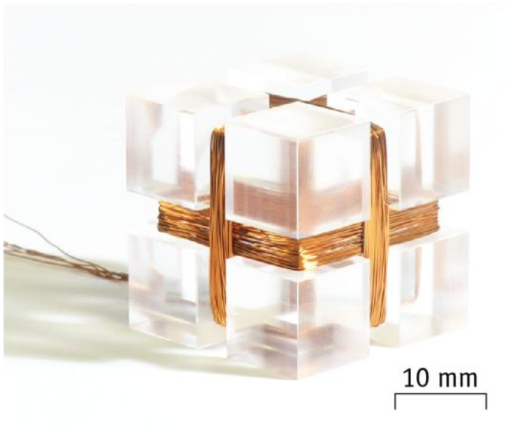


▲ Custom field probe for verification

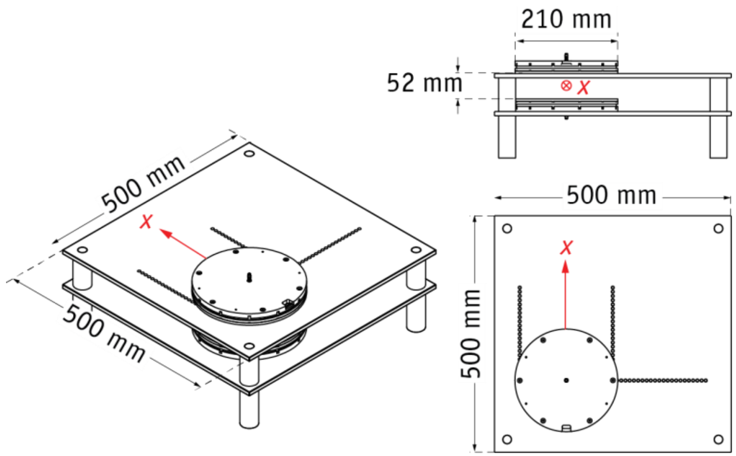


- FE Models for Prediction of Stray Field Accurate: < 10% error
- Prototype Complies with ICNIRP 2010 at 300 mm

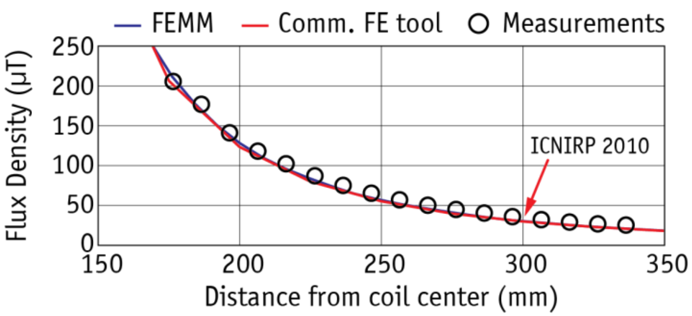


▲ Measured stray field @ 5 kW

# Σ Inductive Power Transfer

- **Resonant Circuit Design**
  - Series/Series Resonance
  - Load Matching
- **Coil Modeling**
  - Power Loss Estimation
  - Calculation of Stray Field
- **Optimization**
  - High Transmission Efficiency
  - High Power Density
  - Cost, Reliability, ...

# $\eta$-$\alpha$-Pareto Optimization

*Multi-Objective Optimization*
*Design of Scaled Prototype System*
*Experimental Verification*

## DESIGN TASK

# *Transfer of 5 kW Across Air Gap of 52 mm*

▶ **Specifications:**

| | |
|---|---|
| Output Power | 5 kW |
| Air Gap | 52 mm |
| Input Voltage | 400 V |
| Output Voltage | 350 V |

▶ **Degrees-of-Freedom:**

- Type of Litz Wire
- Core Shape and Material
- Transmission Frequency
- Coil Size / Area
- (Compensation Method)

▶ **Performance Measures:**

- Transfer Efficiency: $\eta = P_{out}/P_{in}$ [%]
- Area-Related Power Density: $\alpha = P_{out}/A_{coil}$ [kW/dm$^2$]

▶ **R. Bosshard, J. W. Kolar et al.,** "Modeling and $\eta$-$\alpha$-Pareto optimization of inductive power transfer coils for electric vehicles," IEEE J. Emerg. Sel. Topics Power Electron. (accepted for publication), 2014.

# $\eta$-$\alpha$-Pareto Optimization of IPT Coils

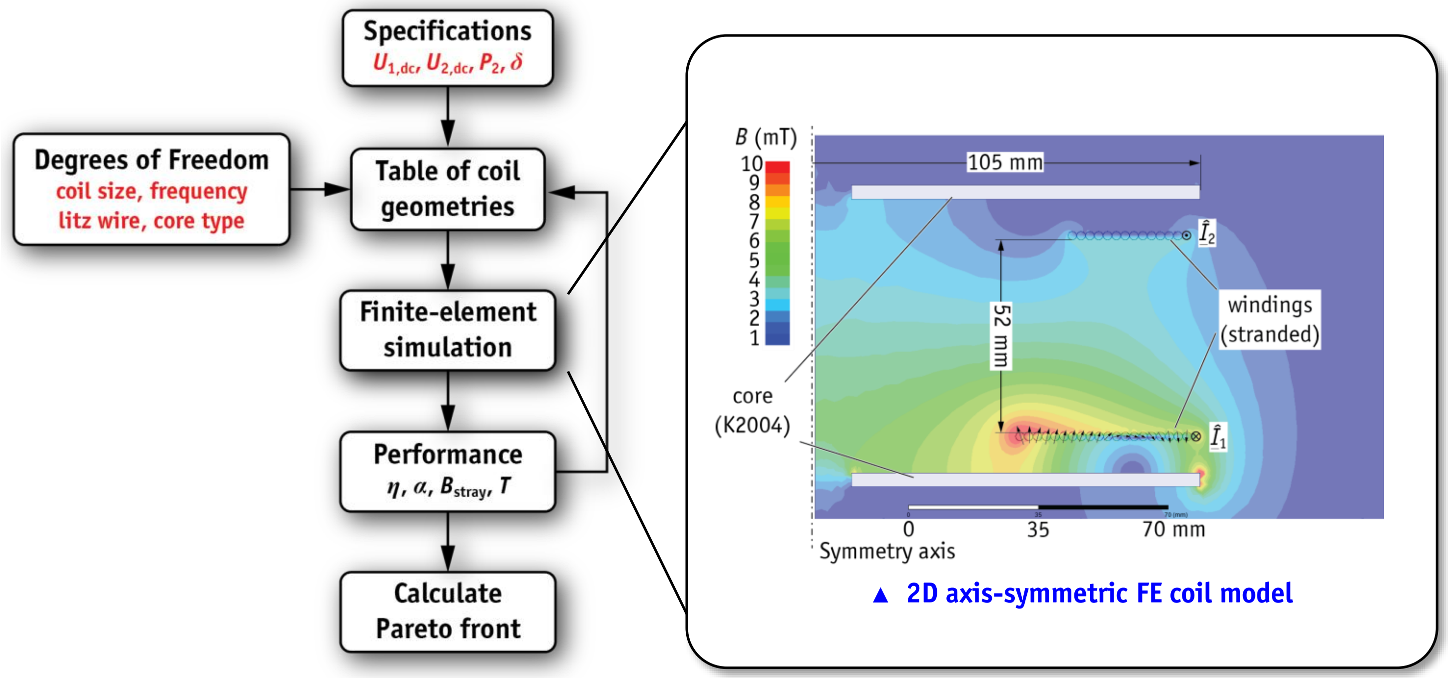


▲ 2D axis-symmetric FE coil model

# $\eta$-$\alpha$-Pareto Optimization – Results (1)

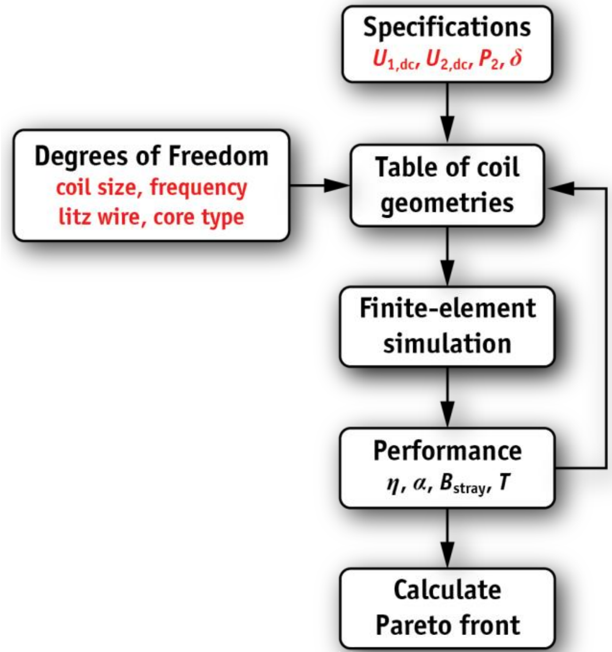


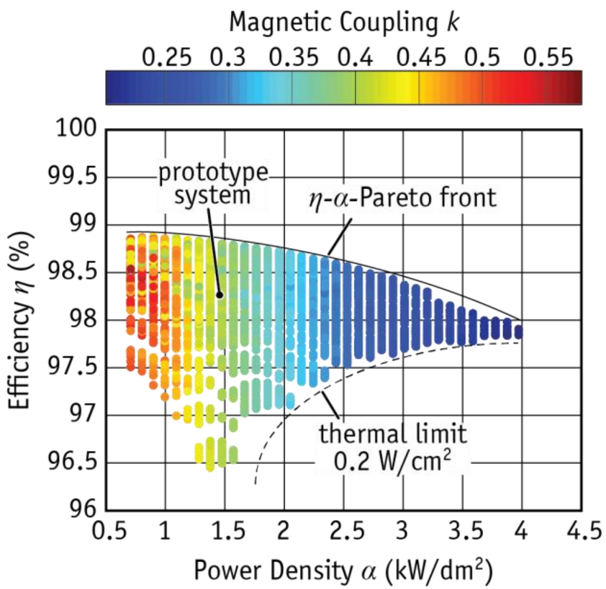


▲ Calculated efficiency vs. power density of >12k IPT coils with 5 kW output power

# $\eta$-$\alpha$-Pareto Optimization – Results (2)

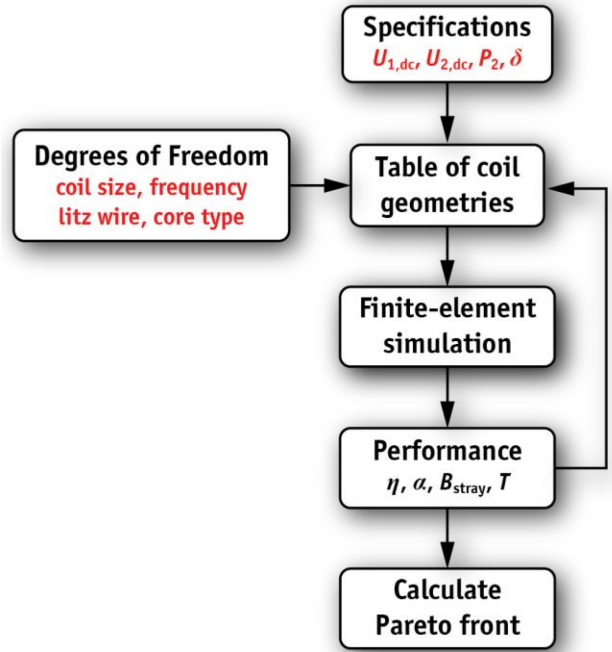


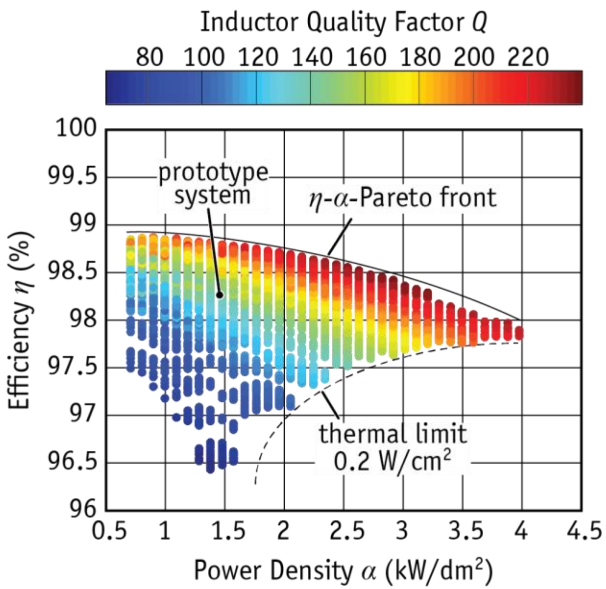


▲ Calculated efficiency vs. power density of >12k IPT coils with 5 kW output power

# $\eta$-$\alpha$-Pareto Optimization – Results (3)

- **Higher Transmission Frequency Leads Reduced Coil Losses!**
  - **Reason:**

**Matching Condition:** $$\left(\frac{R_L}{\omega_0 L_2}\right)_{opt,SS} \approx k$$

**Higher $\omega_0$ → Lower $L_2$ → Lower $N$**
**→ Shorter Windings**
**→ Lower $R_{ac}$**

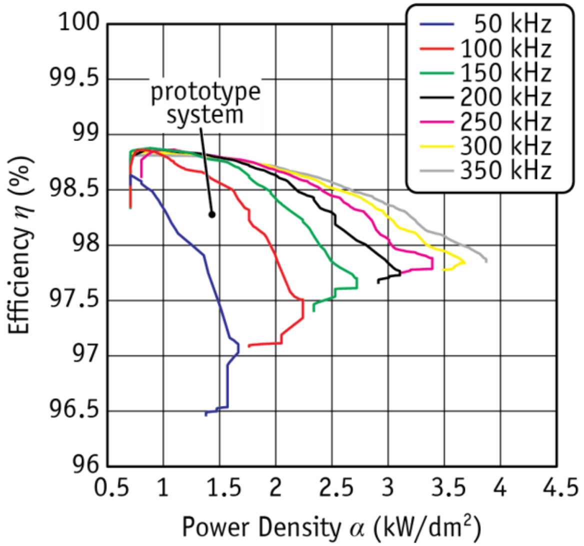


▲ **Calculated efficiency vs. power density, divided by transmission frequency**

# Selection of a Transmission Frequency

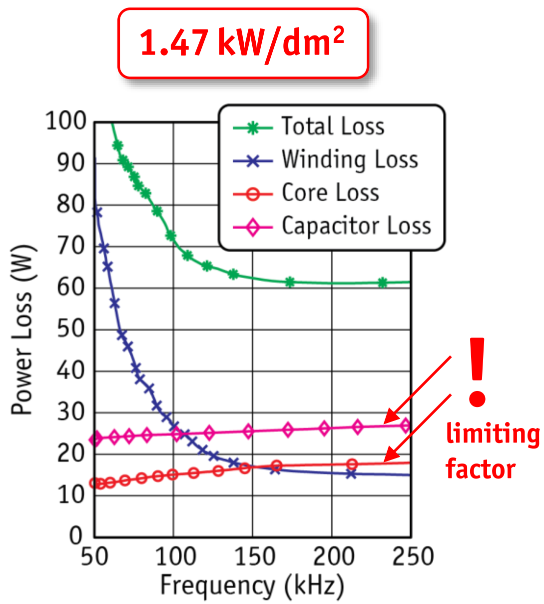


▲ Power loss breakdown at 1.47 kW/dm²
(power density of prototype)

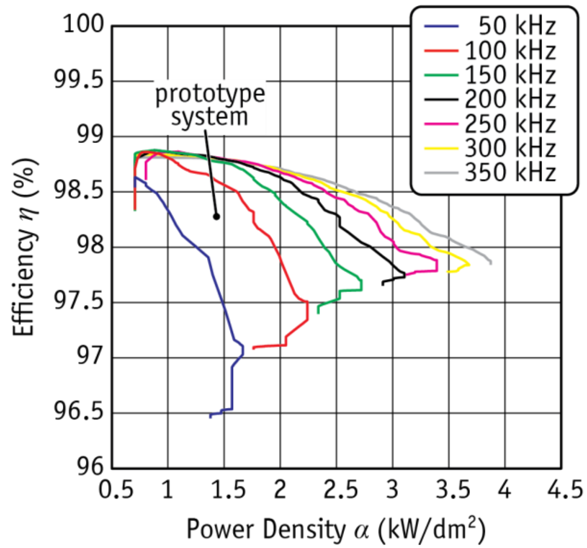


▲ Calculated efficiency vs. power density, divided by transmission frequency

# Benefit from Ideal Components

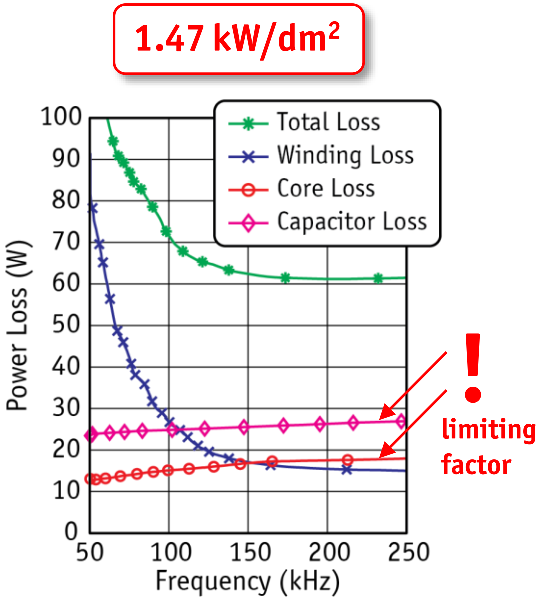


▲ Power loss breakdown at 1.47 kW/dm²
(power density of prototype)

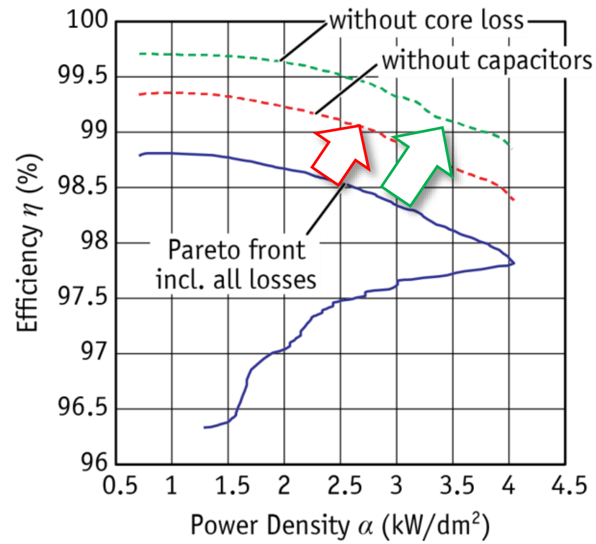


▲ Calculated efficiency vs. power density,
for ideal capacitors and core material

# Transmission Frequency – Further Limitations

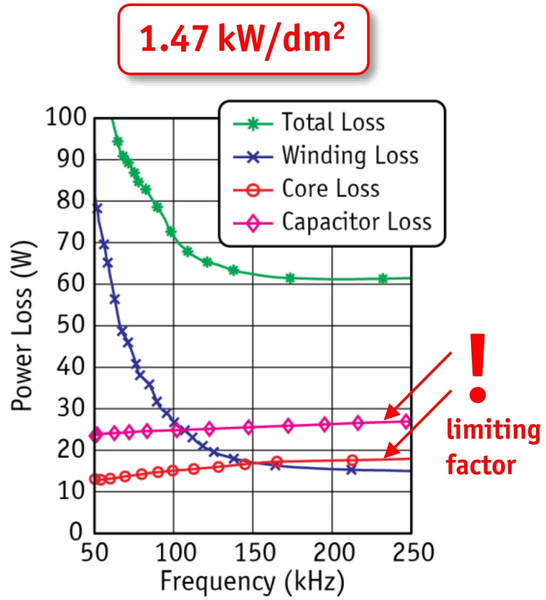


▲ Power loss breakdown at 1.47 kW/dm²
(power density of prototype)

▶ **Other Limiting Factors:**

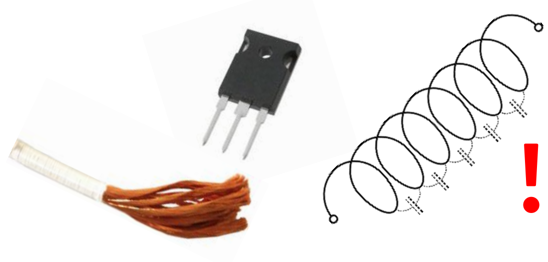

- Availability / Cost of Litz Wire
- Frequency Dependent Losses of Power Electronic Converter (e.g. Gate Driver)
- Parasitics of Coil and Converter (Coil Self-Resonance)
- Switching Speed of Semiconductors

# Trade-Off: Efficiency vs. Stray Field

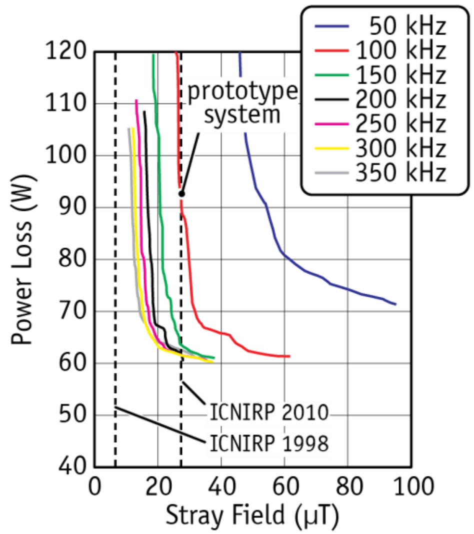


▲ Calculated efficiency vs. stray field at 30 cm distance from coil center

- Smaller Coils have Higher Losses
- ... and Lower Stray Field

} Trade-off!

- Higher Frequency Allows Lower Flux in Air Gap for Equal Power } Trade-off!

– High Frequency Preferred for Low Stray Field & High Efficiency !

- Matching Condition: $\left(\frac{R_L}{\omega_0 L_2}\right)_{\mathrm{opt,SS}} \approx k$

– Higher $\omega_0$ → Lower $L_2$ → Lower $N$ → Lower $R_{ac}$ → Lower Flux!

# Designed 5 kW Prototype IPT Coil

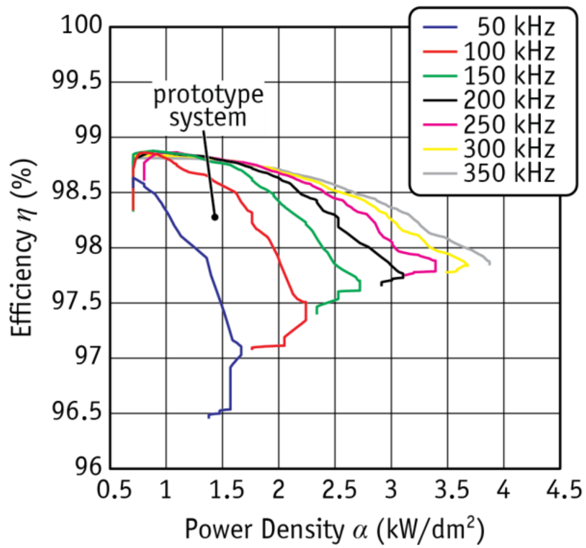


| Coil Diameter | 210 mm* |
|---|---|
| Transm. Efficiency | 98.25% |
| Power Density | 1.47 kW/dm$^2$ |
| Stray Field | 26.16 μT |

* Air Gap 52 mm, Ratio ≈ 4

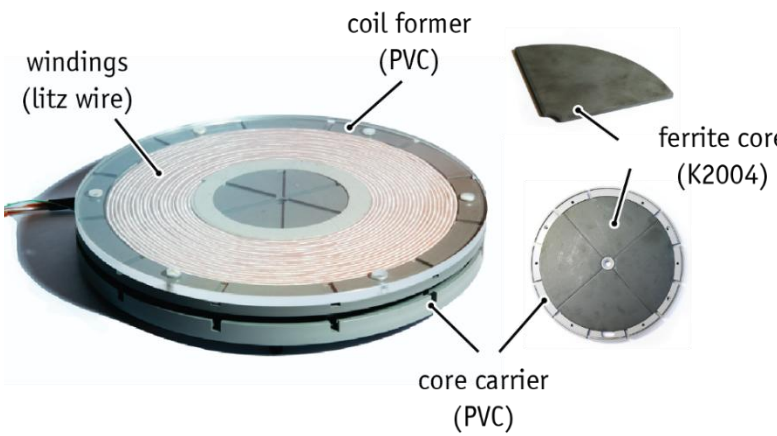


▲ Scaled 5 kW prototype IPT coil

# DC-to-DC Power Loss Measurement

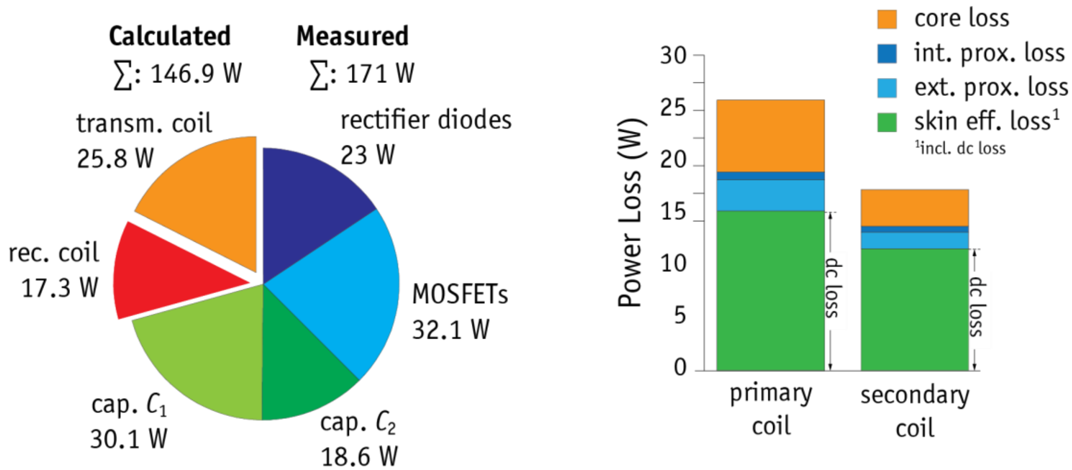


▲ Breakdown of power losses at 5 kW output power

- **FE-Based Power Loss Models are Accurate: < 14% error**
- **DC-to-DC Efficiency > 96.5% (incl. Capacitors & Semiconductors)**

# Thermal Model & Verification

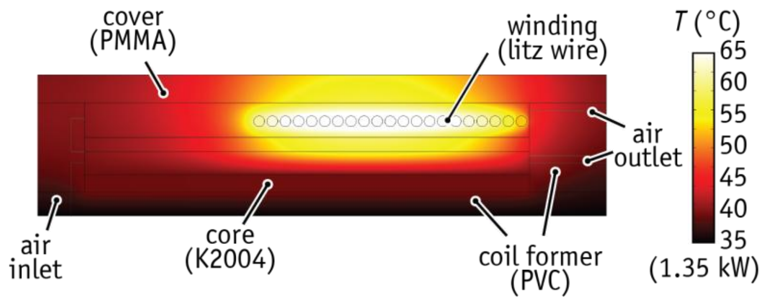


▲ Thermal simulation of prototype IPT coil

- **Thermal Modeling with FE tool for Design Verification**
- **Accuracy: < 5% Error of Steady-State Temperature**

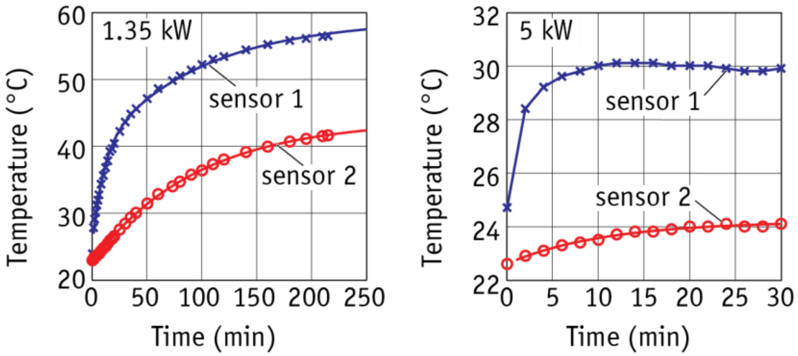


▲ Thermal measurements with thermocouples
(with and without forced air cooling)

# Control Methods for IPT Systems

*Frequency Control Methods*
*Controlled DC-Link Voltages*
*Measured Performance Comparison*

# Frequency Control Methods

# Frequency Control Method

- **Frequency Control Above Resonance**
  - **Regulation of Output Voltage / Power**
  - **Zero Voltage Switching of Inverter in Inductive Region of Input Impedance**
  - **Simplicity & Robustness**
- **Most Widely used Control Method for High-Power IPT Systems**

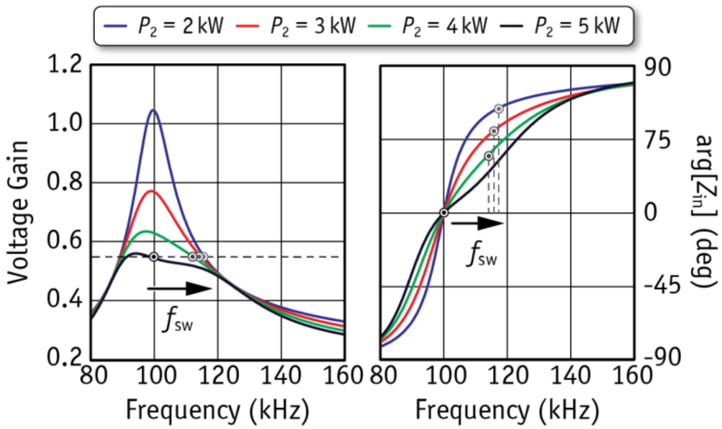


▲ **Voltage transfer function / input phase angle**

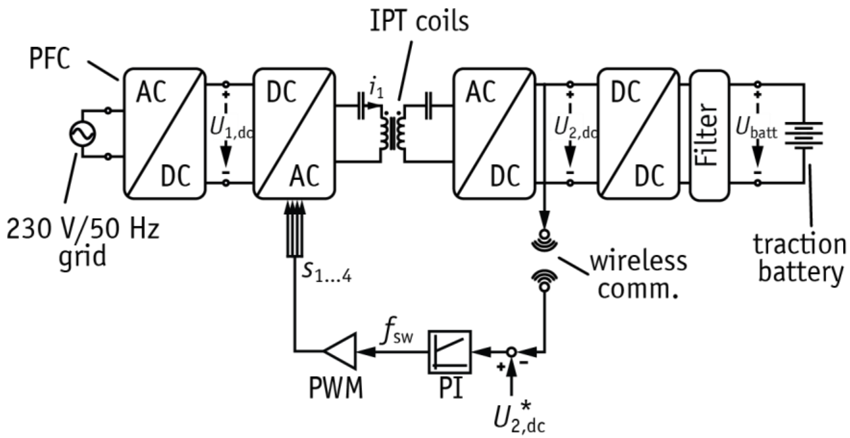


◀ **Control-diagram for a PI-based frequency controller**

# Dual / Self-Oscillating Control Method

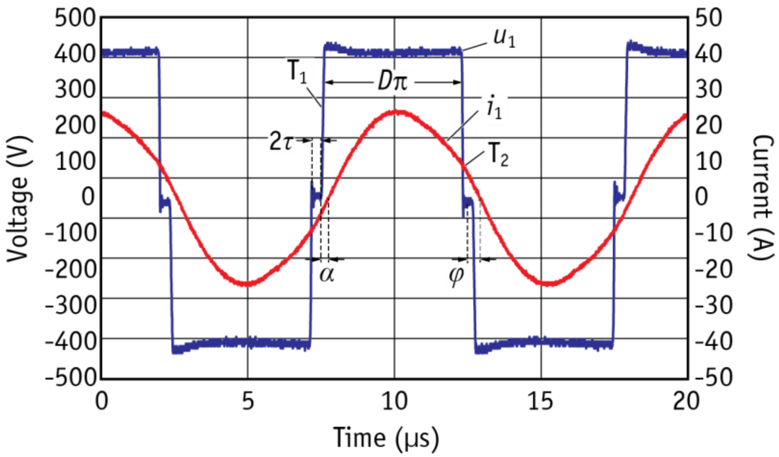


▲ Working principle of self-oscillating controller

- **Tracking of Transmitter Coil Current Zero Crossings**
  - Automatically Follow Resonance
  - Guaranted Zero Voltage Switching

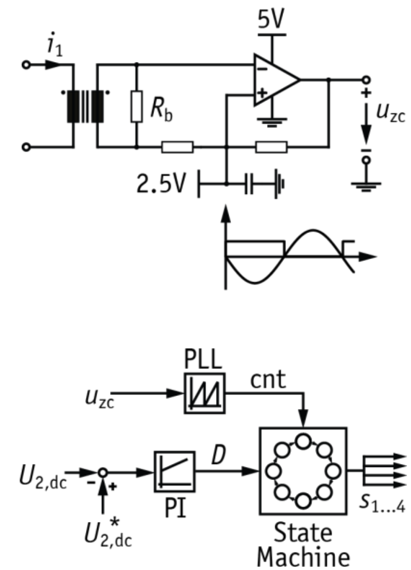


▲ Current zero crossing detection and control-diagram

**J. A. Sabate, M. M. Jovanovic, F. C. Lee, and R. T. Gean,** "Analysis and design-optimization of LCC resonant inverter for high-frequency AC distributed power system," in *IEEE Trans. Ind. Electron.*, vol. 42, no. 1, pp. 63–71, 1995.

# Dual / Self-Oscillating Control – Measured Performance

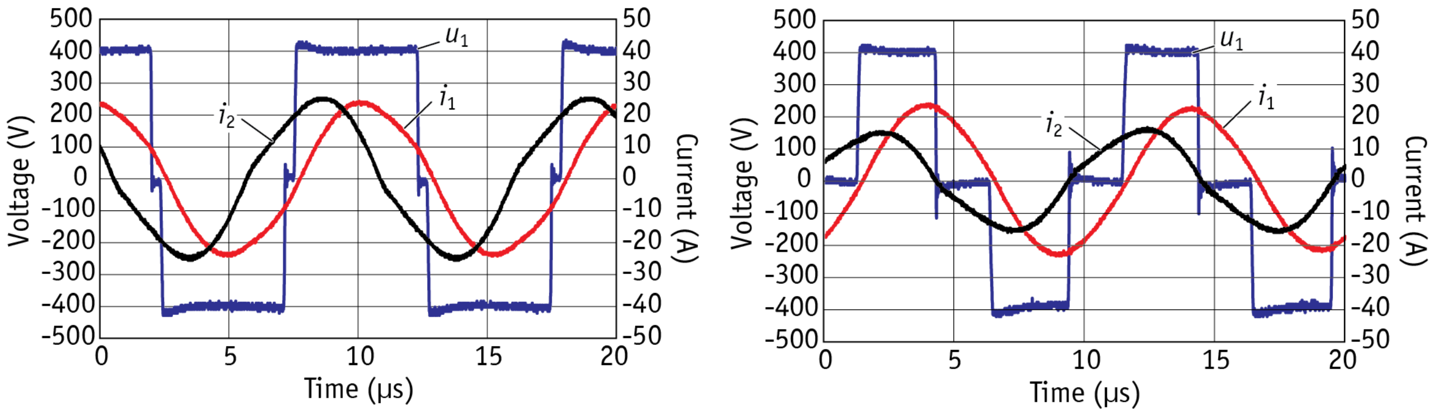


▲ Measured waveforms for dual control
at duty cycles $D$ = 0.95 / 0.65

- **Small Reduction of Transmitter Coil Current**
- **Transition from Active to Reactive Power**
  - Due to Increased Frequency into Inductive Region
  - Partial-Load Efficiency?

(same is Observerd for Frequency Control)

# Variable DC-Link Voltage Control Method

# Variable Amplitude Control

- **Duty-Cycle Control**

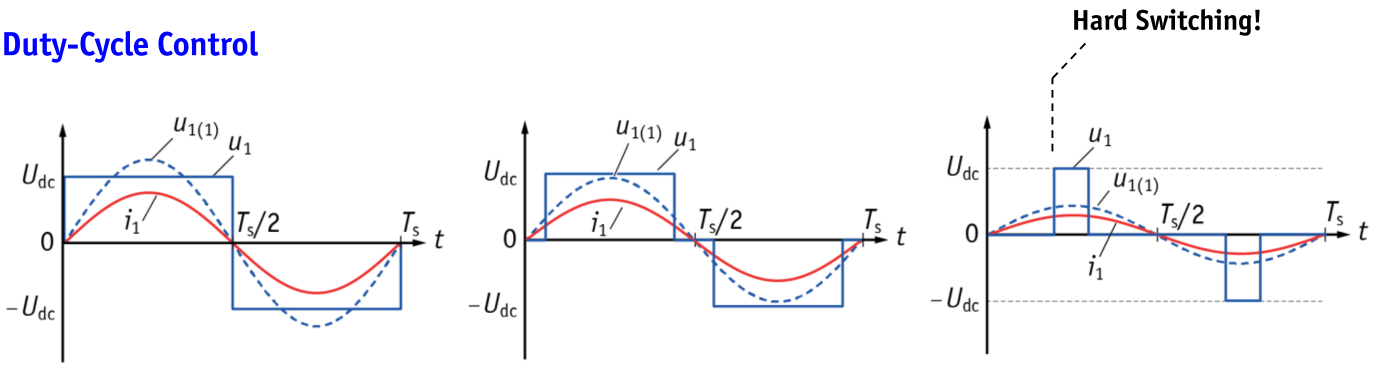


- **Control of the DC-link Voltage**

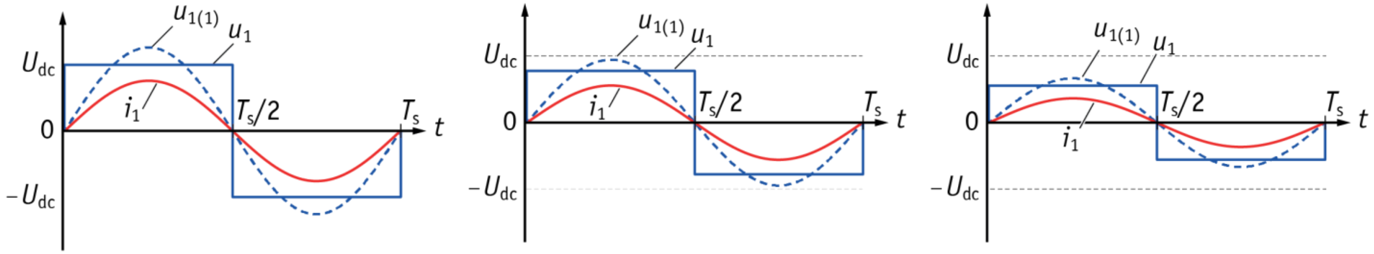

# Proposed System Topology (1)

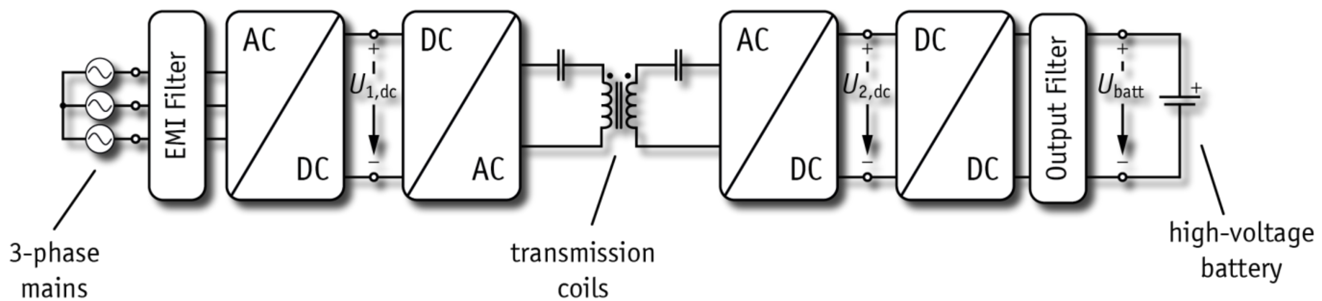


▲ Structure of a 3-phase 2-stage IPT charging system

- **Controlled DC-Link on Both Sides**
  - **Buck-Type PFC: Controls $U_{1,dc}$ from Grid Side**
  - **DC-DC-Converter: Controls $U_{2,dc}$ from Battery Side**

- **Calculated Output Power**

$$P_2 = \frac{8}{\pi^2} \frac{U_{1,dc} U_{2,dc}}{\omega_0 L_h}$$

**Several Options for Optimization!**

# Proposed System Topology (2)

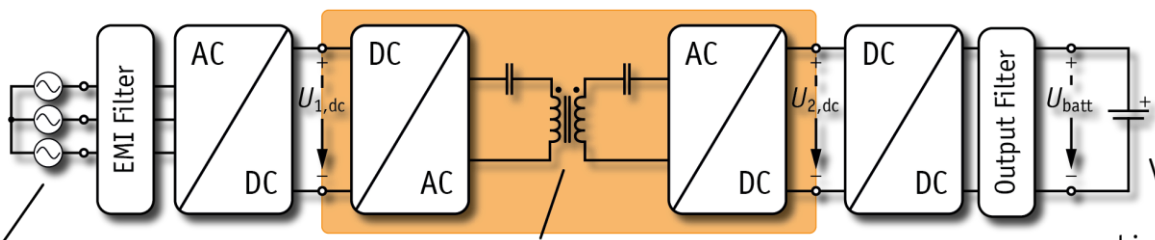


▲ Structure of a 3-phase 2-stage IPT charging system

- Buck-Type PFC Rectification
  - Controls Charging Power
  - Power Factor Correction
- IPT Link: Operation at Resonance
  - Only Active Power Transmitted
  - Operation at Efficiency Maximum
- Vehicle-Side DC-DC Converter
  - Monitoring/Control of Battery Current and Voltage (SoC)
  - «Active Impedance Matching»

# Proposed System Topology (3)

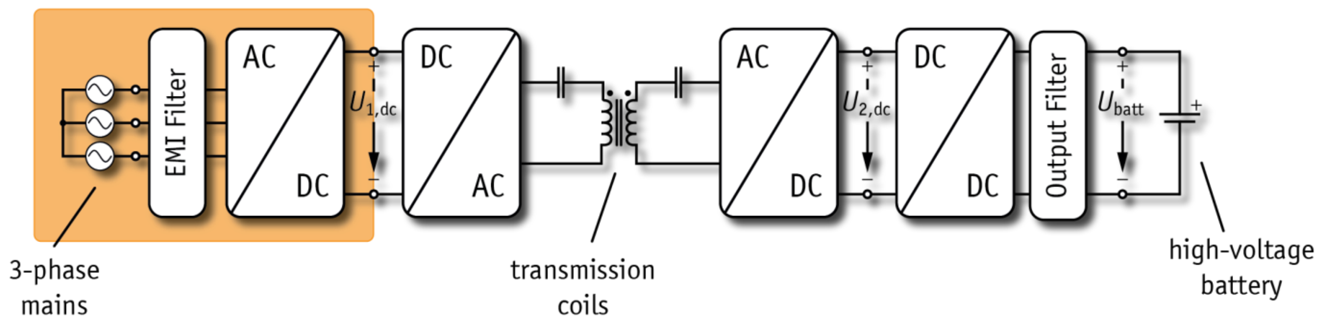


▲ Structure of a 3-phase 2-stage IPT charging system

- **Buck-Type PFC Rectification**
  - Controls Charging Power
  - Power Factor Correction
- **IPT Link: Operation at Resonance**
  - Only Active Power Transmitted
  - Operation at Efficiency Maximum
- **Vehicle-Side DC-DC Converter**
  - Monitoring/Control of Battery Current and Voltage (SoC)
  - «Active Impedance Matching»

# Proposed System Topology (4)

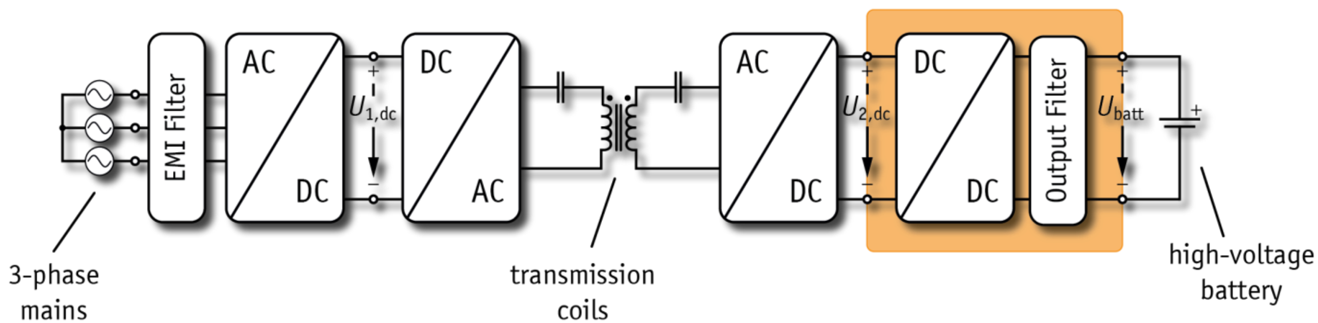


▲ Structure of a 3-phase 2-stage IPT charging system

- **Buck-Type PFC Rectification**
  - Controls Charging Power
  - Power Factor Correction
- **IPT Link: Operation at Resonance**
  - Only Active Power Transmitted
  - Operation at Efficiency Maximum
- **Vehicle-Side DC-DC Converter**
  - Monitoring/Control of Battery Current and Voltage (SoC)
  - «Active Impedance Matching»

# Measured Voltage/Current Waveforms

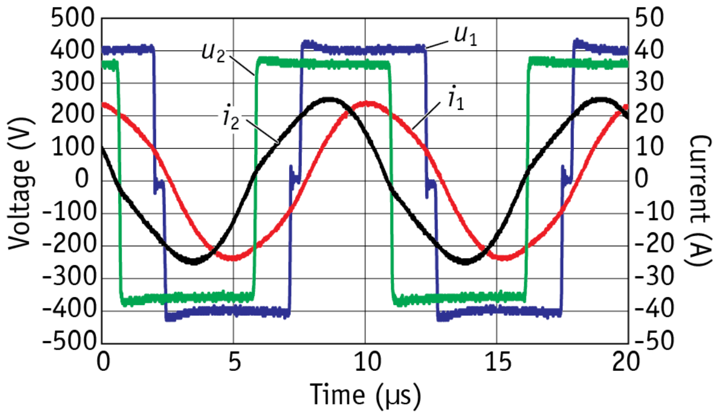


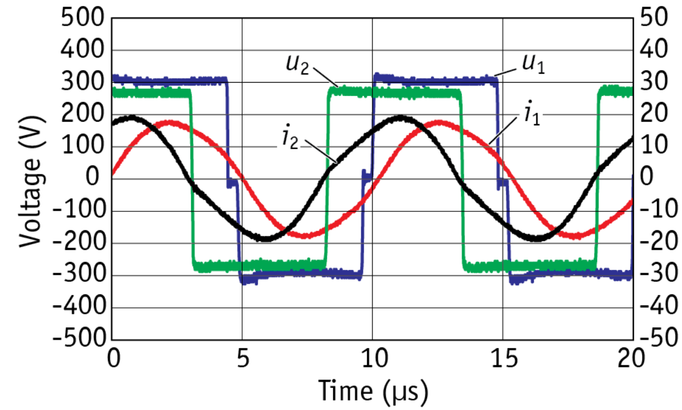


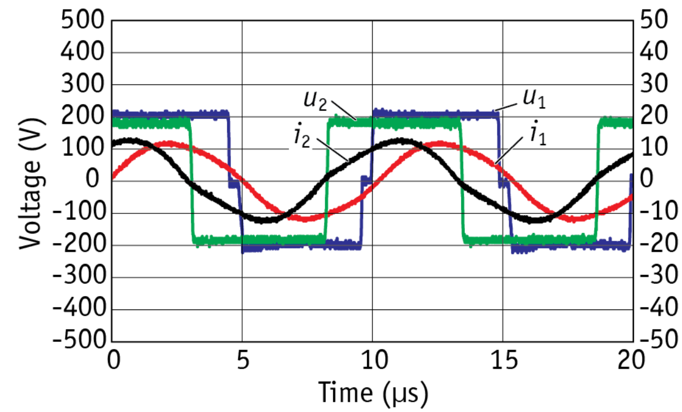


**Measured waveforms for voltage control at output power levels $P_2$ = 5.7 / 3.2 / 1.4 kW**

- **Linear Reduction of Transmitter Current**
  - **Always Only Active Power Transmitted**
  - **Improved Partial-Load Efficiency**

# Comparison to Existing Control Methods

- **Reduced Current in Transmitter Coil due to Operation at Resonance**

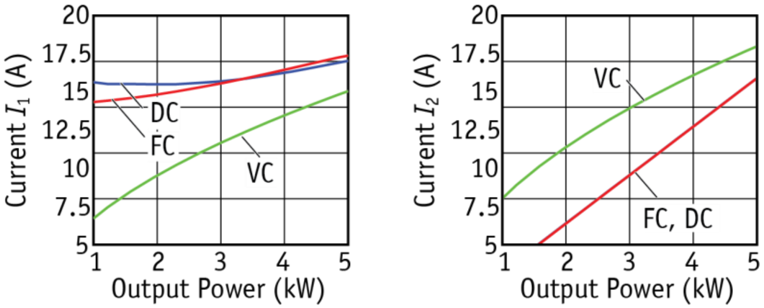


▲ Calculated transmitter and receiver coil currents

- **Controlled DC-Link Voltages Provide Reduced Power Loss in**
  - Transmission Coils
  - Resonant Capacitor ESR
  - Semiconductor Conduction

Calculated power loss components ►

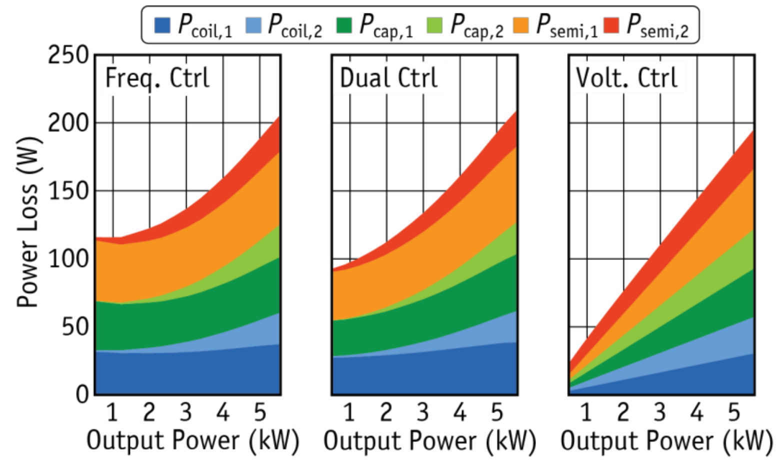

# Misalignment: «Active Impedance Matching»

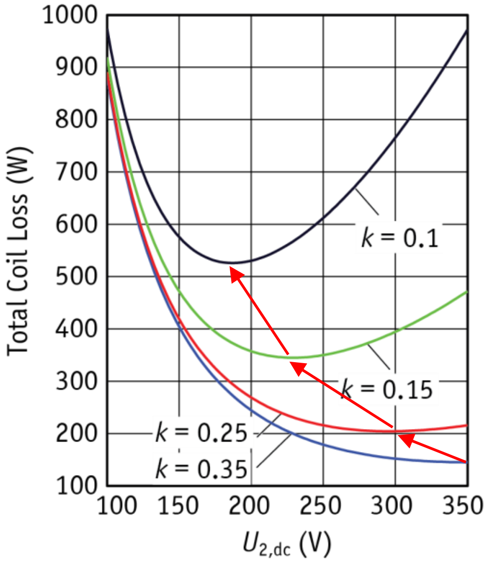


▲ **Tracking of efficiency optimum under misalignment**

- **Impedance Matching is Needed for Max. Transmission Efficiency**
- **«Apparent» Load Depends on $U_{2,dc}$**

- **Active Impedance Matching with Vehicle-Side DC-DC Converter**
- **On-Line Efficiency Optimization e.g. with Tracking Algorithm**

**R. Bosshard, J. W. Kolar et al.,** "Control Method for Inductive Power Transfer with High Partial-Load Efficiency and Resonance Tracking," in *Proc. Int. Power Electron. Conf. (IPEC, ECCE Asia)*, pp. 260–271, 2014.

# DC-to-DC Power Loss Measurement

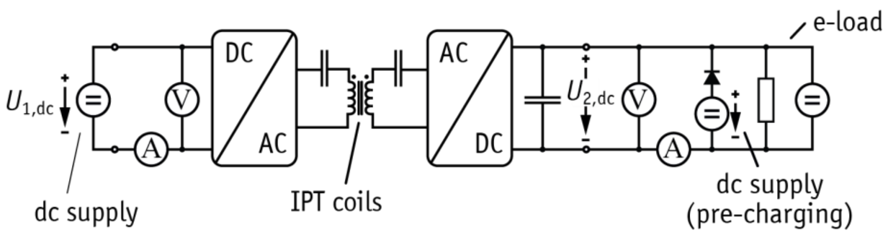


▲ Efficiency measurement setup with electronic load

- **DC-to-DC Measurement with ...**
  - **DC-Supply to Control $U_{1,dc}$**
  - **Electronic Load to Control $U_{2,dc}$**

- **Efficiency > 96% down to 1 kW**

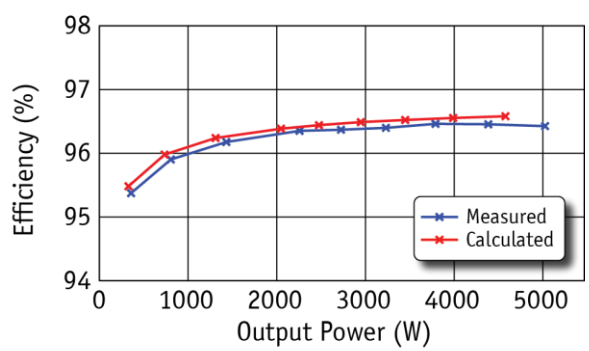


▲ Efficiency measurement @ 52 mm air gap

# Requirements for DC-DC-Converter

► **Additional DC-DC converter**

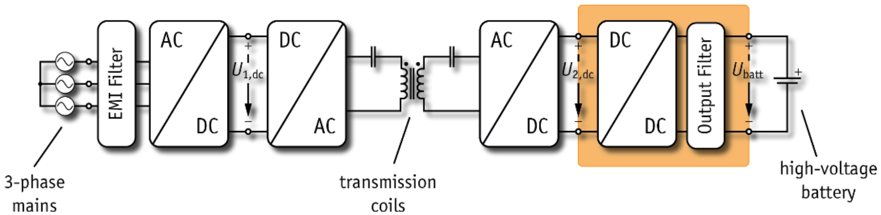


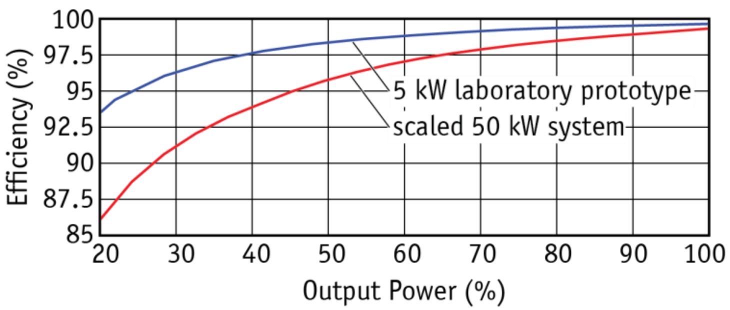


▲ **Efficiency Requirement for DC-DC Converter**

**Example Solution:**
**12 kW, 99.3%, 30 kW/dm³**

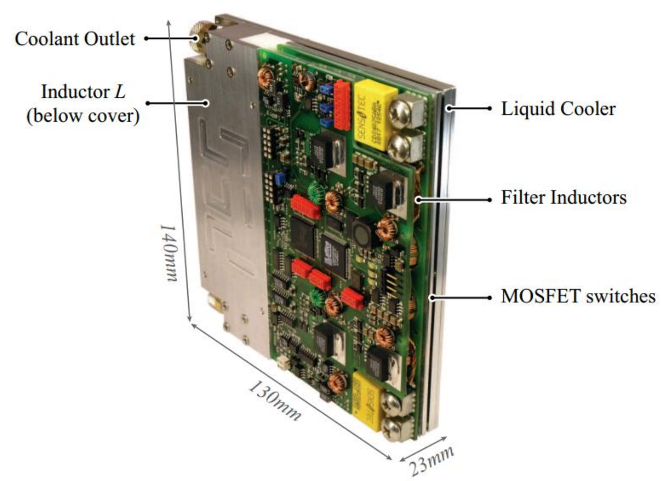


**S. Waffler and J. Kolar**, "Efficiency optimization of an automotive multiphase bi-directional DC-DC converter," in *Proc. 6th Int. Power Electron. and Motion Control Conf. (ECCE Asia)*, 2009, pp. 566–572.

# Control of IGBT Switching Conditions

▼ Measured transmitter coil current and inverter output voltage

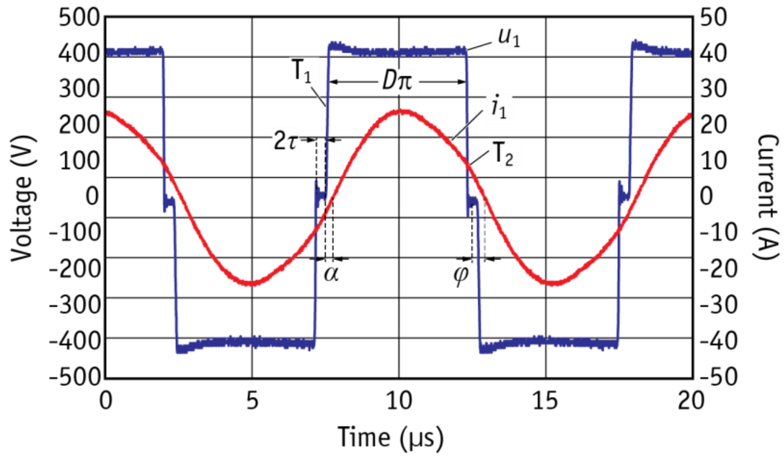


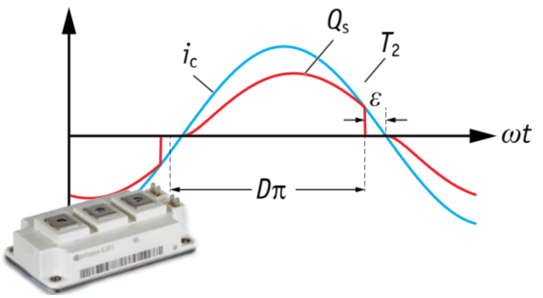


▲ Calculated stored charge in IGBT junction

- ▶ System Structure Allows Full Control of IGBT Switching Conditions
- ▶ Switching Loss due to Stored Charge in IGBT Junction Minimized

**P. Ranstad and H.-P. Nee,** "On dynamic effects influencing IGBT losses in soft-switching converters," *IEEE Trans. Power Electron.*, vol. 26, no. 1, pp. 260–271, 2011.

**G. Ortiz, H. Uemura, D. Bortis, J. W. Kolar, and O. Apeldoorn,** "Modeling of soft-switching losses of IGBTs in high-power high-efficiency dual-active-bridge dc/dc converters," *IEEE Trans. Electron Devices*, vol. 60, no. 2, pp. 587–597, 2013.

# Summary: IPT for EV

Image:
ddpavumba
FreeDigitalPhotos.net

# Σ Inductive Power Transfer for EV Charging

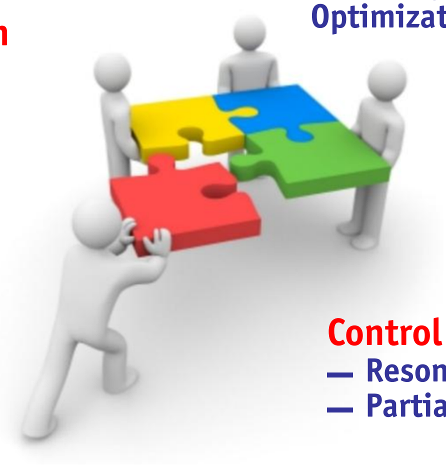

**Coil Design & Optimization**
- Magnetic Modeling & Design
- Multi-Objective Optimization

**Resonant Circuit Design**
- Compensation Topology
- Impedance Matching

**Control Method**
- Resonance Tracking
- Partial-Load Efficiency

**Power Electronic Converter**
- Modulation & Soft-Switching
- Semiconductor Devices

## Inductive Power Transfer

# Applications ... on the Hype Cycle

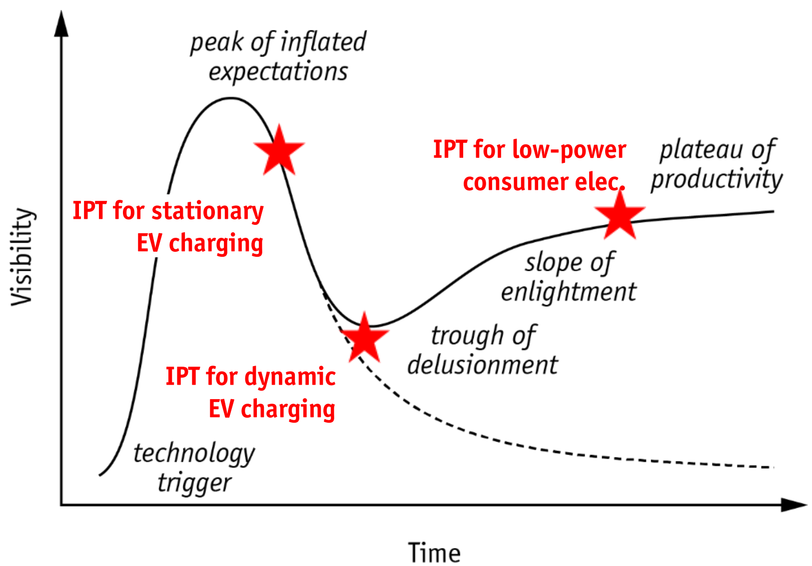

## Inductive Power Transfer for

# Dynamic EV Charging

- Large & Expensive Installation
  vs. Improving Battery Technology
- Medium-Voltage Supply & Distribution of Power along 1% of all Highways
- Efficiency of Dynamic IPT
  vs. Increasing Energy Cost?
- Possible Applications:
  Electrification @ Traffic Lights, Bus Stops,
  Transportation Vehicles @ Industrial Sites ...

## Inductive Power Transfer for

# Stationary EV Charging


- ▶ Stationary EV Charging for Private Domestic Use
  - Simplified / Safer Charging Process
  - Large Market Potential
- ▶ Stationary EV Charging for Public Transportation Systems
  - Simplified Quick-Charging at Bus Stops
  - Reduced Battery Volume
  - Reduced Number of Fleet Vehicles

→ Reduced Investments & Operating Costs!

# 3-Φ Buck-Type
# PFC Rectifier Systems

– Unidirectional
– Bidirectional

# ► Classification of Unidirectional Rectifier Systems

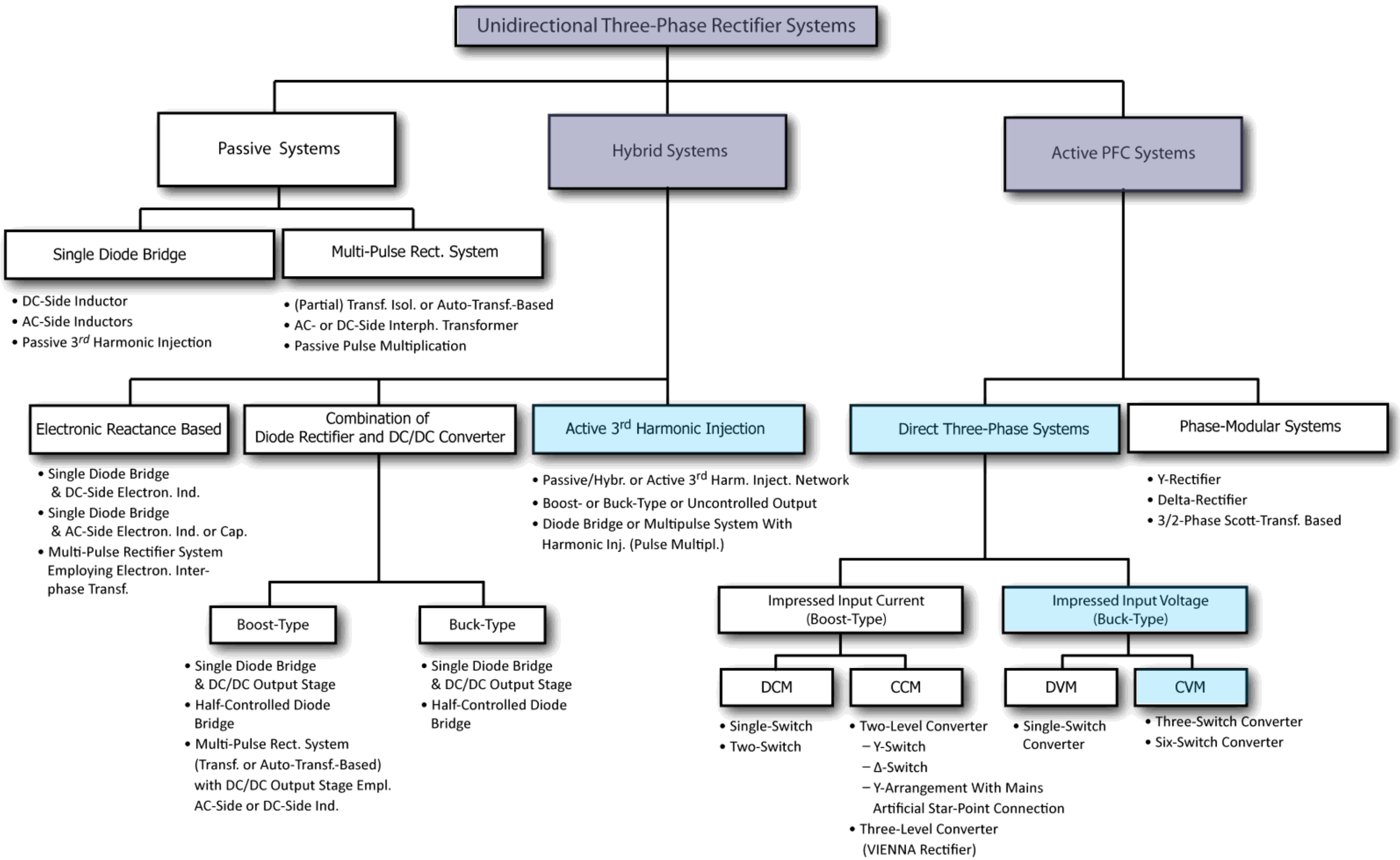

# Active 3-Φ Buck-Type
# PFC Rectifier Systems

*Three-Switch Rectifier*
*Six-Switch Rectifier*

# Three-Switch PFC Rectifier

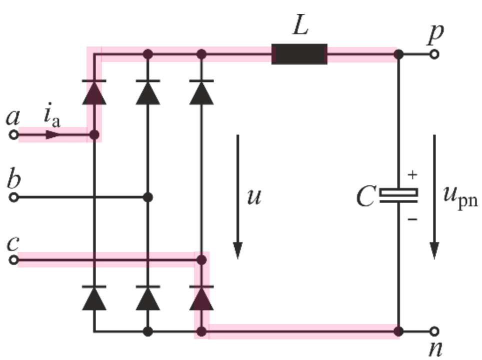


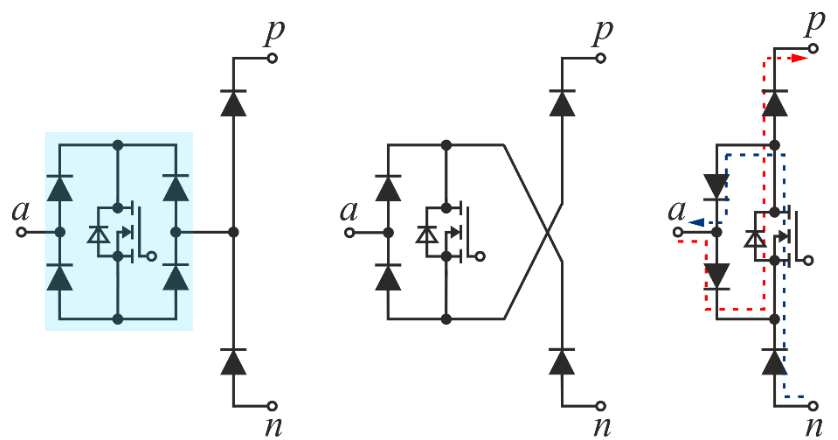


- **Derivation of Rectifier Topology**

→ **Controllability of Conduction State**
→ **Phase-Symmetry / Bridge-Symmetry**

# Three-Switch PFC Rectifier

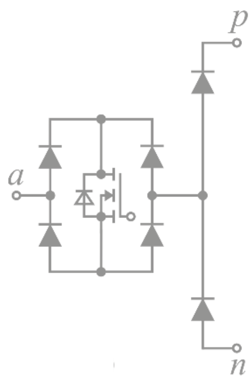


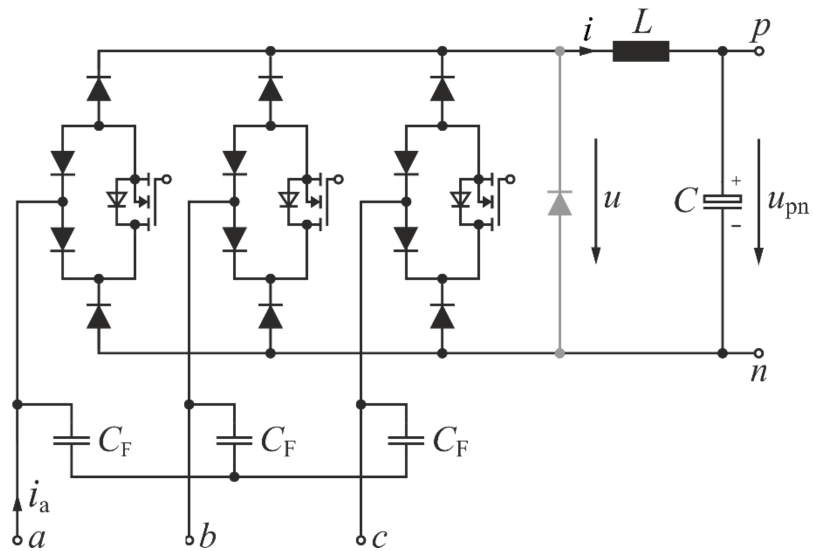


- Output Voltage Control
- Sinusoidal Mains Current Control
- $\Phi$ = (-30°,+30°)

# Three-Switch PFC Rectifier

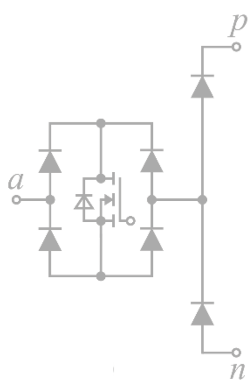


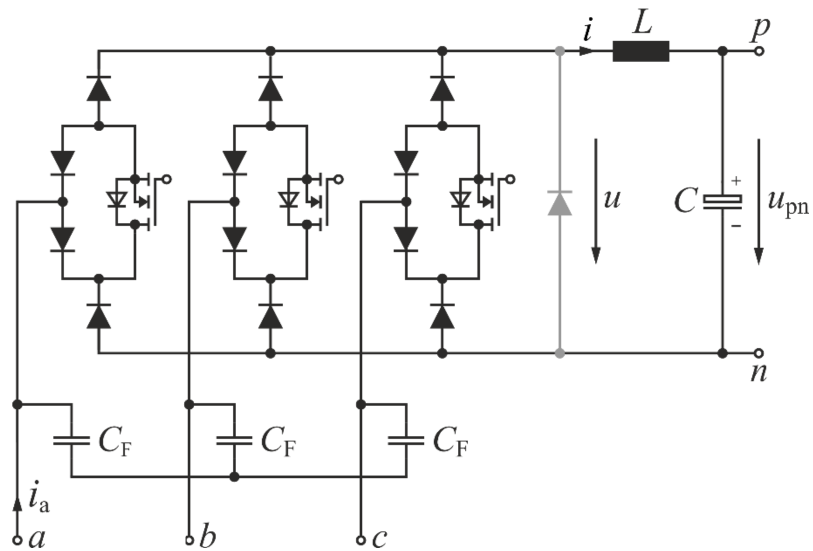


- Output Voltage Control
- Sinusoidal Mains Current Control
- $\Phi$ = (-30°,+30°)

→ Relatively High Conduction Losses

# Six-Switch PFC Rectifier

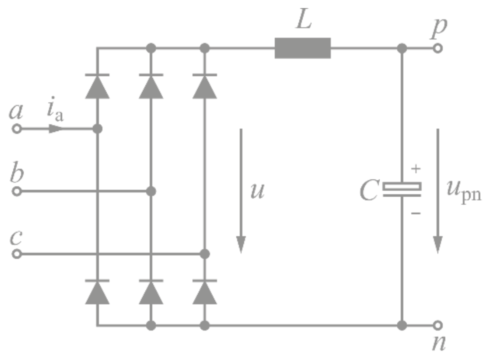


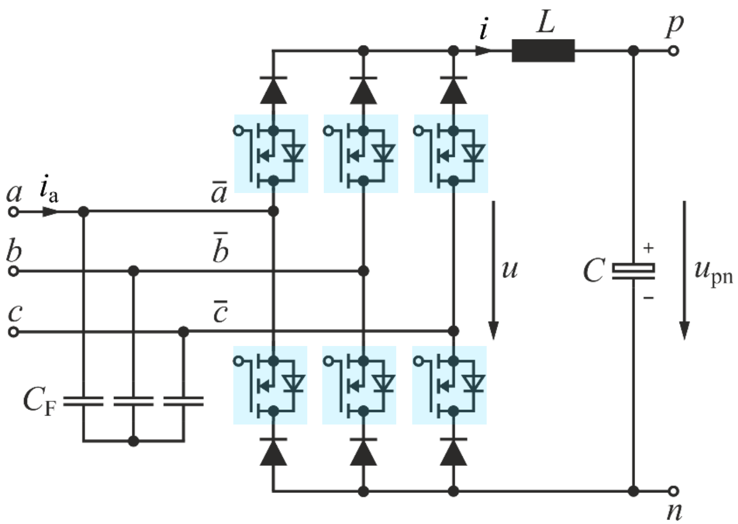


- **Derivation of Rectifier Topology**

→ **Controllability of Conduction State**
→ **Phase-Symmetry / Bridge-Symmetry**

# Six-Switch PFC Rectifier

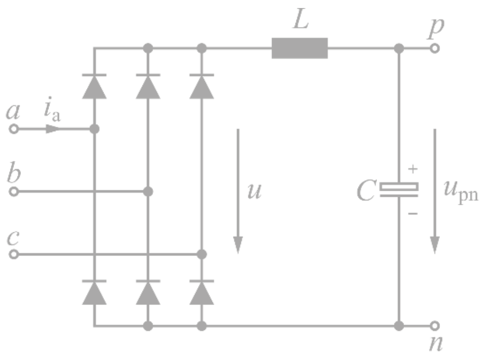


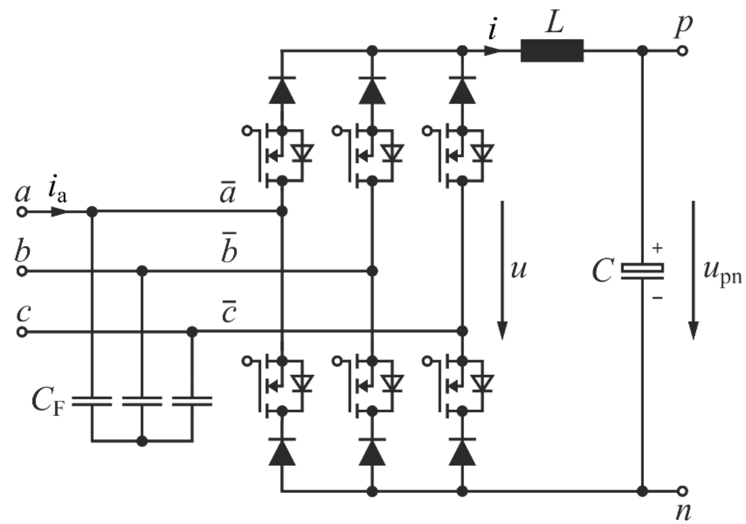


- Output Voltage Control
- Sinusoidal Mains Current Control
- $\Phi$ = (-90°,+90°)

# Control Structure

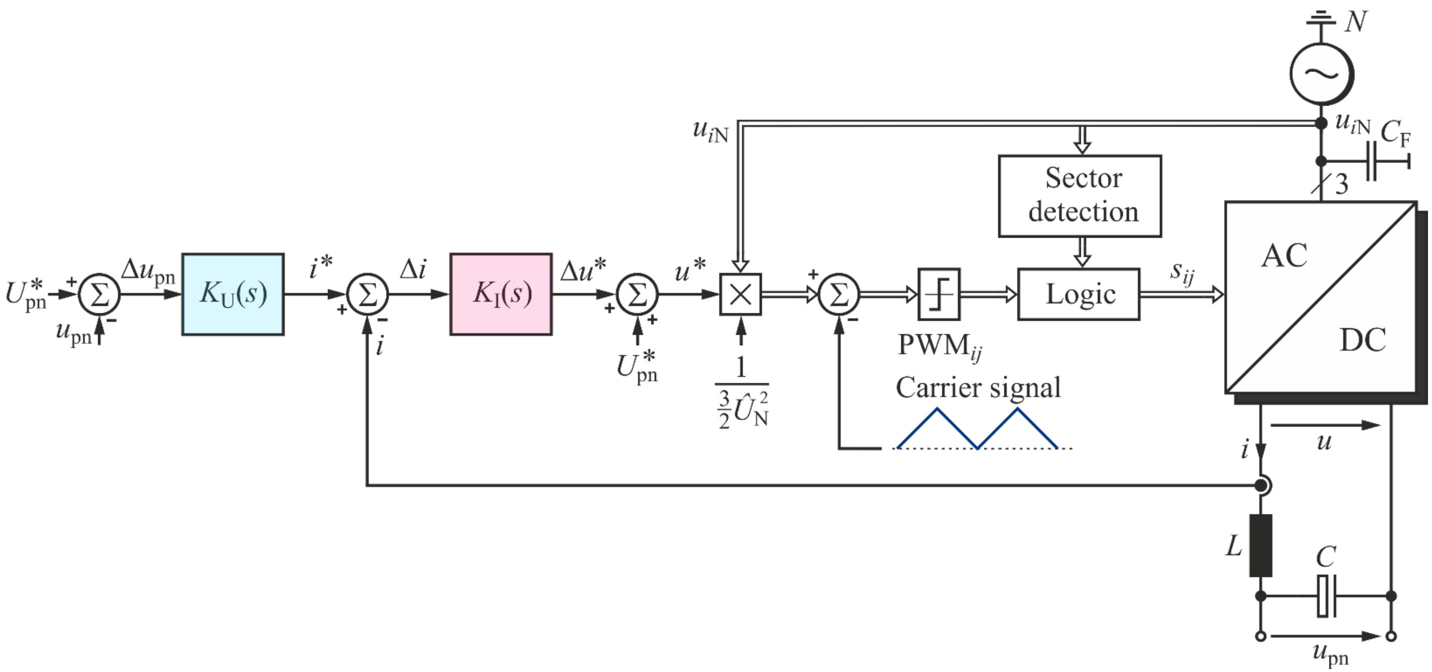


- Output Voltage Control & Inner Output Current Control

# Detailed Functional Analysis

- *Modulation*
- *Input Current Formation*
- *Output Voltage Formation*
- *Demonstrator System*

# ▶ Modulation Scheme

- Consider 60°-Wide Segment of the Mains Period; Suitable Switching States Denominated by ($s_a$, $s_b$, $s_c$)

- Clamping to Phase with Highest Absolute Voltage Value, i.e.

- Phase *a* for $\omega t \in \left(-\frac{\pi}{6}, +\frac{\pi}{6}\right)$,
- Phase *c* for $\omega t \in \left(+\frac{\pi}{6}, +\frac{\pi}{2}\right)$ etc.

- Assumption: $\omega t \in \left(0, +\frac{\pi}{6}\right)$

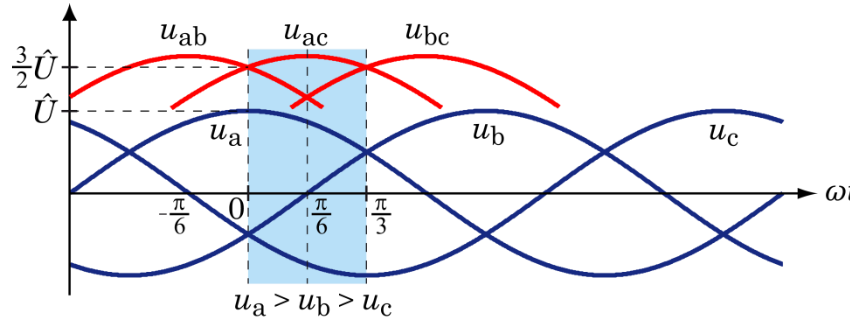


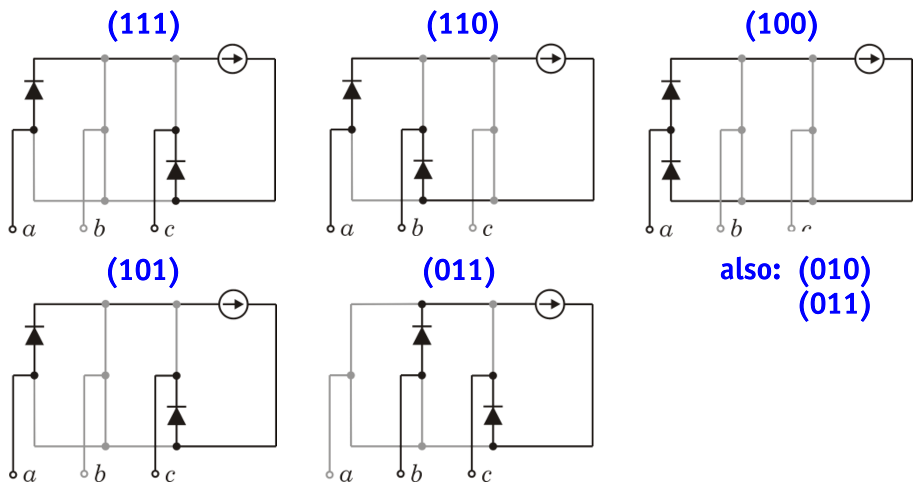


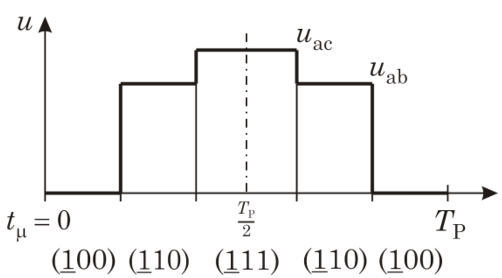


- Clamping and "Staircase-Shaped" Link Voltage in Order to Minimize the Switching Losses

# ▶ Input Current and Output Voltage Formation (1)

**- Assumption:** $\omega t \in \left(0, +\frac{\pi}{6}\right)$

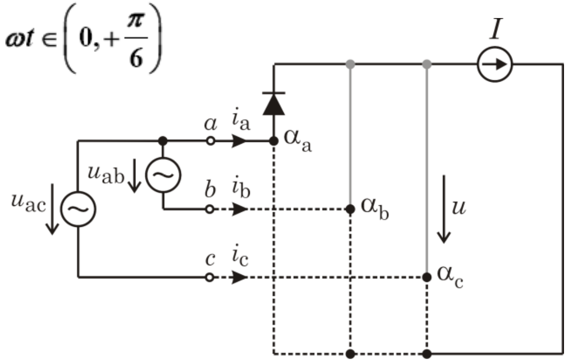


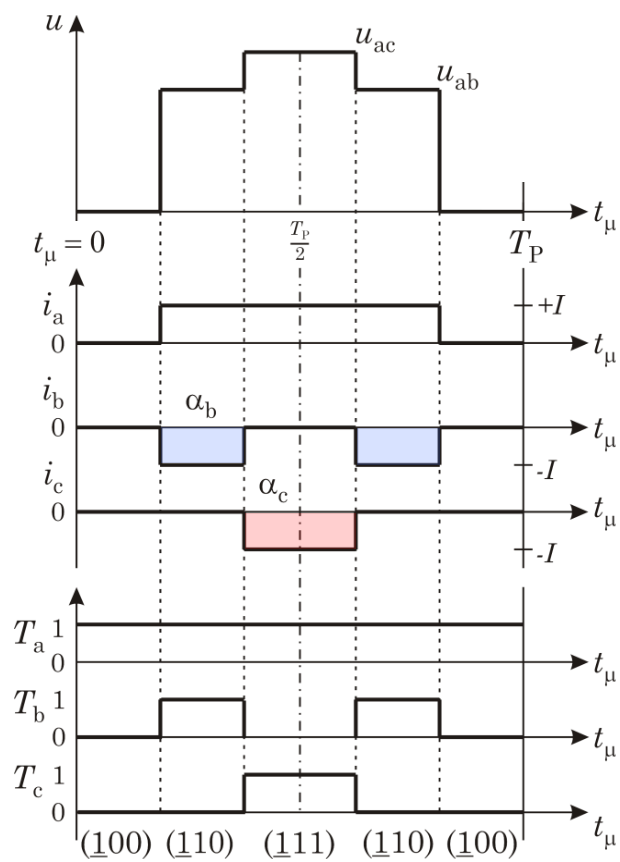


**- Ohmic Mains Behavior:**

$$i_a = G^* u_a = (\alpha_b + \alpha_c) \cdot I$$

$$i_b = G^* u_b = -\alpha_b \cdot I$$

$$i_c = G^* u_c = -\alpha_c \cdot I$$

**- Example:**

$$\alpha_b + \alpha_c = \frac{G^* u_a}{I} = \frac{G^* \hat{U}}{I} \cdot \cos(\omega t) = M \cdot \cos(\omega t)$$

$$\alpha_b = -\frac{G^* u_b}{I} = M \cdot \cos\left(\omega t - \frac{2\pi}{3}\right)$$

$M \in (0 \ldots 1), I \geq \hat{I}^*$

$$\alpha_c = -\frac{G^* u_c}{I} = M \cdot \cos\left(\omega t + \frac{2\pi}{3}\right)$$

# ▶ Input Current and Output Voltage Formation (2)

**- Assumption:** $\omega t \in \left(0, +\frac{\pi}{6}\right)$

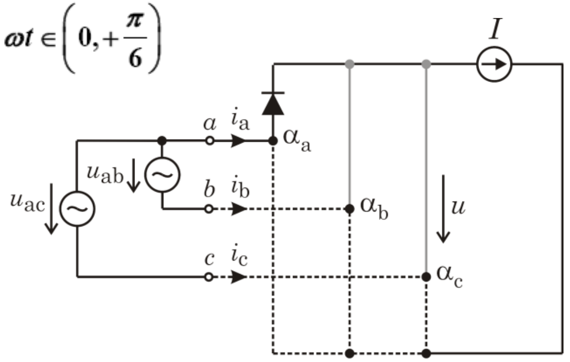


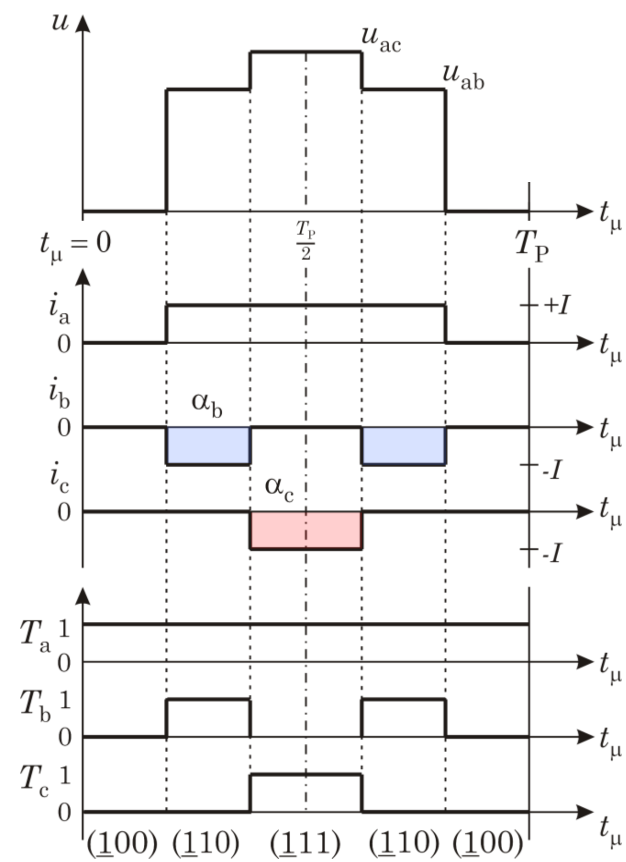


**- Output Voltage Formation:**

$$\overline{u} = u_{ab} \cdot \alpha_b + u_{ac} \cdot \alpha_c$$

$$P_{link} = P_{input}$$

$$\overline{u} \cdot I = \frac{3}{2} \cdot \hat{U} \cdot \hat{I}^*$$

$$\overline{u} = \frac{3}{2} \cdot \hat{U} \cdot \frac{\hat{I}^*}{I} = \frac{3}{2} \cdot \hat{U} \cdot M$$

- **Output Voltage is Formed by Segments of the Input Line-to-Line Voltages**
- **Output Voltage Shows Const. Local Average Value**

# ▶ Experimental Results

## ■ Ultra-Efficient Demonstrator System

$U_{LL}$ = 3 x 400 V (50 Hz)
$P_o$ = 5 kW
$U_o$ = 400 V
$f_s$ = 18 kHz
$L$ = 2 x 0.65 mH

η = 98.8% (Calorimetric Measurement)

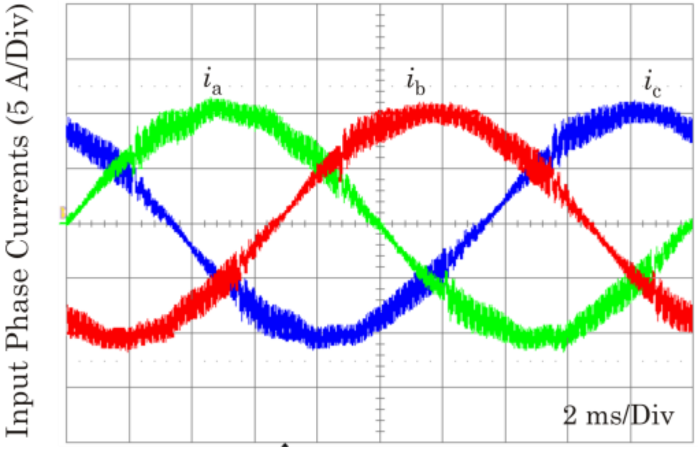

# Experimental Results

## Ultra-Efficient Demonstrator System

$U_{LL}$ = 3 x 400 V (50 Hz)
$P_o$ = 5 kW
$U_o$ = 400 V
$f_s$ = 18 kHz
$L$ = 2 x 0.65 mH

$\eta$ = 98.8% (Calorimetric Measurement)

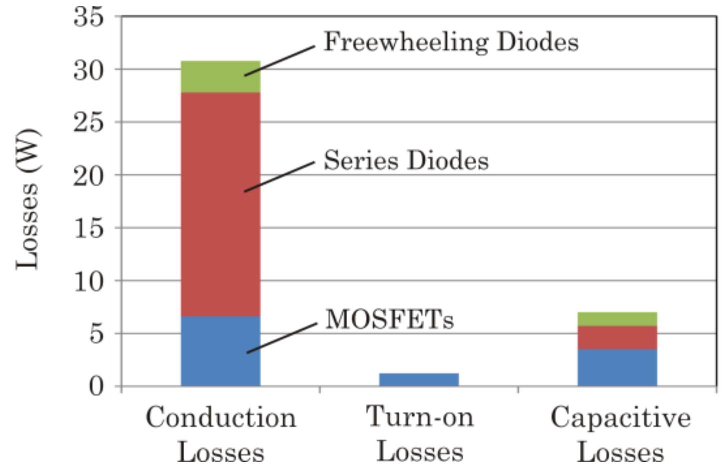


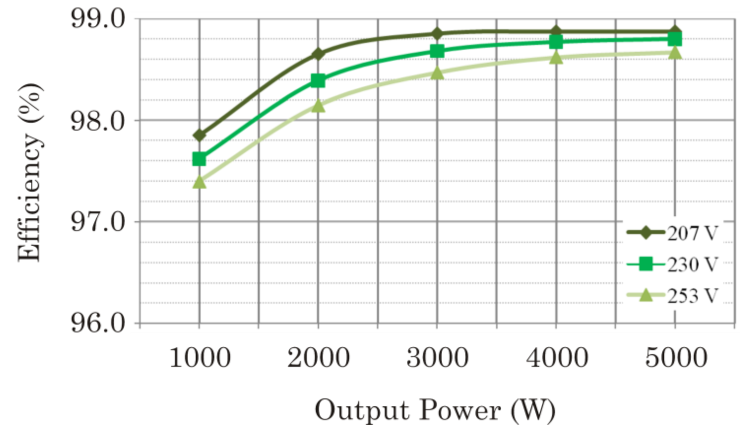

# Remark: Matrix-Type Approaches

## ▶ Integrated Isolation / Single-Stage Energy Conversion

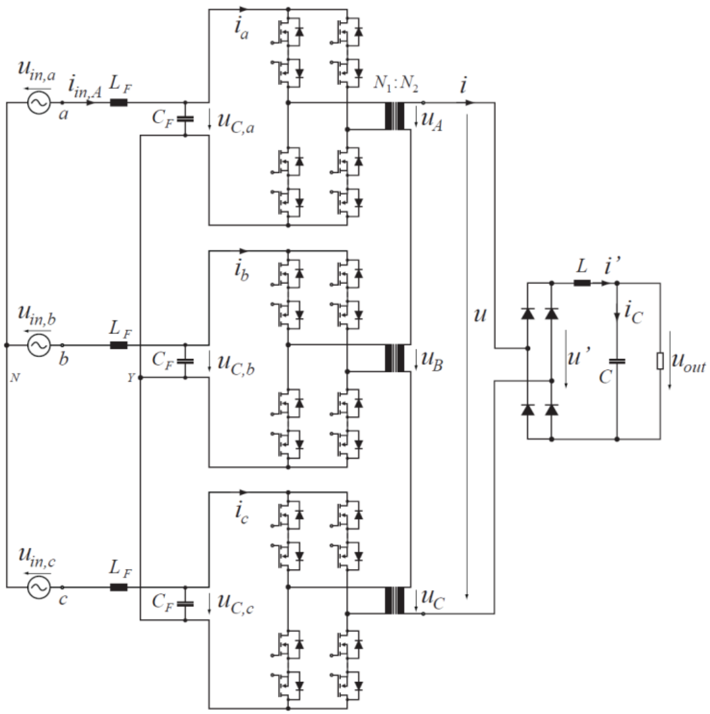


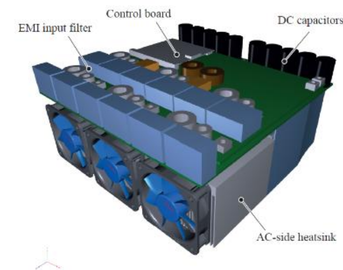


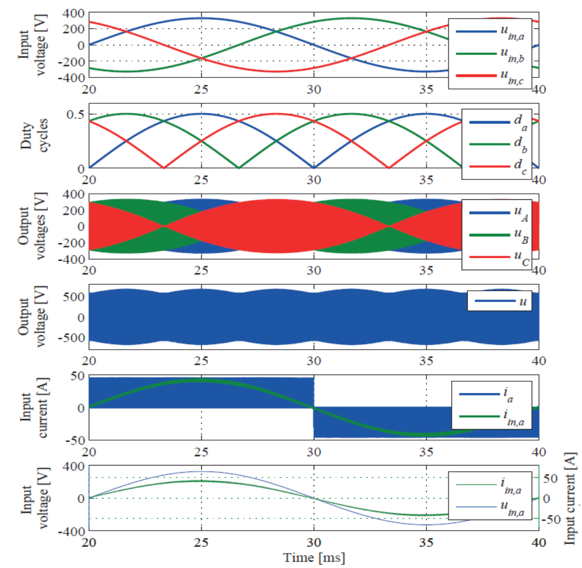


- Higher Control Complexity / Limited Control Flexibility
- Typ. Lower (!) Efficiency Compared to Two-Stage Concepts

# $3^{rd}$ Harmonic Inj. Buck-Type PFC Rectifier Systems

*SWISS Rectifier*

# SWISS Rectifier

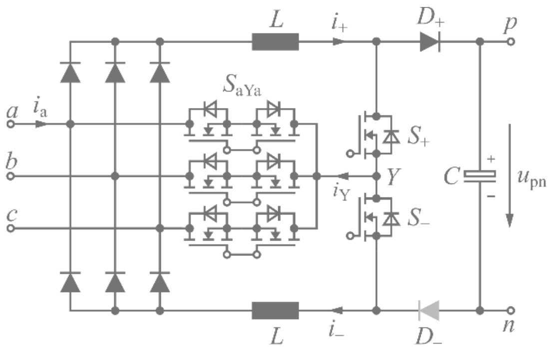


- **3rd Harmonic Inj. Concept**

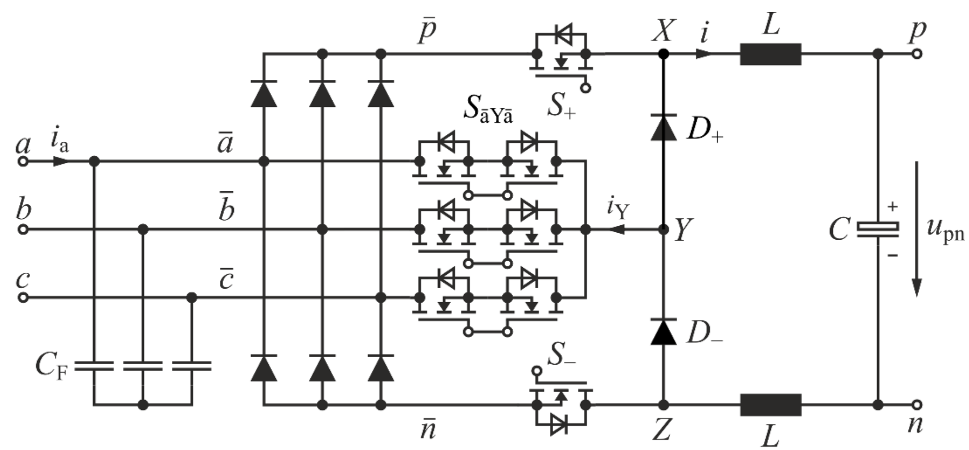

# SWISS Rectifier

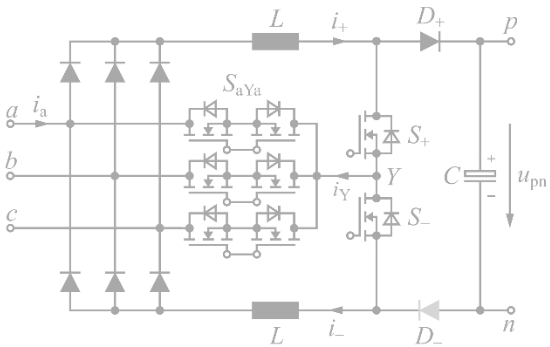


- Output Voltage Control
- Sinusoidal Current Control

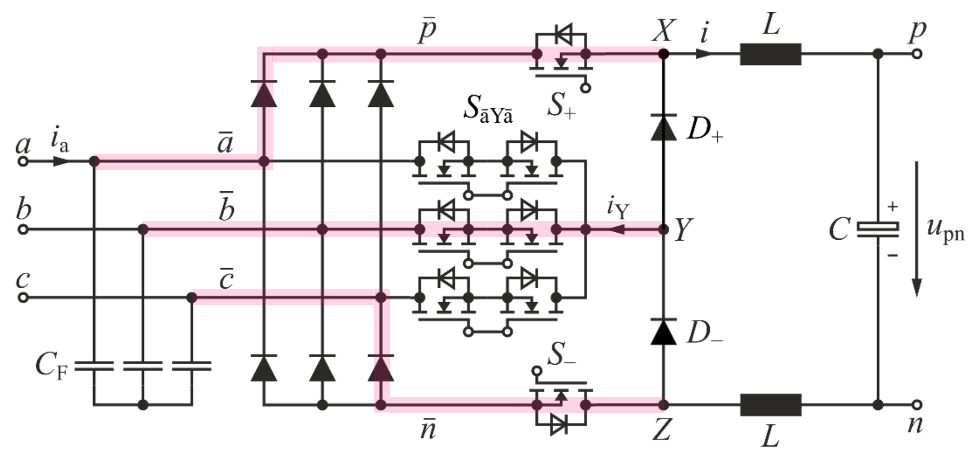

# SWISS Rectifier

- Output Voltage Control
- Sinusoidal Current Control

→ Low Complexity

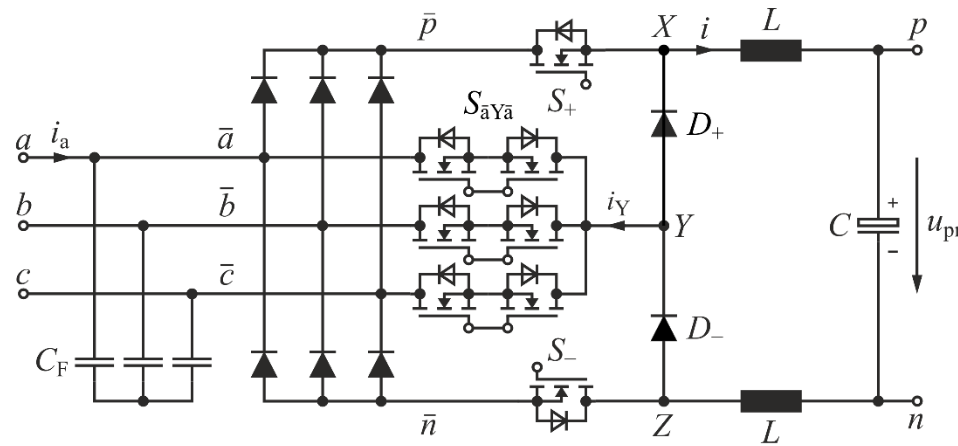

# SWISS Rectifier

## ▶ Control Structure

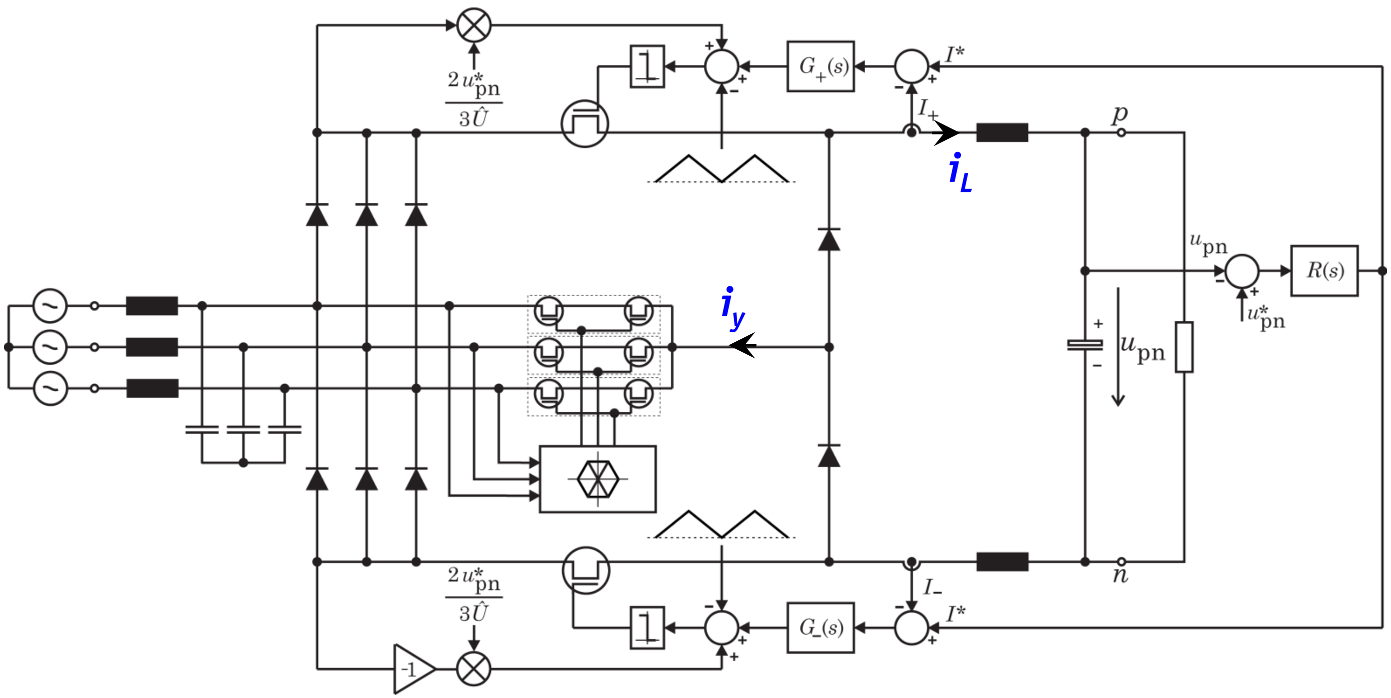


▶ Gating of $T_+$, $T_-$: - Synchronous Control Minimizes $i_y$-Ripple / Maximizes Ripple of $i_L$
- Interleaving Minimizes Ripple of $i_L$ / Maximizes $i_y$-Ripple

# Comparison of Buck-Type Systems

*Six-Switch Rectifier*
*SWISS-Rectifier*

# Buck-Type PFC Rectifiers

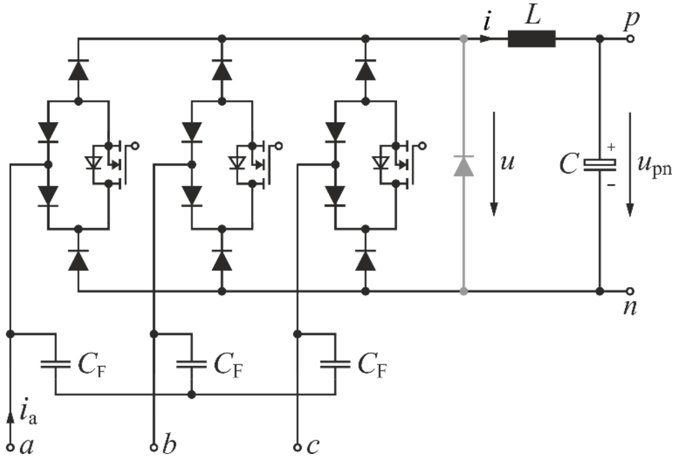


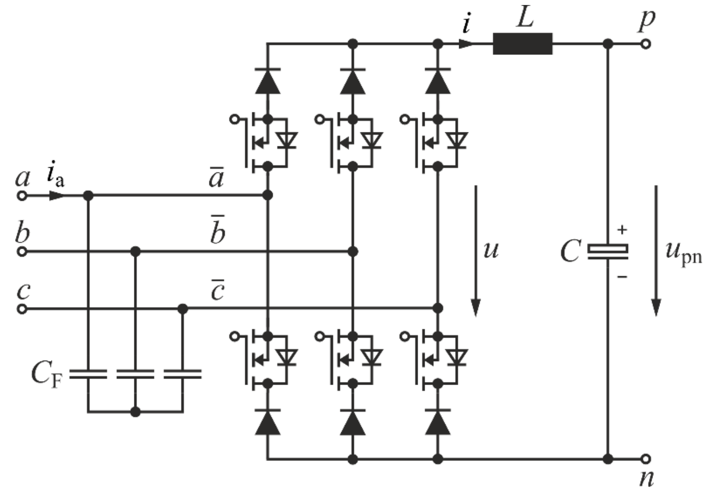


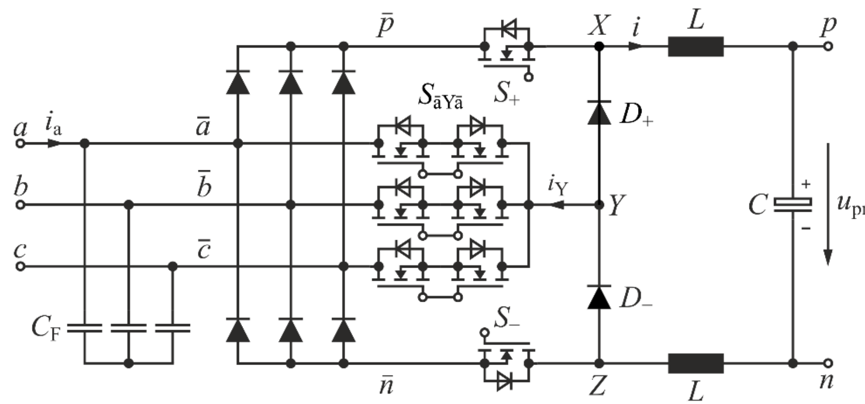


- $3^{rd}$ Harmonic Inj. Type
- Diode Bridge Cond. Modulation

# Buck-Type PFC Rectifiers

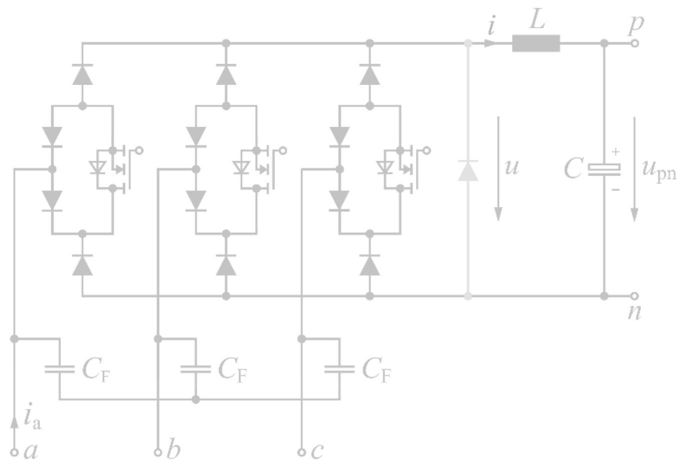


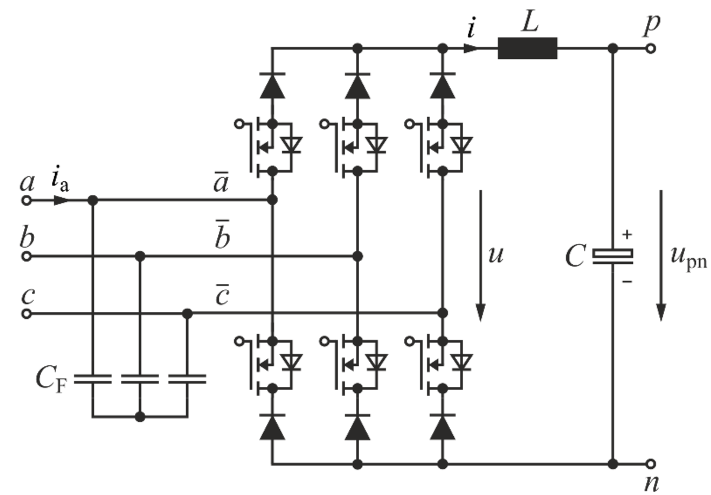


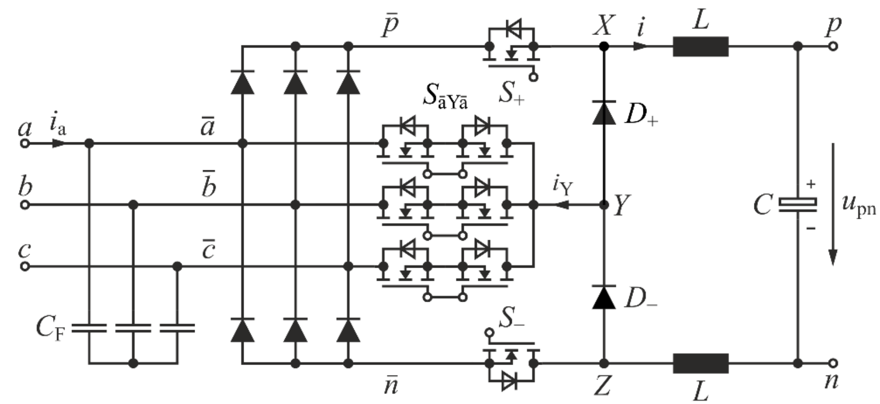


- Three-Switch Rectifier
  → Conduction Losses

# SWISS Rectifier vs. Six-Switch Rectifier

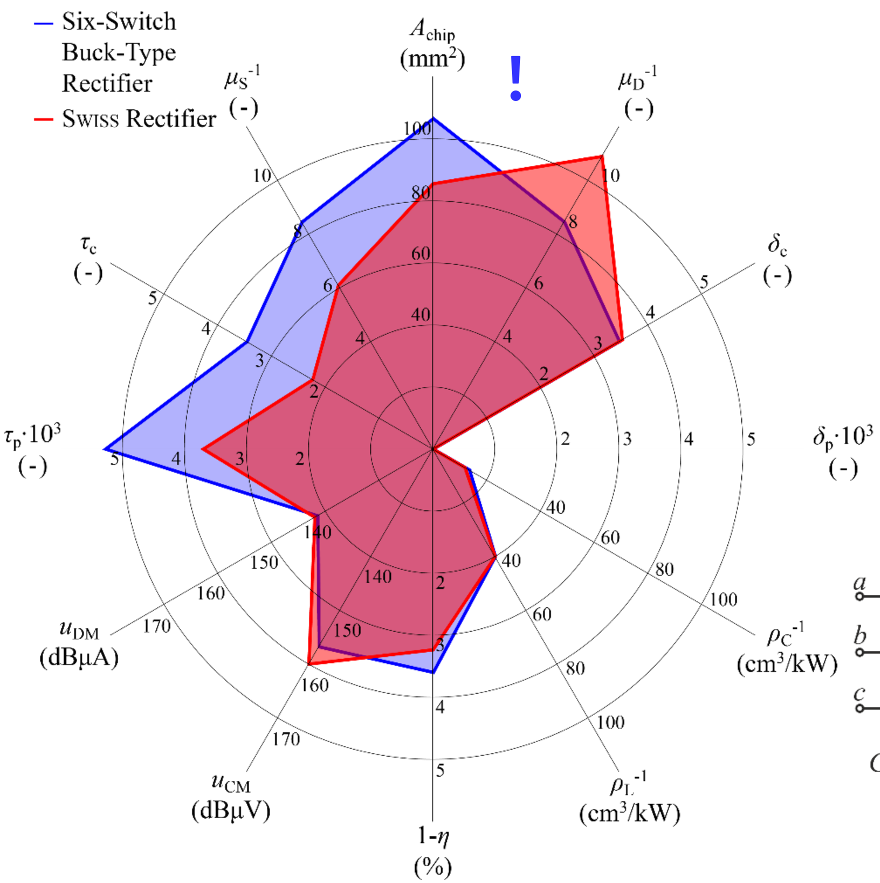


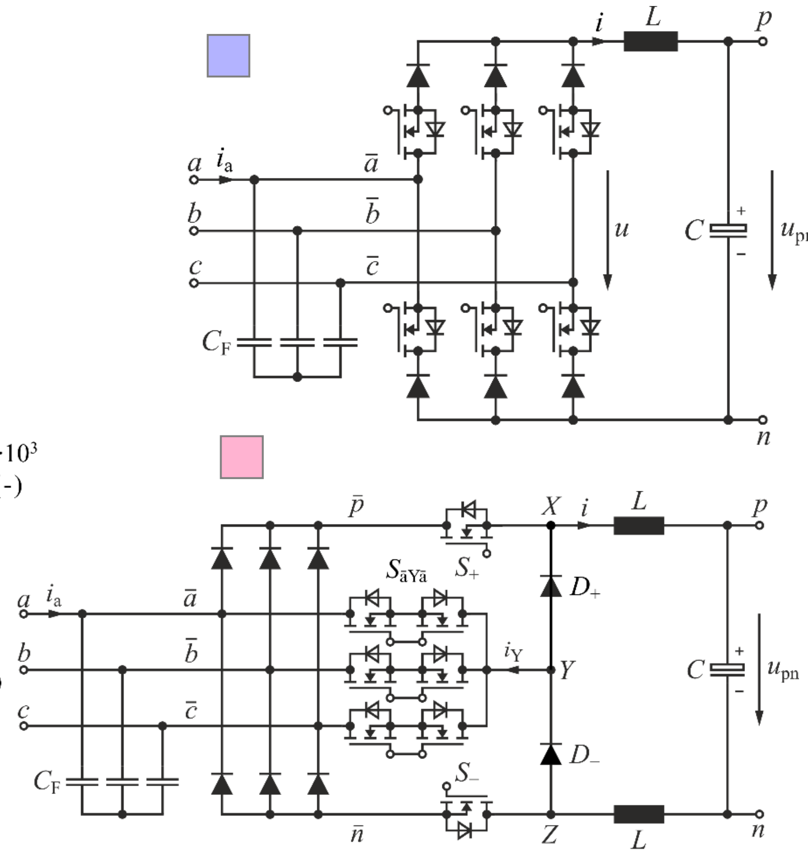

# Bidirectional PFC Rectifier Systems

- *Boost-Type Topologies*
- *Buck-Type Topologies*

# Boost-Type Topologies

# ► Classification of Bidirectional Boost-Type Rectifier Systems

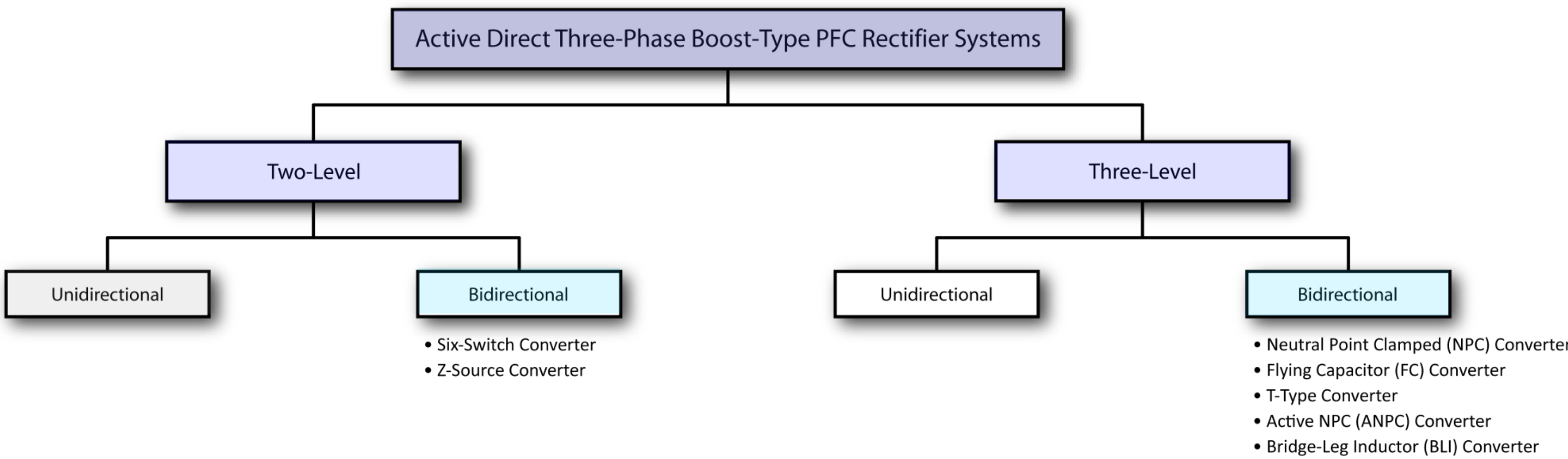

# ▶ Derivation of Two-Level Boost-Type Topologies

- **Output Operating Range**

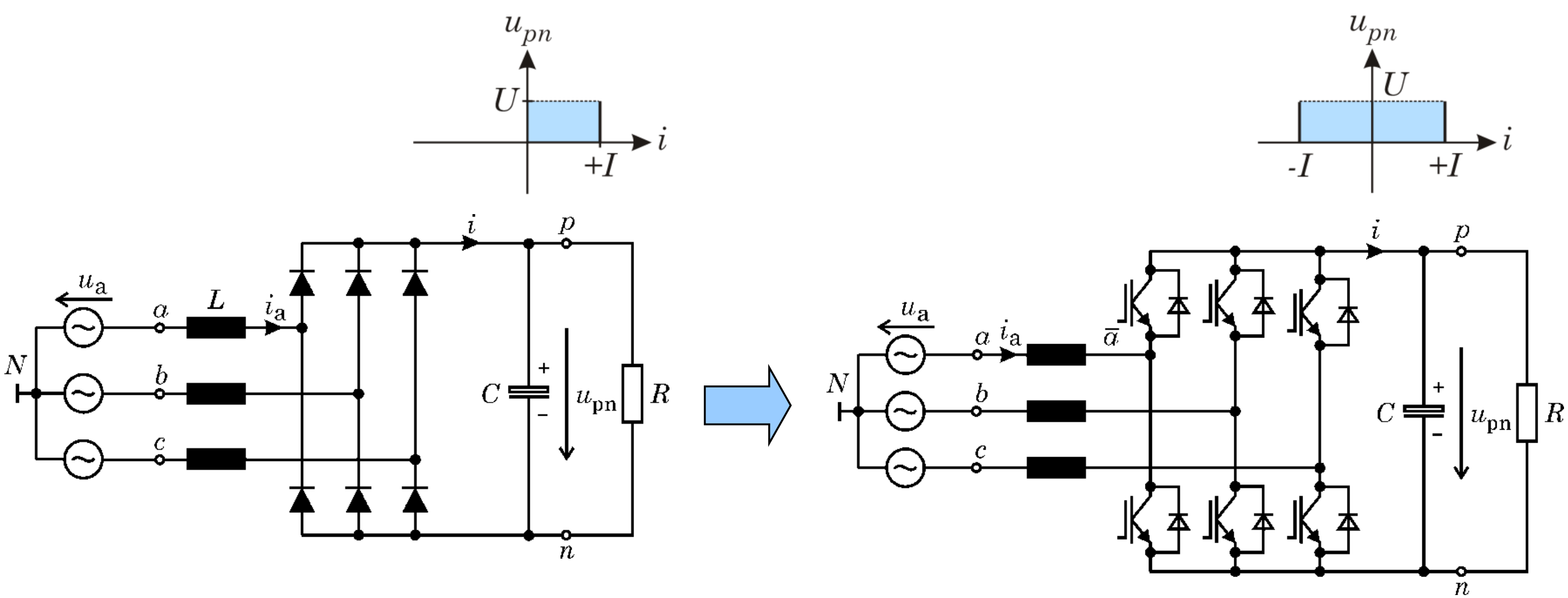

# ▶ Derivation of Three-Level Boost-Type Topologies

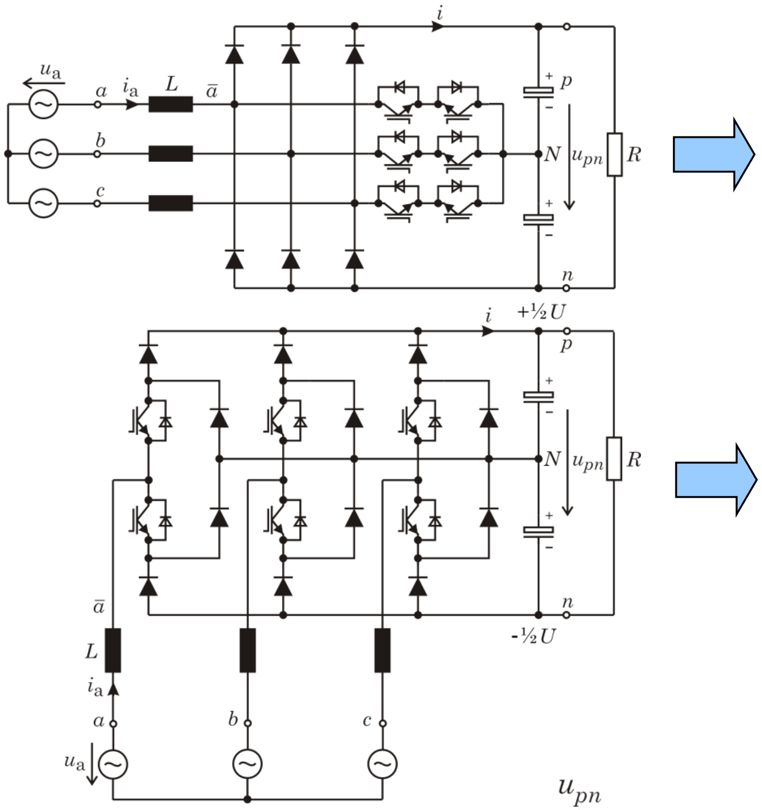


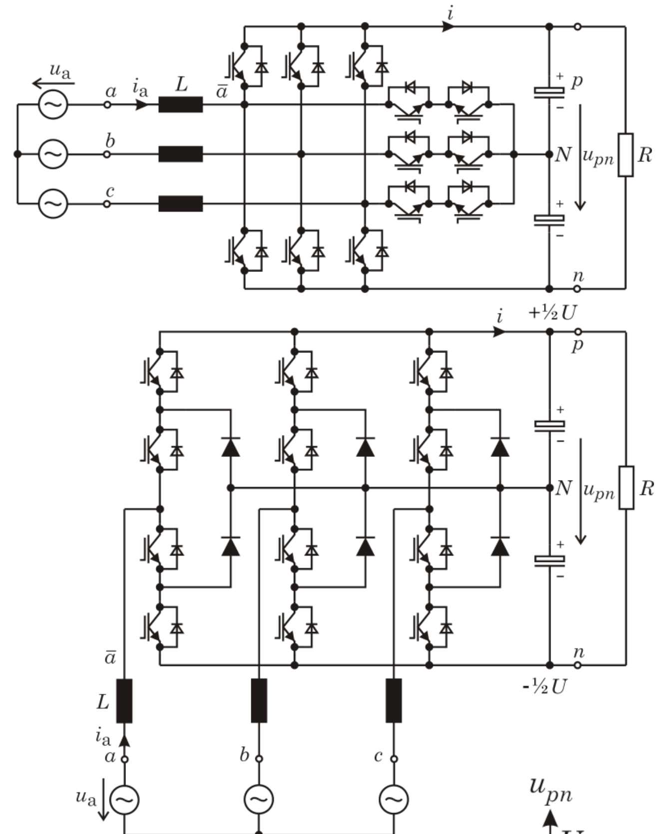


- **Output Operating Range**

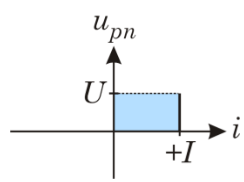


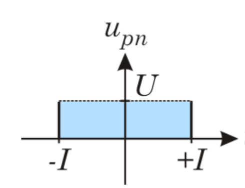

# ▶ Comparison of Two-Level/Three-Level NPC Boost-Type Rectifier Systems

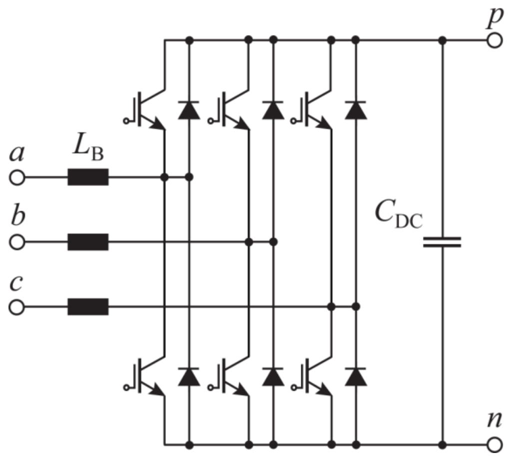


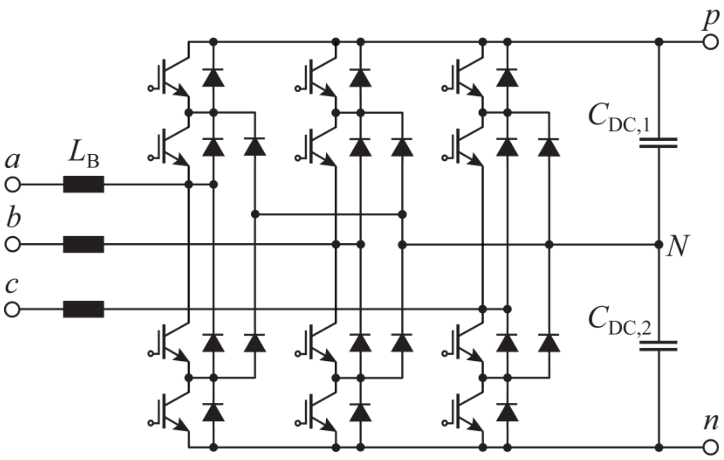


- Two-Level Converter Systems

+ State-of-the-Art Topology for LV Appl.
+ Simple, Robust, and Well-Known
+ Power Modules and Auxiliary Components Available from Several Manufacturers

- Limited Maximum Switching Frequency
- Large Volume of Input Inductors

- Two-Level → Three-Level Converter Systems

+ Reduction of Device Blocking Voltage Stress
+ Lower Switching Losses
+ Reduction of Passive Component Volume

– Higher Conduction Losses
– Increased Complexity and Implementation Effort

# ▶ Active Neutral Point Clamped (ANPC) Three-Level Boost-Type System

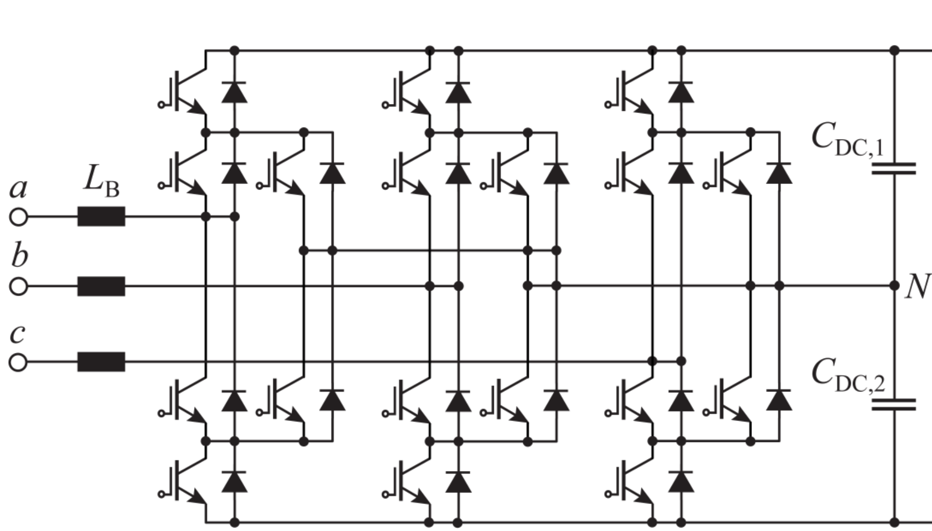


- \+ Active Distribution of the Switching Losses Possible
- \+ Better Utilization of the Installed Switching Power Devices

- – Higher Implementation Effort Compared to NPC Topology

# ▶ T-Type Three-Level Boost-Type Rectifier System

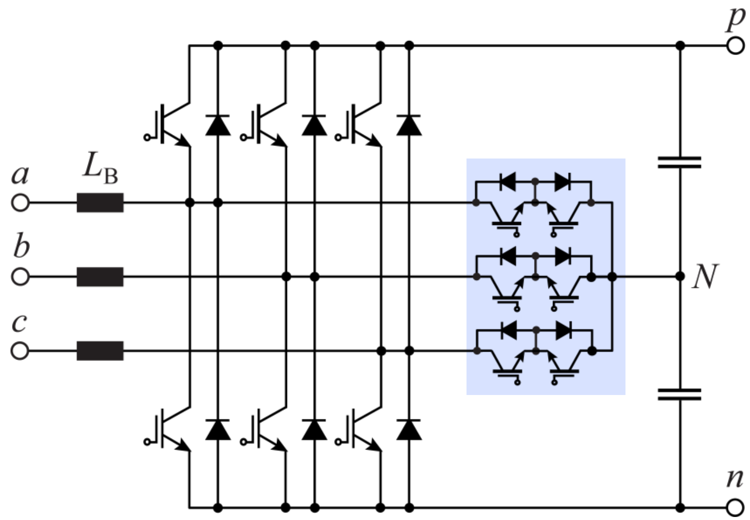


- \+ Semiconductor Losses for Low Switching Frequencies Lower than for NPC Topologies
- \+ Can be Implemented with Standard Six-Pack Module

- − Requires Switches for 2 Different Blocking Voltage Levels

# ▶ Three-Level Flying Capacitor (FC) Boost-Type Rectifier System

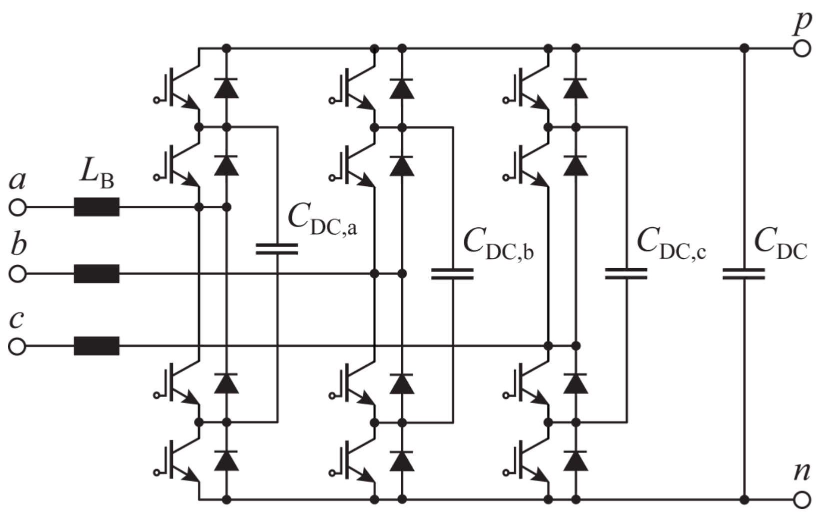


+ Lower Number of Components (per Voltage Level)
+ For Three-Level Topology only Two Output Terminals

– Volume of Flying Capacitors
– No Standard Industrial Topology

# ▶ Three-Level Bridge-Leg Inductor (BLI) Boost-Type Rectifier System

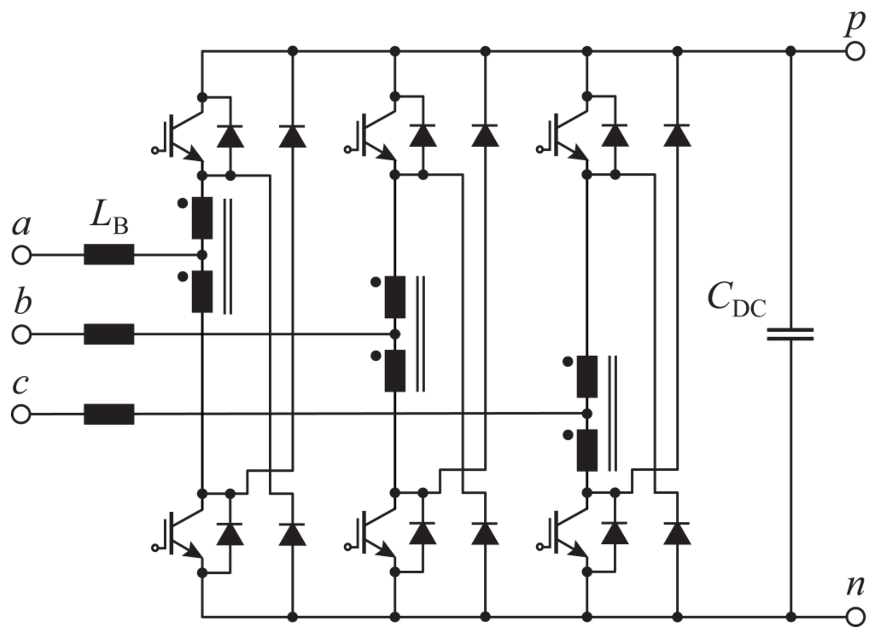


+ Lower Number of Components (per Voltage Level)
+ For Three-Level Topology only Two Output Terminals

– Additional Volume due to Coupled Inductors
– Semiconductor Blocking Voltage Equal to DC Link Voltage

# ▶ Pros and Cons of Three-Level vs. Two-Level Boost-Type Rectifier Systems

+ Losses are Distributed over Many Semicond. Devices; More Even Loading of the Chips → Potential for Chip Area Optimization for Pure Rectifier Operation
+ High Efficiency at High Switching Frequency
+ Lower Volume of Passive Components

− More Semiconductors
− More Gate Drive Units
− Increased Complexity
− Capacitor Voltage Balancing Required
− Increased Cost

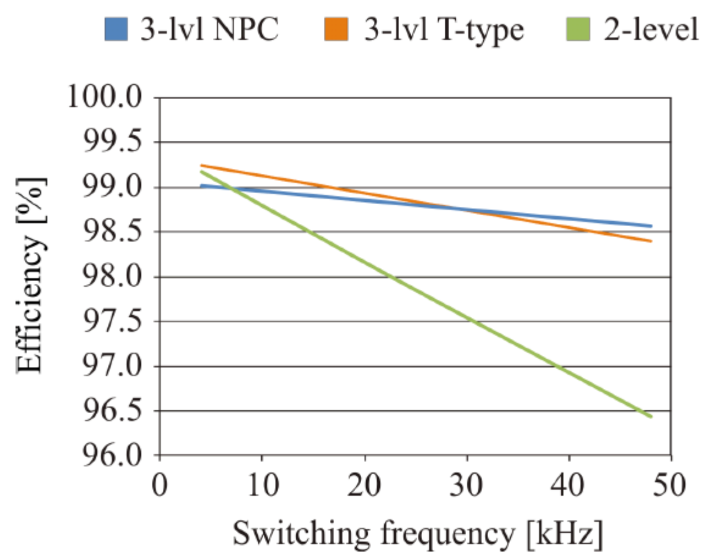


- Moderate Increase of the Component Count with the T-Type Topology

Consideration for 10kVA/400$V_{AC}$ Rectifier Operation; Min. Chip Area, $T_{j,max}$= 125°C

▶ Multi-Level Topologies are Commonly Used for Medium Voltage Applications but Gain Steadily in Importance also for Low-Voltage Renewable Energy Applications

# Buck-Type Topologies

# ▶ Derivation of Unipolar Output Bidirectional Buck-Type Topologies

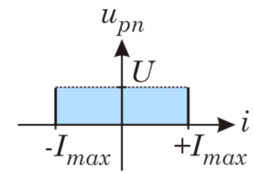


- **Output Operating Range**

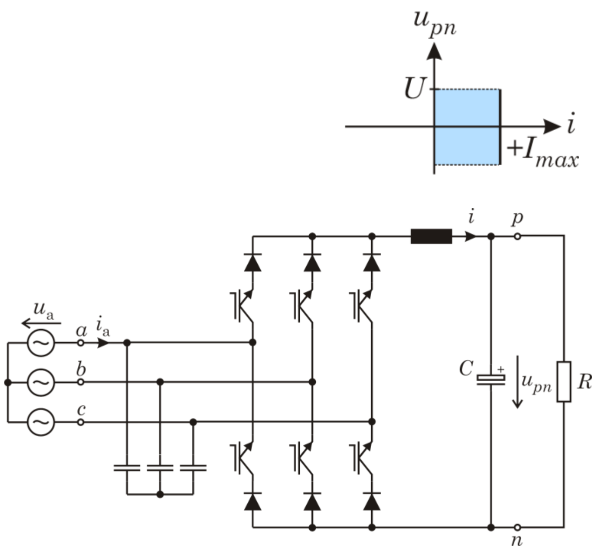


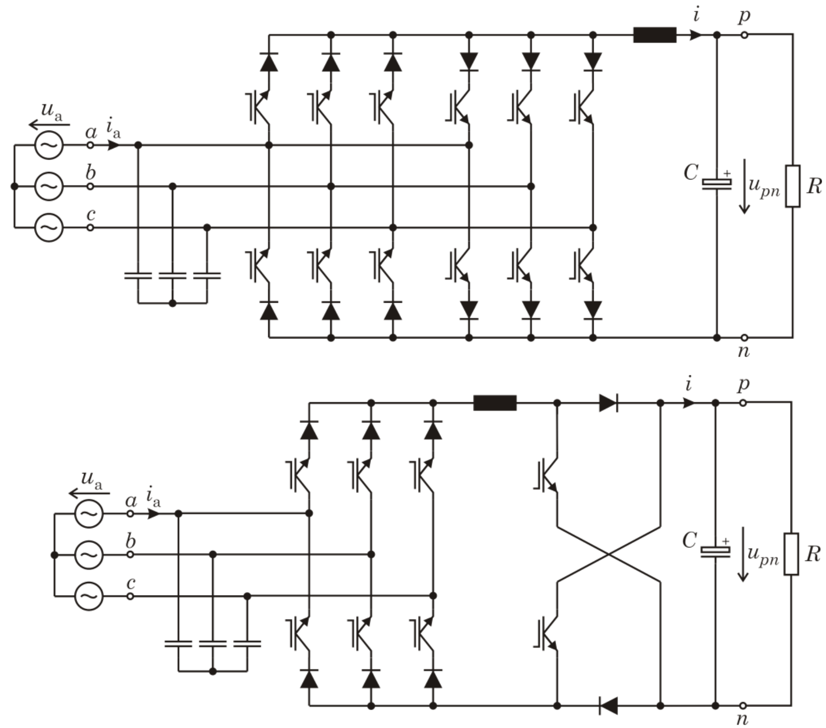


- System also Features Boost-Type Operation

# ▶ Derivation of Unipolar Output Bidirectional Buck-Type Topologies

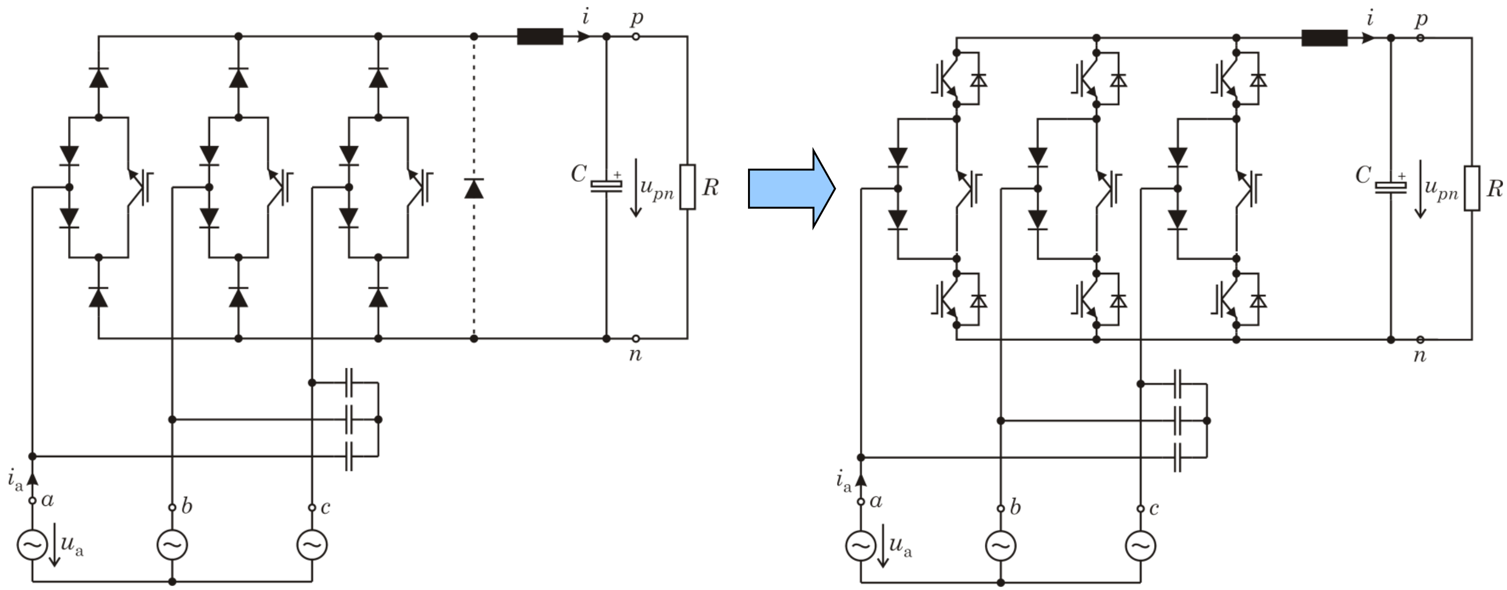


- **Output Operating Range**

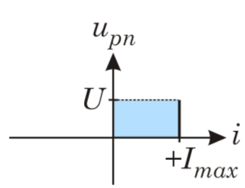


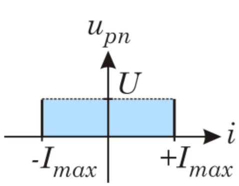

# EMI Filtering

*Vienna Rectifier*
*Six-Switch Buck-Type Rectifier*

# EMI Filtering of Active 3-Φ PFC Rectifier Systems

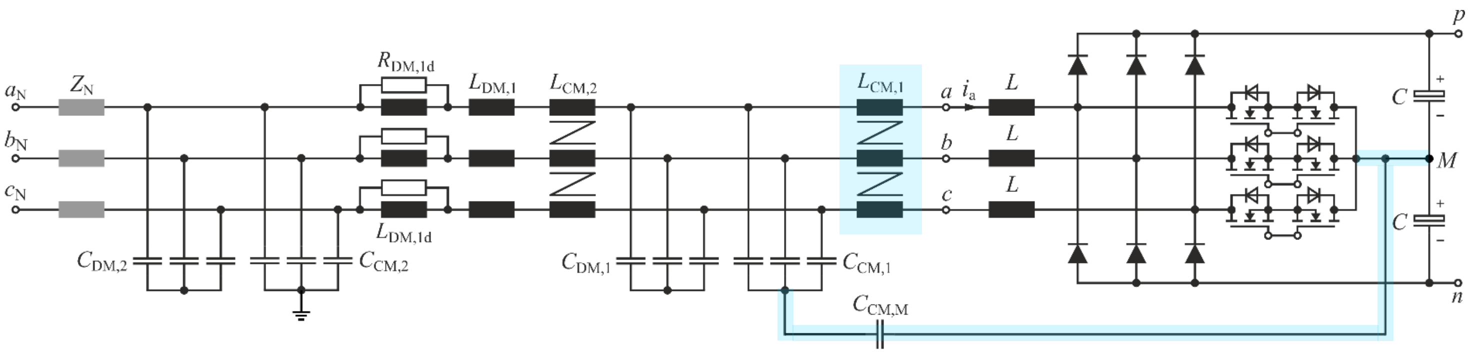


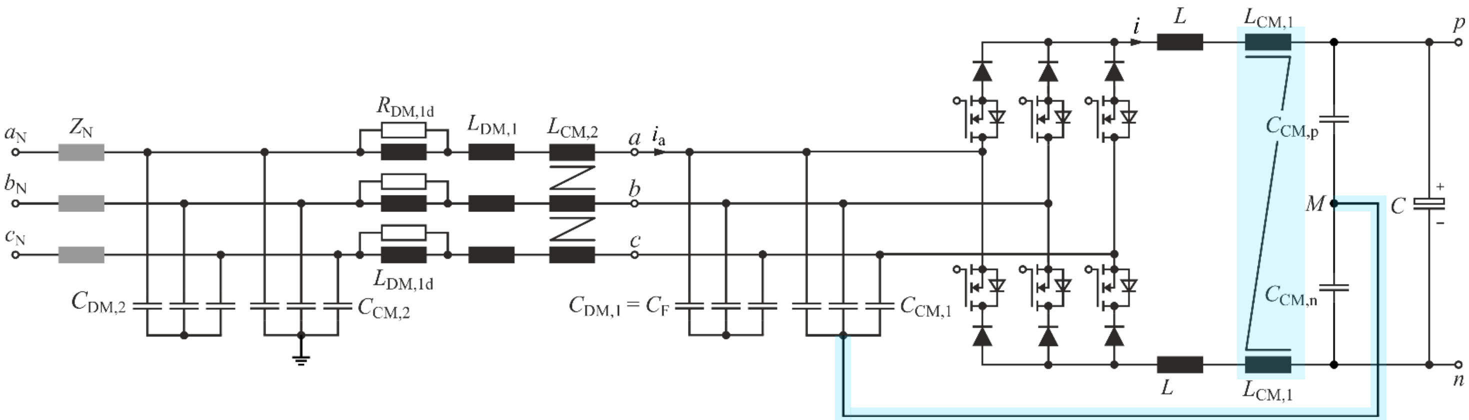


- Internal CM EMI Filtering

# Summary of Unidirectional PFC Rectifier Systems

- *Block Shaped Input Current Systems*
- *Sinusoidal Input Current Systems*

# ▶ Block Shaped Input Current Rectifier Systems

+ Controlled Output Voltage
+ Low Complexity
+ High Semicond. Utilization
+ Total Power Factor $\lambda \approx 0.95$
– $THD_I \approx 30\%$

## Boost-Type

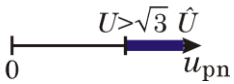


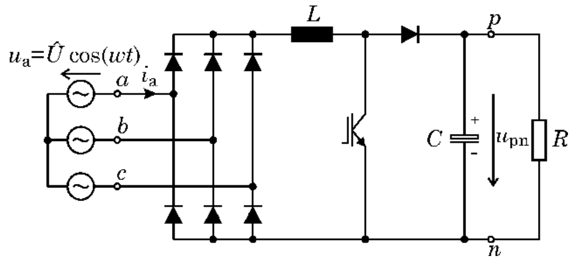


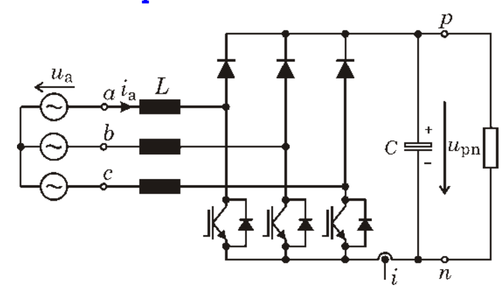


## Buck-Type

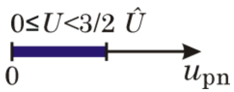


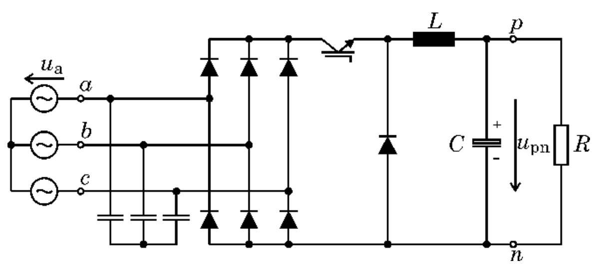


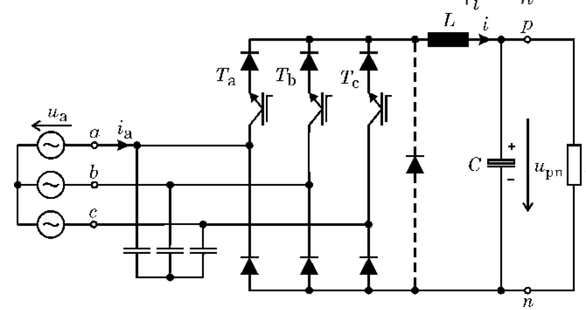


## Buck+Boost-Type


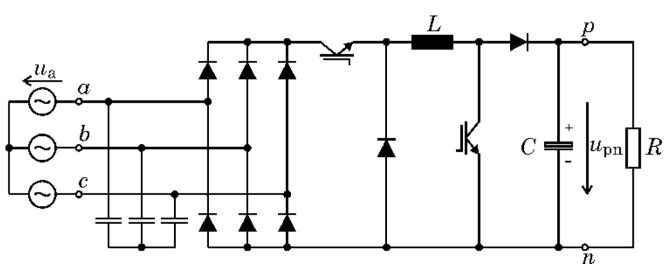


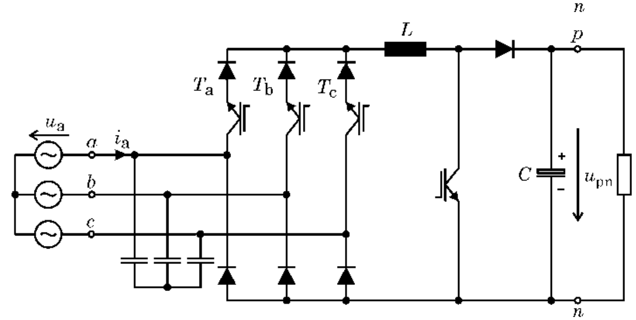

# ▶ Sinusoidal Input Current Rectifier Systems (1)

+ Controlled Output Voltage
+ Relatively Low Control Complexity
+ Tolerates Mains Phase Loss

− 2-Level Characteristic
− Power Semiconductors Stressed with Full Output Voltage

**Boost-Type**

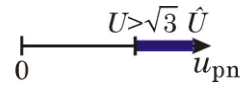


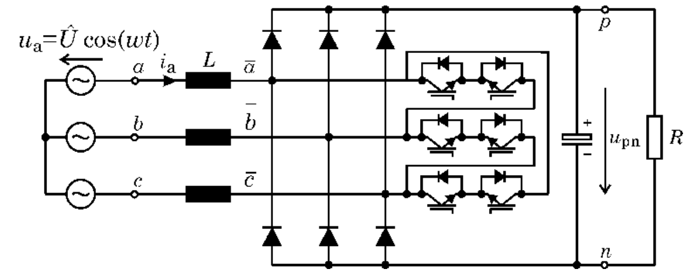


+ Controlled Output Voltage
+ 3-Level Characteristic
+ Tolerates Mains Phase Loss
+ Power Semicond. Stressed with Half Output Voltage

− Higher Control Complexity

**Boost-Type**

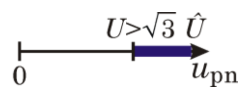


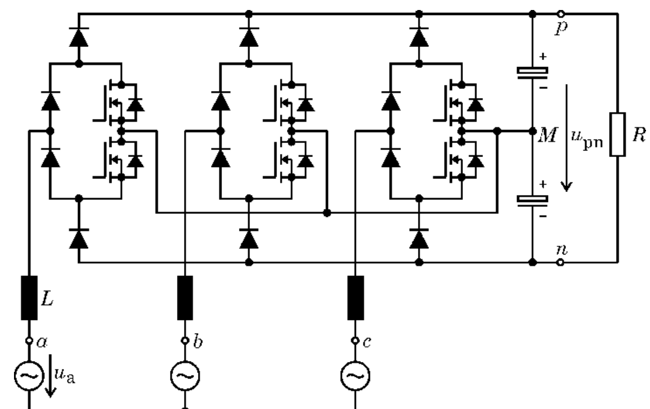


+ Low Current Stress on Power Semicond.
+ In Principal No DC-Link Cap. Required
+ Control Shows Low Complexity

− Sinusoidal Mains Current Only for Const. Power Load
− Power Semicond. Stressed with Full Output Voltage
− Does Not Tolerate Loss of a Mains Phase

**Unregulated Output**

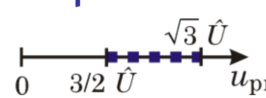


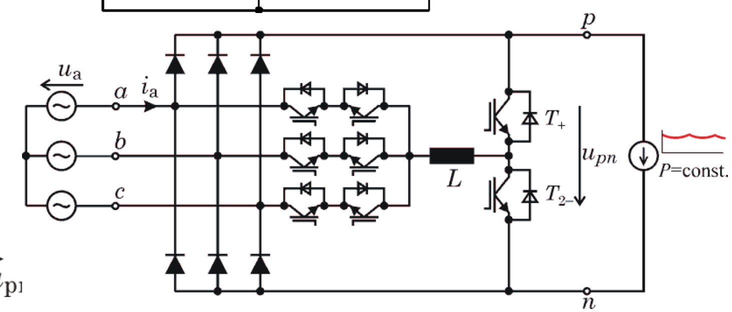

# ▶ Sinusoidal Input Current Rectifier Systems (2)

**Buck-Type**

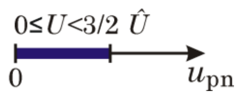


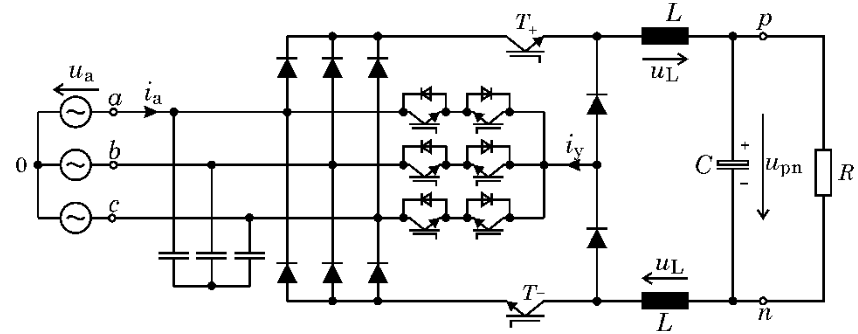


- \+ Allows to Generate Low Output Voltages
- \+ Short Circuit Current Limiting Capability
- – Power Semicond. Stressed with LL-Voltages
- – AC-Side Filter Capacitors / Fundamental Reactive Power Consumption

**Buck+Boost-Type**


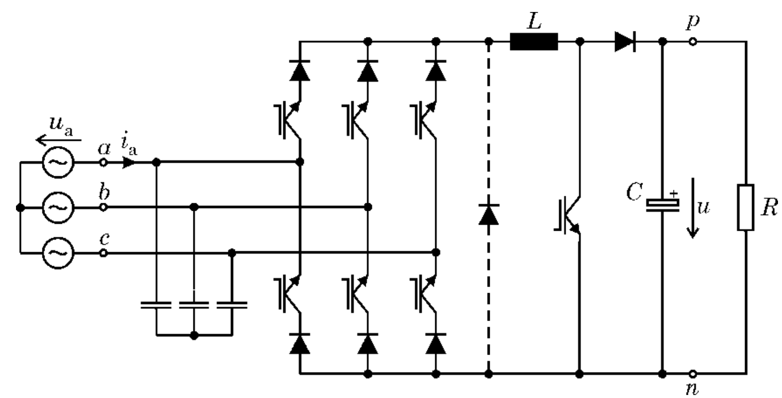


- \+ See Buck-Type Converter
- \+ Wide Output Voltage Range
- \+ Tolerates Mains Phase Loss, i.e. Sinusoidal Mains Current also for 2-Phase Operation
- – See Buck-Type Converter (6-Switch Version of Buck Stage Enables Compensation of AC-Side Filter Cap. Reactive Power)

# Appendix A

## 3-Φ Active PFC Rectifier Design Equations

# Current Stresses – VIENNA Rectifier

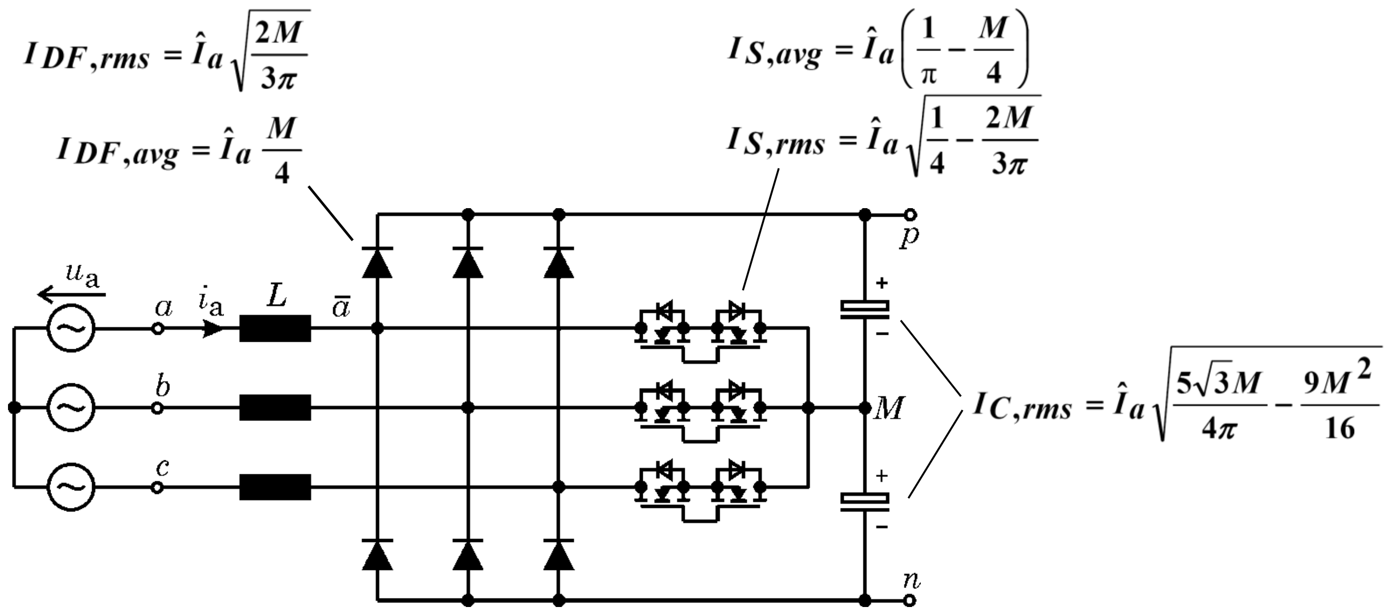


**Modulation Index:** $M = \frac{\hat{U}_a}{(U_{pn}/2)}$

# Current Stresses – Δ–Switch Rectifier

$$I_{DF,avg} = \hat{I}_a \frac{M}{2\sqrt{3}}$$

$$I_{DF,rms} = \hat{I}_a \sqrt{\frac{M(5+2\sqrt{3})}{12\pi}}$$

$$I_{\frac{D}{S},avg} = \hat{I}_a \left( \frac{1}{2\pi} - \frac{M}{4\sqrt{3}} \right)$$

$$I_{\frac{D}{S},rms} = \hat{I}_a \sqrt{\left( \frac{1}{6} - \frac{\sqrt{3}}{8\pi} \right) - \frac{M}{2\sqrt{3}\pi}}$$

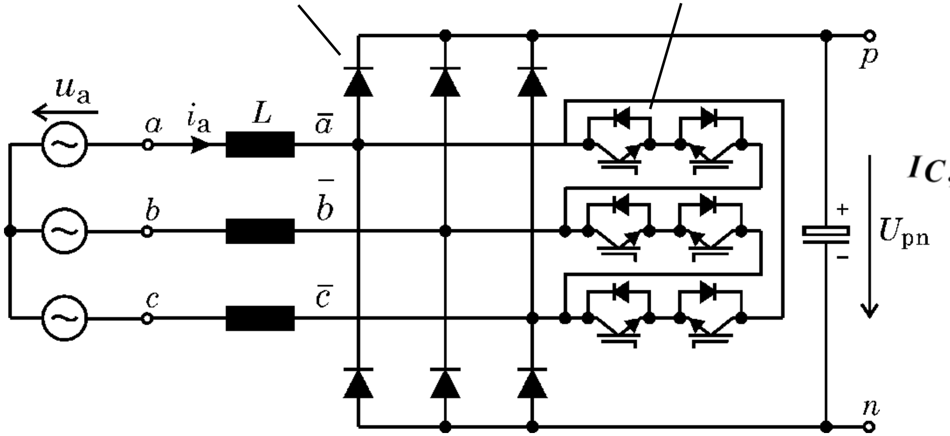


$$I_{C,rms} = \hat{I}_a \sqrt{\frac{5M}{2\pi} - \frac{3M^2}{4}}$$

**Modulation Index:** $M = \frac{\sqrt{3}\hat{U}_a}{U_{pn}}$

# Current Stresses – Integrated Active Filter Rectifier

$$I_{D,avg} = \hat{I}_a \frac{\sqrt{3}}{2\pi}$$

$$I_{D,rms} = \hat{I}_a \sqrt{\frac{1}{6} + \frac{\sqrt{3}}{8\pi}}$$

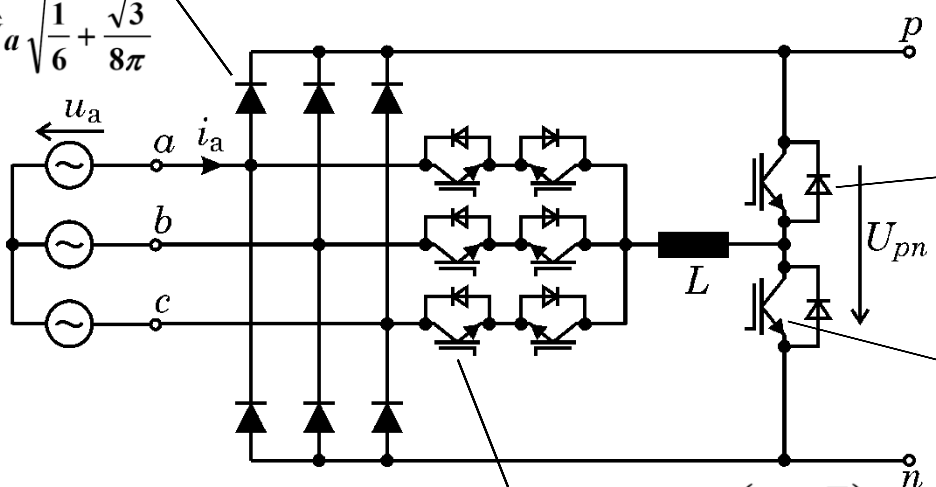


$$I_{D,avg} \approx \hat{I}_a \frac{3}{2\pi}\left(1 + \frac{3}{\pi} - \sqrt{3}\right)$$

$$I_{D,rms} = \hat{I}_a \sqrt{\frac{1}{8} + \frac{3\sqrt{3}}{4\pi}\left(\ln\left(\frac{4}{3}\right) - \frac{1}{2}\right)}$$

$$I_{S,avg} = \hat{I}_a \frac{3}{4\pi}\left(2 + \sqrt{3}\ln\left(\frac{1}{3}\right)\right)$$

$$I_{S,rms} = \hat{I}_a \sqrt{\frac{1}{8} + \frac{3\sqrt{3}}{4\pi}\ln\left(\frac{3}{4}\right)}$$

$$I_{\frac{D}{S},avg} = \hat{I}_a \left(\frac{2 - \sqrt{3}}{2\pi}\right)$$

$$I_{\frac{D}{S},rms} = \hat{I}_a \sqrt{\frac{1}{12} - \frac{\sqrt{3}}{8\pi}}$$

**Modulation Index:** $M = \frac{\sqrt{3}\hat{U}_a}{U_{pn}}$

# Current Stresses – SWISS Rectifier

$$I_{D,avg} = I_{DC} M \frac{\sqrt{3}}{2\pi}$$

$$I_{D,rms} = I_{DC} M \sqrt{\frac{\sqrt{3}}{8\pi} + \frac{1}{6}}$$

$$I_{S,avg} = I_{DC} M \frac{3\sqrt{3}}{2\pi}$$

$$I_{S,rms} = I_{DC} \sqrt{\frac{3\sqrt{3} M}{2\pi}}$$

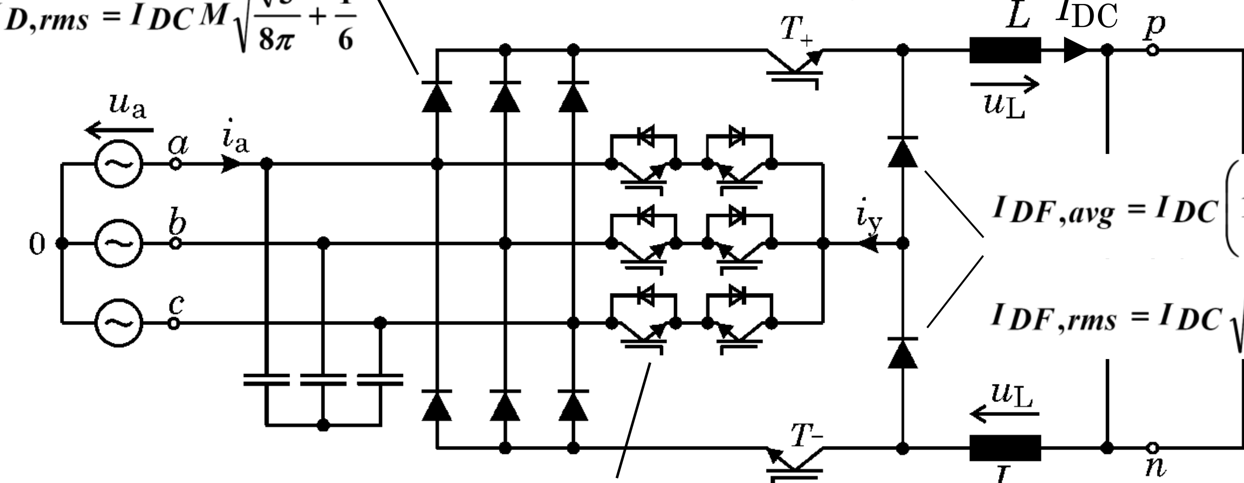


$$I_{DF,avg} = I_{DC} \left(1 - \frac{3\sqrt{3}}{2\pi} M\right)$$

$$I_{DF,rms} = I_{DC} \sqrt{1 - \frac{3\sqrt{3}}{2\pi} M}$$

$$I_{\frac{D}{S},avg} = I_{DC} M \frac{2 - \sqrt{3}}{2\pi}$$

$$I_{\frac{D}{S},rms} = I_{DC} M \sqrt{\frac{1}{12} - \frac{\sqrt{3}}{8\pi}}$$

**Modulation Index:**

$$M = \frac{\hat{I}_a}{I_{DC}}$$

# Current Stresses – 6S Buck-Type Rectifier (1)

$$I_{\frac{D}{S},avg} = I_{DC}\frac{M}{\pi}$$

$$I_{\frac{D}{S},rms} = I_{DC}\sqrt{\frac{M}{\pi}}$$

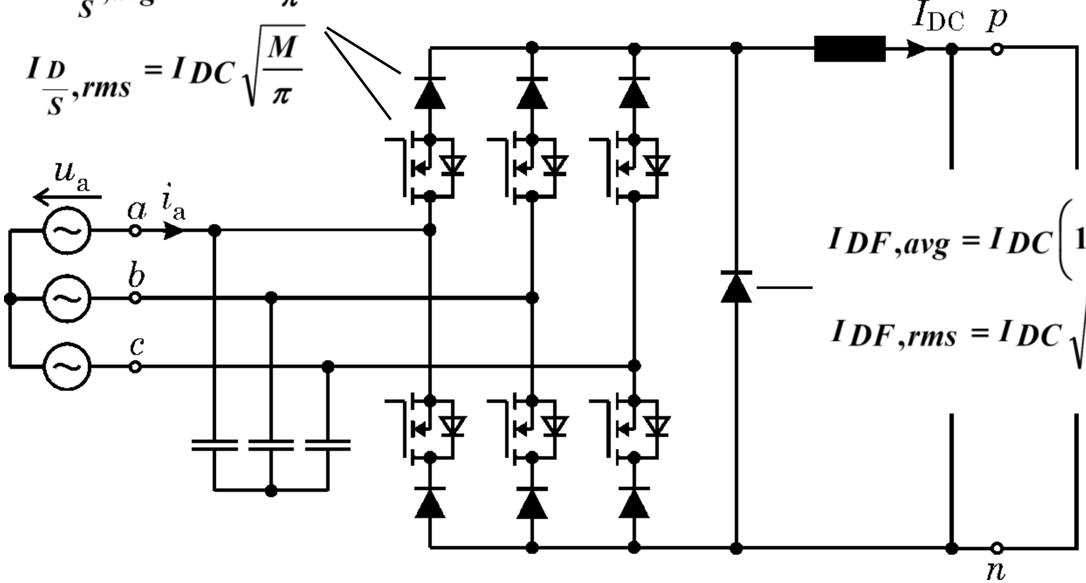


$$I_{DF,avg} = I_{DC}\left(1-\frac{3M}{\pi}\right)$$

$$I_{DF,rms} = I_{DC}\sqrt{1-\frac{3M}{\pi}}$$

**Modulation Index:** $M = \frac{\hat{I}_N}{I_{DC}}$

# Current Stresses – 6S Buck-Type Rectifier (2)

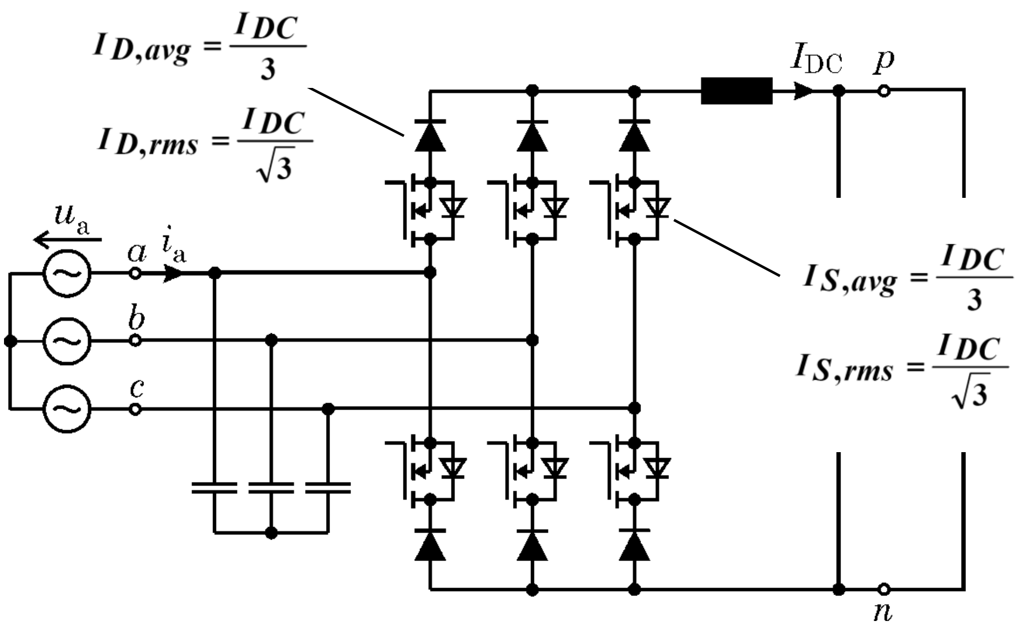


**Modulation Index:** $M = \frac{\hat{I}_N}{I_{DC}}$

# Thank you!

**Contact**

kolar@lem.ee.ethz.ch
bosshard@lem.ee.ethz.ch

# About the Instructors

**Johann W. Kolar (**F´10) received his M.Sc. and Ph.D. degree (summa cum laude / promotio sub auspiciis praesidentis rei publicae) from the University of Technology Vienna, Austria. Since 1984 he has been working as an independent international consultant in close collaboration with the University of Technology Vienna, in the fields of power electronics, industrial electronics and high performance drives. He has proposed numerous novel converter topologies and modulation/control concepts, e.g., the VIENNA Rectifier, the SWISS Rectifier, the Delta-Switch Rectifier, the isolated Y-Matrix AC/DC Converter and the three-phase AC-AC Sparse Matrix Converter. Dr. Kolar has published over 450 scientific papers at main international conferences, over 180 papers in international journals, and 2 book chapters. Furthermore, he has filed more than 110 patents. He was appointed Assoc. Professor and Head of the Power Electronic Systems Laboratory at the Swiss Federal Institute of Technology (ETH) Zurich on Feb. 1, 2001, and was promoted to the rank of Full Prof. in 2004. Since 2001 he has supervised over 60 Ph.D. students and PostDocs.

The focus of his current research is on AC-AC and AC-DC converter topologies with low effects on the mains, e.g. for data centers, More-Electric-Aircraft and distributed renewable energy systems, and on Solid-State Transformers for Smart Microgrid Systems. Further main research areas are the realization of ultra-compact and ultra-efficient converter modules employing latest power semiconductor technology (SiC and GaN), micro power electronics and/or Power Supplies on Chip, multi-domain/scale modeling/simulation and multi-objective optimization, physical model-based lifetime prediction, pulsed power, and ultra-high speed and bearingless motors. He has been appointed an IEEE Distinguished Lecturer by the IEEE Power Electronics Society in 2011.

He received 9 IEEE Transactions Prize Paper Awards, 8 IEEE Conference Prize Paper Awards, the PCIM Europe Conference Prize Paper Award 2013 and the SEMIKRON Innovation Award 2014. Furthermore, he received the ETH Zurich Golden Owl Award 2011 for Excellence in Teaching and an Erskine Fellowship from the University of Canterbury, New Zealand, in 2003.

He initiated and/or is the founder/co-founder of 4 spin-off companies targeting ultra-high speed drives, multi-domain/level simulation, ultra-compact/efficient converter systems and pulsed power/electronic energy processing. In 2006, the European Power Supplies Manufacturers Association (EPSMA) awarded the Power Electronics Systems Laboratory of ETH Zurich as the leading academic research institution in Power Electronics in Europe.

Dr. Kolar is a Fellow of the IEEE and a Member of the IEEJ and of International Steering Committees and Technical Program Committees of numerous international conferences in the field (e.g. Director of the Power Quality Branch of the International Conference on Power Conversion and Intelligent Motion). He is the founding Chairman of the IEEE PELS Austria and Switzerland Chapter and Chairman of the Education Chapter of the EPE Association. From 1997 through 2000 he has been serving as an Associate Editor of the IEEE Transactions on Industrial Electronics and from 2001 through 2013 as an Associate Editor of the IEEE Transactions on Power Electronics. Since 2002 he also is an Associate Editor of the Journal of Power Electronics of the Korean Institute of Power Electronics and a member of the Editorial Advisory Board of the IEEJ Transactions on Electrical and Electronic Engineering.

# About the Instructors (Cont'd)

**Roman Bosshard** received the M.Sc. degree from the Swiss Federal Institute of Technology (ETH) Zurich, Switzerland, in 2011. During his studies, he focused on power electronics, electrical drive systems, and control of mechatronic systems. As part of his M.Sc. degree, he participated in a development project at ABB Switzerland as an intern, working on a motor controller for traction converters in urban transportation applications. In his Master Thesis, he developed a sensorless current and speed controller for a ultrahigh-speed electrical drive system with CELEROTON, an ETH Spin-off founded by former Ph.D. students of the Power Electronic Systems Laboratory at ETH Zurich.

In 2011, he joined the Power Electronic Systems Laboratory at the Swiss Federal Institute of Technology (ETH) Zurich, where he is currently pursuing the Ph.D. degree. His main research area is inductive power transfer systems for electric vehicle battery charging, where he published five papers at international IEEE conferences and one paper in the IEEE Journal of Emerging and Selected Topics in Power Electronics.